Quantum reactive scattering: the time - independent approach (Part I)

Ralph Jaquet

Theoretische Chemie, Universität Siegen, D-57068 Siegen, Germany

ralph.jaquet@theo.chemie.uni-siegen.de

1. Introduction

Reactive scattering events are those in which the "chemical identity" of at least some of the particles changes. Included in this would be chemical exchange reactions, dissociation, ionisation, charge transfer, and electronic excitations, or a combination of these. Since the "chemical identity" of the species in a scattering process is a persistent asymptotic property, the theory of such processes must include all relevant asymptotic states which may occur or are measured.

The four volume set edited by Baer [1] and the book edited by Clary [2] describe the state of the theory of chemical reaction dynamics up to 1986. The two volume set edited by Miller [3] is an earlier review of the field. The book edited by Bernstein [4] gives a detailed review of theory in chemical dynamics. Other more recent collections of reviews are the volume by Bowman (1994) [5], Zhang and Wyatt (1996) [6], by Tsipis et al. (1997) [7] and the new special issues in Physical Chemistry Chemical Physics (1999), Faraday Discussion 110 (1998) and Faraday Transactions Vol. 93 (1997). Reviews about numerical techniques are given in the volumes by Cerjan [8] and Lagana [9].

These lecture notes are based mostly on the work of Kuppermann [10], Schatz and Kuppermann [11], Kouri and Hoffmann [12], Miller [13], Manolopolous and Clary [14], Mrugala [15], Launay [16] and Jaquet et al. [17].

In order to describe correctly the intention of the different authors mentioned above part of their work is taken nearly unmodified and some other parts have been rephrased in order to keep this review of finite size. In the appendix a detailed list of the used work from the literature will be given.

The intention of this review is to give an introduction into the field of time-independent quantum reactive scattering which will be exemplified mostly in form of triatomic systems (A + BC). The state-of-the-art are nowadays four atomic systems (AB + CD, A + BCD), but in order to summarize this 'field' too, it would burst the size of this contribution and as a consequence new developments will be quoted only in a shorter way. In this 'Part I' we will give an introduction of what elastic, inelastic and reactive scattering means, then we discuss coordinate systems and at the end we will present the historical way how in the 1970's the first numerically exact calculations for H + H_2 had been performed. For further reading we strongly refer to the work of Kuppermann [10].

1.1 Remarks to quantum reactive scattering

The detailed study of the dynamics of simple chemical reactions in the gas phase and on solid surfaces is a major area of modern physical chemistry. Experimental progress in this field has developed to such an extent that it is possible to get a "complete" picture of the state-to-state dynamics of atom-diatom reactions such as

$$\mathrm{A} + \mathrm{BC}(v,j) \rightarrow \mathrm{AB}(v',j') + \mathrm{C} \tag{1.1}$$

where (v,j) labels a rovibrational state of the reactant molecule BC and (v',j') is a rovibrational state of the product molecule AB. Work on the state-to-state dynamics of atom / diatom - polyatom reactions is in progress. Experimental work has stimulated in the last 10 - 15 years theoretical research into developing exact quantum mechanical methods and performing calculations on the dynamics of reactions in three dimensions (3D). Not only does this theory provide results for comparing with the experimental data on state-to-state dynamics, but it also provides a first principle approach for predicting rate- coefficients over a wide range of temperatures.
Up to 1986, accurate quantum mechanical calculations had then only been performed on the simplest 3D chemical reactions

$$\mathrm{H} + \mathrm{H}_2(v=0, j=\mathrm{even}) \rightarrow \mathrm{H}_2(v'=0, j'=\mathrm{odd}) + \mathrm{H} \tag{1.2}$$

although classical trajectory calculations were already possible on a wide range of reactions, including those involving polyatomic molecules. Since 1986 there has been remarkable progress in the quantum mechanical description of 3D chemical reactions. Indeed several important 'benchmark' calculations, on reactions considerably more difficult than (1.2), have been performed.
The most detailed quantity that can be measured in a reaction dynamics experiment is the differential cross section [18]

$$\frac{d\sigma_{v,j\rightarrow v',j'}(\theta,E)}{d\Omega} \tag{1.3}$$

which gives a measure of the probability of producing the product state (v',j') from the reactant state (v,j) with a solid scattering angle $\Omega = (\theta,\phi)$ and fixed collision energy E. Crossed molecular beam experiments enable these differential cross sections to be fully resolved with respect to θ. Averaging over the scattering angle gives the integral cross sections [18]

$$\sigma_{v,j\rightarrow v',j'}(E) = 2\pi \int_0^{\pi} \frac{d\sigma_{v,j\rightarrow v',j'}(\theta,E)}{d\Omega} sin\theta d\theta, \tag{1.4}$$

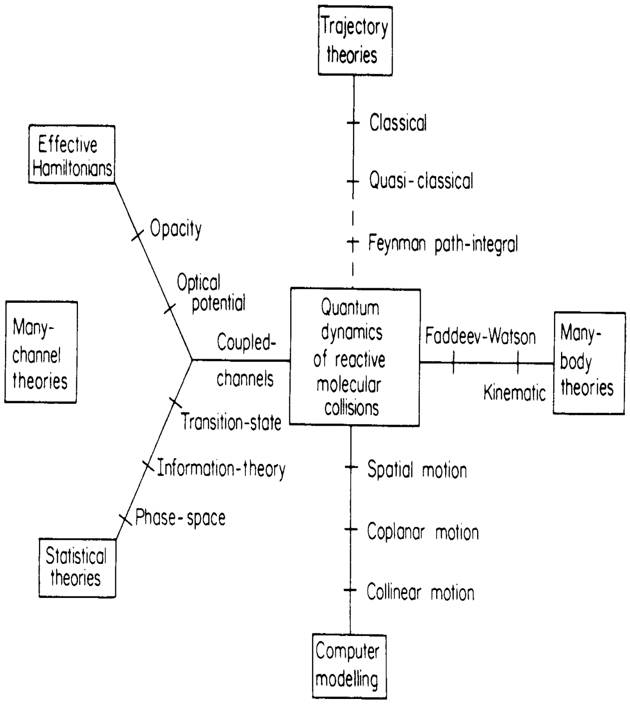

Fig. 1.1. Different theoretical approaches for reactive molecular collisions. (Adapted from Micha, D.: *Adv. Chem. Phys.* **30** (1975) 7.)

which can in principle be measured in less sophisticated bulk experiments. Thermal rate constants to specified product states are obtained by Boltzmann averaging these integral cross sections over the initial rovibrational state (v, j) and collision energy E. These rate constants can then be summed over all possible product states, (v', j'), to give the total reactive thermal rate coefficient $k(T)$. This thermal rate coefficient, in turn, can be measured quite directly in a bulb.

The theoretical methods reviewed in the next chapters produce all of these quantities, ranging from state and energy selected differential cross sections to temperature dependent rate coefficients. Thus the theory of chemical reaction dynamics provides a crucial link between the results obtained in detailed state selective molecular beam experiments and thermally averaged bulb measurements. Exact quantum mechanical methods are now well established for solving inelastic scattering (energy transfer) problems [19] and practical and general quantum mechanical methods for the 3D reactive scattering problem have begun to become "routine". The reason for the comparatively slow progress in reactive scattering is that the coordinates which most conveniently describe the reactants of a chemical reaction are not particularly convenient for describing the products, and vice versa (see Fig. 1.2). Therefore, in order to obtain a complete description of the reactive scattering event, one has either simultaneously to retain all convenient sets of coordinates, both for the reactants and the products, or else to define a new set of (inevitably more complicated) coordinates which somehow encompass all possibilities at once. While each of these approaches has its pros and cons it was clear that new technical difficulties would inevitably arise. But because of the recent availability of large memory supercomputers and workstations, these new technical difficulties can be overcome.

One might wonder since *classical trajectory* calculations on quite complicated reactions have been performed for some time [20], why the coordinate problem described above really is so obtrusive in the quantum mechanical case. The reason for this is simply that quantum mechanical calculations must, by virtue of the Uncertainty Principle describe *all* regions of the available coordinate space at once. Classical trajectory calculations effectively access only a single point in this space at a time, which by comparison is a great deal easier to arrange. In fact the coordinate problem encumbers classical calculations so little that just about any well defined (e.g. Cartesian) coordinate system will do.

An overview [21] of the great variety of approaches to the calculation of cross sections for reactive molecular collisions is given in Fig. 1.1. This variety reflects the different interests and backgrounds of investigators in the field, which has attracted both chemists and physicists. Although some approaches will eventually prove more general and efficient than others, no single approach is likely to provide the answer for each of the many collision problems that arise when going from some chemical species to others or when changing physical parameters. One can distinguish four main categories: computer modelling, many-channel theories, many-body theories and trajectory theories. We will focus mainly on that part of quantum theories, which is related to the time-independent coupled-channels approach using linear algebraic variational methods or propagation methods.

1.2 Overview of quantum reactive methods and remarks to the coupled equations problem

In the description of molecular reactive scattering, the problem of accounting for the change of chemical identity between reagents and products is essential. The following section is extracted from the work of Mrugala [15]. Two formal approaches to this problem have become important in the quantum theory of atom-diatom reactive scattering. In the *traditional ordinary Schrödinger equation* approach, the difference between reagents and products is accounted for essentially by an appropriate design of coordinate system, i.e., on the '*kinematical level*' of description. In the approach offered by the arrangement channel quantum mechanics (Kouri and Baer (1986) [22]), called

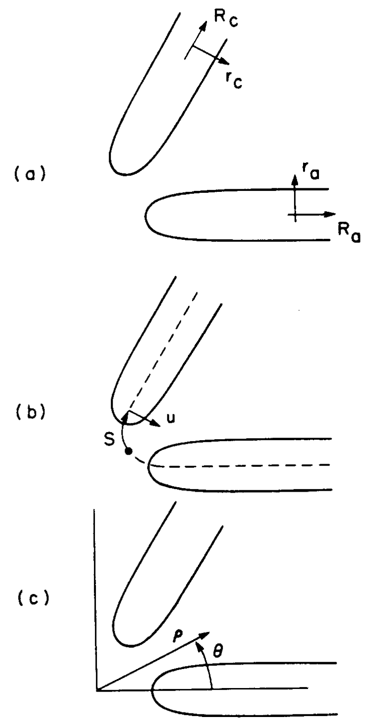

Fig. 1.2. Schematic depiction of a collinear A + BC → AB + C potential energy surface and different ways of choosing coordinates. (a) Jacobi coordinates for arrangement a (A + BC) and c (AB + C), (b) reaction path ('natural coordinates') coordinates, (c) hyperspherical (here simply polar) coordinates. (Adapted from Miller, W.H. in: *Methods in Computational Molecular Physics*, Wilson, S., Diercksen, H.F. (Eds.) NATO ASI Series B 293 (Plenum, NY, 1992)

here the *generalised Schrödinger equation* approach, the problem of existence of different asymptotic in reactive collisions is resolved on the '*dynamical level'*, by intervening into the structure of the equation of motion. Most of the coordinate systems (see Fig. 1.2) which have been especially 'designed or adapted' to description of atom-diatom reactive scattering fall into the category of *natural reaction coordinates* (Marcus 1966 [23], Light 1971 [24]) or into the category of *hyperspherical coordinates* (Smith 1960 [25, 26], Johnson 1980 [27]). The essential difference between these categories concerns construction of the so-called *scattering coordinate.* In general terms, this is a coordinate which measures the progress the collision system has made from (or to) the condensation stage to (or from) the fragmentation stage. There are, of course, three different atom-diatom fragmentations - arrangement channels - possible in a triatomic system and the three-atom dissociation channel which is usually excluded from consideration.
In the *natural reaction coordinate* systems, the scattering coordinate is defined separately for every atom-diatom arrangement channel, usually as an are length along some reference curve in the space of relative configurations of the three atomic nuclei which is placed possibly close to the path of minimum electronic energy within a respective arrangement channel region ('tube') of

this space. Obviously, when the Schrödinger equation for the nuclear motion on a given potential surface is solved in the natural reaction coordinates, the necessity arises for matching the solutions from the different arrangement channel tubes at some surfaces in the condensation (strong interaction) region of the configuration space. The natural reaction coordination systems have been particularly popular and useful in solving collinear models of reactive collisions (see the reviews: Walker and Light (1980 [28]), Kuppermann (1981) [10], Baer (1982) [29], Basilevsky and Ryaboy (1982) [30]). In a rigorous description of reactive collisions, usefulness of the natural reaction coordinates approach has been found to be rather severely limited by considerable complexity and possible inaccuracies of the matching procedure.
In the *hyperspherical coordinate* systems, the scattering coordinate - the hyperradius - is defined to describe simultaneously all the fragmentation channels possible in a collision system. There is no need for troublesome matching of solutions arising in the strong interaction region. The hyperspherical coordinates become inadequate, however, in describing the system at the fragmentation stage, with atom and diatom fragments infinitely separated. This causes some complications in asymptotic analysis of solutions of the Schrödinger equation.
In the *generalised Schrödinger* equation approach, a decomposition of the total wavefunction into pieces - each describing only one atom-diatom arrangement channel - is made which corresponds, in a sense, to the division of the configuration space into the separate arrangement channel regions in the natural reaction coordinate-ordinary Schrödinger approach. The matching of the total wave function generated in the different arrangement channel regions is replaced with a coupling of the different arrangement channel components of the total wavefunction which is introduced explicitly into the generalised Schrödinger equation, usually in the form of potential-like terms. The choice of coordinate representation is not as essential for overall adequacy of description of reactive collision as in the case of the ordinary Schrödinger equation but it still matters a lot when the generalised equation is to be practically solved. Of some importance is the fact that each component of the total wavefunction may be represented in its own coordinate system, most suitable for describing a given atom-diatom arrangement. All the channel coordinate systems may have a common scattering coordinate or three different channel scattering coordinates may be employed.
Concerning practical approaches aimed at solving eventually the ordinary or the generalised Schrödinger equation, two categories of methods may be distinguished: close-coupling methods and variational methods. Actually, methods of both categories have been (or could have been) derived on a basis of some variational principle connected with the quantum-mechanical equations of motion. The difference lies in the assumed form of trial solutions of these equations, the 'best' of which is sought for by any individual method.

In the *close-coupling methods*, trial wavefunctions or their arrangement channel components are in the form of expansions in some basis functions which span the parts of the entire configuration space available to the collision system on surfaces with fixed values of the scattering coordinate or the parts of the particular arrangement channel regions on surfaces with fixed values of respective channel scattering coordinates. The basis functions may be modified, stepwise or continuously, with changing the parameters of the surfaces and the expansion coefficients have to be, of course, functions of the scattering coordinate(s). For the coefficient functions which correspond to the actual (approximate) solution of the ordinary or of the generalised Schrödinger equation, sets of coupled equations-differential or integro -differential in cases with multiple scattering coordinates-are obtained. The number of equations in a set is made finite by retaining only the most closely coupled ones-the close-coupling approximation. Obviously, the strength of coupling depends on the shape of the potential surface, on properties of the basis functions and on the coordinate system employed. For usefulness of the close-coupling methods, it is important that a kind of quasi-separability exists in the collision system between motion along the scattering coordinate and motions along the remaining coordinates in the coordinate system chosen which allows truncation of the coupled equations to a small set.

In the *variational methods*, trial solutions are expanded in basis functions which describe all degrees of freedom of the collision system. From the condition of stationarity of the functional employed, sets of algebraic equations are obtained for the expansion coefficients. Since the choice of coordinates and of basis functions is not limited by any quasi-separability requirement these direct variational (algebraic) methods are potentially more flexible than the close-coupling methods in describing collision systems at the condensation stage and therefore are particularly suitable for reactive systems. Some remarkable research has been carried out in recent years on utilisation of the algebraic approach in atom-diatom reactive scattering calculations. Methods have been developed using various versions of the Kohn principle for the scattering S-matrix (Zhang and Miller 1987 [31], 1989 [32]), for the log-derivative matrix (Manolopoulos et al. 1989 [34]), and for the Wigner R matrix (Linderberg et al. 1989 [35]). These methods can be exploited to carry out calculations within the generalised as well as within the ordinary Schrödinger equation approaches. A parallel (actually an earlier) trend in the search for efficient algebraic methods for molecular reactive scattering calculations has been concerned with the generalised Lippmann-Schwinger equations rather than with the Schrödinger equations and has resulted in developing methods which use the Schwinger or Schwinger-like expressions for the reactance matrix (Schwenke et al. 1988 [36], Zhang et al. 1988 [37]) and the methods based on the Newton variational principle (Schwenke et al. 1988 [36], 1989 [38]) and on the scattering wave variational principle (Sun et al. 1990 [39, 40]).

The *close-coupling methods*, being undoubtedly the most powerful and convenient methods of investigating non- reactive molecular scattering processes (Lester (1976) [41]), have played the leading role in advancing the description of reactive atom-diatom collisions from the stage of collinear models to the present level of rigorous quantum-mechanical treatment in full dimensionality (see the reviews: Wyatt (1979) [42], Walker and Light (1980) [28], Schatz (1986-89) [43, 44, 45]). These methods continue to be useful tools in the branch of reactive scattering investigations (Pack, Parker et al. (1987-91) [46, 47, 48, 49, 50]) despite the rapid development and impressive achievements of the algebraic approach. Using a close-coupling method seems to be the most natural choice within the ordinary Schrödinger equation approach. Numerous formulations of the coupled equations for atom-diatom reactive scattering have appeared in the literature. Representative of the class of formulations using natural reaction coordinates and involving matching procedures are those by Elkowitz and Wyatt (1975 [51]) (see also Wyatt (1979 [42])), by Schatz and Kuppermann (1976 [11]) (see also Kuppermann (1981 [10])), and by Walker et al. (1976 [52]) (see also Light and Walker (1976 [53]), Walker and Light (1980 [28])). Formulations using hyperspherical coordinates were proposed by Kuppermann and co-workers (1980 [54], 1986 [55], 1989 [56]), by Hauke et al. (1980 [57]) and Römelt (1980 [58]) for collinear reactions, and by Pack and Parker (1987 [46], 1989 [47]).
Within the generalised Schrödinger approach, the close-coupling methods have had much less popularity. Several interesting attempts, however, have been made to derive coupled equations within this approach in an ordinary differential equation form (Diestler 1971 [59], Stechel et al. 1979 [60], Top and Shapiro 1983 [61], Schwenke et al. 1987 [62]). Successful calculations based on one of such formulations (which also employs hyperspherical coordinates) have been reported by Schatz (1986-89 [43, 44, 45]).
For further references on the coupled equations problems and the relation of the coordinate problem to quantum reactive methods see the reviews of Mrugala [15] and Manolopolous and Clary [14].

2. Some aspects to quantum molecular scattering in chemical dynamics

Chemical dynamics is the link between the potential energy surface (or surfaces) and physically observable chemical phenomena. The *potential surface* comes in principle from an ab initio quantum chemistry calculation (within the Born-Oppenheimer approximation) though in practice it is often constructed by some more approximate model, e.g., semiempirical quantum chemistry or totally empirical "force field" models. First a brief overview of the present state of the methodology and scope of applications in this area is given. We will concentrate on chemical dynamics in the gas phase, though

much of the methodology of this field has carried over to the study of dynamical processes in condensed phases, gas-surface collision processes, and also dynamics in biomolecular systems.
In the next three subsections (extracted from the work of Miller [13]) we will discuss briefly molecular collision processes (elastic, inelastic and reactive scattering), perhaps the most well-defined and rigorous approach to studying chemical dynamics.

2.1 Elastic Scattering

The study of elastic scattering was in the early days of chemical dynamics (the 1960's) an important project, both experimentally and theoretically, for developing the tools to be used to study more interesting processes, e.g., elastic scattering of the rare gas atoms [63]. Y.T.Lee's (1986 Nobel Prize with M. Polanyi and D. Herschbach) measurements of the differential scattering cross sections allowed the definitive determination of the intermolecular potential energy function $V(r)$ of essentially all the rare gas atoms with each other.
The fully rigorous quantum mechanical elastic differential cross section is given by [64]

$$\sigma_E(\theta) = \left| \frac{1}{2ik} \sum_{l=0}^{\infty} (2l+1) P_l(\cos\theta)(e^{2i\eta_l(E)} - 1) \right|^2, \tag{2.1}$$

where the phase shift $\eta_l(E)$ for orbital angular momentum l and energy E is determined from the asymptotic form of the regular solution of the radial Schrödinger equation,

$$\left(-\frac{\hbar^2}{2\mu}\frac{d^2}{dr^2} + V(r) + \frac{\hbar^2 l(l+1)}{2\mu r^2} - E \right) f_{lE}(r) = 0, \tag{2.2}$$

with asymptotic boundary condition

$$\lim_{r\to\infty} f_{lE}(r) \propto \sin(kr - \frac{\pi l}{2} + \eta_l(E)). \tag{2.3}$$

The procedure is, given the potential function $V(r)$ and a value of the energy E, to solve the Schrödinger equation, (2.2), for all values of l to obtain the phase shifts, and then to compute the cross section from (2.1).
Even though hundreds (or thousands) of values of l's may be needed for the sum in (2.1) to converge, this is nevertheless a trivial calculation nowadays. The potential function $V(r)$ is typically determined by assuming a functional form involving a set of parameters, carrying out the calculation of $\sigma_E(\theta)$ as described, and adjusting the parameters in the potential in a least squares procedure to fit the experimental cross section. Though this least squares fitting procedure is not as elegant as formal "inversion" approaches, it is in practice the most general and straight-forward approach.

Elastic scattering was also the theoretical workhorse in earlier years for developing many approximate theoretical methods, and though these approximations are no longer needed for elastic scattering calculations they still serve as useful guides for dealing with more complex processes.
One of the most important examples of this is the *semi-classical* approximation to quantum mechanics: in 1959 Ford and Wheeler [65] described the explicit sequence of approximations by which the rigorous quantum cross section of (2.1)-(2.3) degenerates to the completely classical cross section,

$$\sigma_E(\theta) = \Sigma_k \frac{bk}{\sin\theta\, |\Theta(b_k)|}, \tag{2.4}$$

where $b_k \equiv b_k(\theta)$ are the values of impact parameters b which classically scatter at angle θ, i.e., the roots of the equation

$$|\Theta(b)| = \theta \tag{2.5}$$

where $\Theta(b)$ is the *classical* deflection angle as a function of b,

$$\Theta(b) = \pi - \int_{r_0}^{\infty} dr \frac{2b}{r^2}\left(1 - \frac{V(r)}{E} - \frac{b2}{r2}\right)^{-\frac{1}{2}}, \tag{2.6}$$

and r_0 is the classical turning point (the largest value r for which the integrand of (2.6) is zero.) The essential approximations are to use the *WKB approximation* for the phase shift and the Legendre polynomial, to replace the sum over l by an integral, and then evaluate the integral by the stationary phase approximation. The result is

$$\sigma_E(\theta) = |\Sigma_k (\frac{bk}{\sin\theta\, |\Theta(b_k)|})^{\frac{1}{2}} e^{i\phi_k/\hbar}|^2, \tag{2.7}$$

where $\{b_k\}$ are the same as in the classical cross section; they emerge semiclassically as the values of l ($l \equiv kb, k = \sqrt{2mE/\hbar^2}$) for which the phase in the integral over l is stationary and thus make the dominate contribution to the sum/integral. The phases $\{\phi_k\}$ are the classical action for the kth trajectory that classically scatters at angle θ.
(2.1), (2.4), and (2.7) show the generic structure relating quantum, classical, and the semiclassical correction in scattering cross sections. (2.7) shows clearly that

$$\sigma_{SC}(\theta) = \sigma_{CL}(\theta) + \text{interference terms}, \tag{2.8}$$

so that it is interference between the different classical contributions to the cross section that is the most fundamental effect of quantum mechanics. Bernstein's 1966 review [64] of the semiclassical description of quantum effects in elastic scattering is still one of the best and most comprehensive, and that by Berry and Mount [66] is also insightful. Recently Child [67] has reviewed semiclassical theory more generally.

2.2 Inelastic Scattering

Inelastic scattering of atoms and molecules is clearly of more physical interest than elastic scattering. This includes excitation or relaxation of rotational and vibrational degrees of freedom and also of electronic states. Rotational/vibrational inelasticity is important in understanding classical transport phenomena in gases, and the vibrational relaxation of highly excited molecules is of crucial importance for describing "unimolecular" reaction in the Lindeman mechanism [68],

$$A + B \rightarrow A^* + B \tag{2.9}$$

$$A^* + B \rightarrow A + B \tag{2.10}$$

$$A^* \rightarrow products \tag{2.11}$$

I.e., after collisional excitation of A to A* by the bath gas B - or A* may be produced "hot" as the product of some preceding chemical reaction - the important consideration is the competition between collisional stabilisation of A* by the bath gas, (2.10), and the unimolecular decomposition of A*, (2.110. Currently, therefore, there is much effort devoted to learning more quantitatively about vibrational de-activation of highly excited vibrational states [69]. Electronically inelastic collisions are important in many gas laser systems, in the upper atmosphere, and in plasmas. Many of these applications involve one of the collision partners being an ion.

The quantum mechanical description of an inelastic scattering process is straightforward. Leaving aside details involving angular momentum, the wavefunction for the generic situation is expanded as

$$\Psi_i(r,\xi) = \sum_j \phi_j(\xi) f_{j\leftarrow i}(r), \tag{2.12}$$

where $\{\phi_j(\xi)\}$ denotes the bound-state eigenfunctions for the internal (rotational, vibrational, and electronic) degrees of freedom (with ξ collectively denoting the appropriate coordinates) of the colliding molecules, and r is the radial (translational) coordinate, i.e., the distance between the centers of mass of the two molecules. The radial function (matrix) $f_{j\leftarrow i}(r)$ is determined by the coupled-channel (channel being the historical term for the various internal states) Schrödinger equation,

$$\left(-\frac{\hbar^2}{2\mu}\frac{d^2}{dr^2} - E_j\right) f_{j\leftarrow i}(r) + \sum_{j'} V_{j,j'}(r) f_{j'\leftarrow i}(r) = 0, \tag{2.13}$$

where $V_{j,j'}(r)$ is the matrix of the interaction potential $V(\xi,r)\}$ with respect to the basis of internal states,

$$V_{j,j'}(r) = \int d\xi \phi_j(\xi) V(\xi,r) \phi_{j'}(\xi), \tag{2.14}$$

and $E_j = E - \epsilon_j$, where E is the total energy and ϵ_j the energy eigenvalue corresponding to ϕ_j (i.e., E_j is the available translational energy for channel j). The boundary conditions for the radial functions are that they be regular for $r \to 0$, and for large r have an incoming radial wave in initial channel i and outgoing waves in all open channels,

$$\lim_{r\to\infty} f_{j\leftarrow i}(r) \sim -\frac{e^{-ik_i r}}{v_i^{\frac{1}{2}}}\delta_{j,i} + \frac{e^{ik_j r}}{v_j^{\frac{1}{2}}} S_{j,i}(E), \tag{2.15}$$

where $v_j = \sqrt{2E_j/\mu}$ is the translational velocity for channels j, and $S_{j,i}$ is the S-matrix, in terms of which all scattering cross sections can be expressed. Using (2.15) in (2.12) shows that the full wavefunction has the following form are large r

$$\Psi_i(r,\xi) \sim -\phi_i(\xi)\frac{e^{-ik_i r}}{v_i^{\frac{1}{2}}}\delta_{j,i} + \sum_j \phi_j(\xi)\frac{e^{ik_j r}}{v_j^{\frac{1}{2}}} S_{j,i}(E), \tag{2.16}$$

from which one more clearly sees that the initial channel i has an incoming radial wave, and all channels have outgoing (scattered) waves. The S-matrix is a unitary matrix and has the interpretation as the probability amplitude for the $i \to j$ transition; the transition probability is thus

$$P_{j\leftarrow i} = |S_{j,i}|^2, \tag{2.17}$$

When one takes account of the total angular momentum, which is a vector sum of the orbital angular momentum of relative motion (i.e., the angular degrees of freedom of the translational coordinate vector $\mathbf{r}$) and any angular momentum from the internal degrees of freedom, one finds that the total angular momentum J is conserved (because of the isotropy of space) and is thus a diagonal label of the S-matrix, $S^J_{j,i}(E)$. The state-to-state differential cross section - the most detailed possible scattering observable - is then given by

$$\sigma_{j\leftarrow i}(\theta) = \left| \frac{1}{2ik_i} \sum_{J=0}^{\infty} (2J+1) d^J_{m_j,m_i}(\theta)(S^J_{j,i}(E) - \delta_{j,i}) \right|^2, \tag{2.18}$$

where $d^J_{m_j,m_i}(\theta)$ is the Wigner rotation function, and m_i, m_j are the projections of the total angular momentum onto the initial and final relative velocity vectors. One can easily recognise the sense in which (2.18) is the generalisation of (2.1) for the elastic scattering of two structureless particles; in the latter case $J \to l$ (i.e., the orbital angular momentum l is the total angular momentum), m_j and $m_i \to 0$, $d^J_{00} = P_l(cos\theta)$, and

$$S^J_{j,i}(E) \to e^{2i\eta_l(E)}. \tag{2.19}$$

The theoretical task, therefore, is to solve (2.13) with the boundary conditions of (2.15) to obtain the S-matrix, in terms of which the inelastic cross sections are given by (2.18). Such calculations are relatively straight-forward nowadays [70], although they can be time consuming if the number of channels is large; the largest calculations which are reasonable at present involve up to $\sim$ 1000 coupled channels. This may seem like a large number, but consider the number of rotational/vibrational states of a diatomic molecule that have an energy below an energy E,

$$N(E) = \sum_{v=0} \sum_{j=0} (2j+1) h(E - \epsilon_{vj}). \tag{2.20}$$

Using a simple rigid rotor-harmonic oscillator approximation for the energy levels,

$$\epsilon_{vj} \cong \hbar\omega(v + \frac{1}{2}) + Bj(j+1), \tag{2.21}$$

where ω is the vibrational frequency and B the rotation constant, gives

$$N(E) \cong \frac{E^2}{2\hbar\omega B}. \tag{2.22}$$

For $E = 0.14$ eV, $\hbar\omega = 2000$ cm^{-1}, and $B = 1$ cm^{-1}, which are typical of a relatively small diatomic molecule (O_2, N_2, CO), (2.22) gives $N \sim 160$, not too large a number of channels. But for I_2 ($\hbar\omega = 215$ cm^{-1}, $B = 0.037$ cm^{-1}) at this energy one has $N \cong 40,000$! And this is the number of channels for only one diatomic molecule; for the collision of two diatomics at energy E one has

$$N(E) \cong \frac{E^4}{4!\hbar\omega_1 \hbar\omega_2 B_1 B_2}, \tag{2.23}$$

$$\cong \frac{1}{6} N_1 N_2, \tag{2.24}$$

where N_1 and N_2 are the number of channels for molecules 1 and 2, respectively. Thus the number of channels involved can become unmanageably large very quickly!

Typically, however, the more channels there are that are strongly coupled in an inelastic collision the better it is to approximate the dynamics by classical mechanics; i.e., there are more channels the heavier the particles, but this is also the limit in which classical mechanics is a better approximation. Thus there have been many classical trajectory simulations of inelastic collision processes [71]. These have the advantage that no approximations other than the use of classical mechanics need be made, and the number of classical equations of motion to be solved (Hamiltonian's equations) grows linearly with the number of particles, while the numbers of coupled channels in the coupled-channel Schrödinger equation grows exponentially with this number. There also exist a wide variety of approximate quantum mechanical and semiclassical theories [72]. In various limits some of the degrees of freedom can

be treated as slow or fast compared to others, leading to sudden or adiabatic approximations, and in some cases the coupling between translational and internal motion can make perturbation theory a useful approximation.
Classical S-matrix theory [67, 73] is a "rigorous" semiclassical theory, rigorous in that it incorporates the full classical mechanics for all degrees of freedom without approximation; it may be viewed as the generalisation of the Ford and Wheeler semiclassical description of elastic scattering. Thus the inelastic transition probability in this theory is of the form

$$P^{SC}_{j\leftarrow i} = |\Sigma_k P^{(k)\,\frac{1}{2}}_{j,i} e^{i\phi^{(k)}_{j,i}/\hbar}|^2, \qquad (2.25)$$

where $P^{(k)}_{j,i}$ is the purely classical contribution to the $i \to j$ transition from the kth trajectory which leads to it - i.e., the completely classical transition probability is

$$P^{CL}_{j\leftarrow i} = \Sigma_k P^{(k)}_{j,i} \qquad (2.26)$$

and $\phi_{i,j}$ is a classical action integral along the corresponding trajectory. The semiclassical transition probability thus has the same structure as in (2.8),

$$P^{SC}_{j\leftarrow i} = P^{CL}_{j\leftarrow i} + \text{interference}. \qquad (2.27)$$

Interference between the different classical trajectories which contribute to the $i \to j$ transition will thus cause interference effects (e.g., "rainbows") in the product distribution of internal states analogous to such effects in the angular distribution (i.e., differential cross section) for elastic scattering.

2.3 Reactive Scattering

Quantum mechanical reactive scattering [4, 5, 14, 74] provides the fundamental, rigorous and the most complete description of a chemical reaction allowed by the basic laws of nature. Thus ever since the 1960's, when crossed molecular beam experiments opened the door to studying reactions at the most detailed state-to-state level, there has been intense interest and effort devoted to developing the theory to the practical stage that calculations can be carried out for real chemical reactions. Unfortunately it is also the most complicated to deal with because of the lack of one physically appropriate set of coordinates for "translation" and "internal" degrees of freedom. This means that the natural coordinates for describing translational and internal degrees of freedom for the reactant molecules are not the natural ones for describing those of the products. See [74] for a fairly detailed discussion of this "coordinate problem" for reactive scattering.

Why a basis set variational approach to reactive scattering?

The theory of reactive scattering is more complicated than that for elastic and inelastic scattering [75, 76, 77], because of coordinates, and different formulations of reactive scattering turn on how one deals with this coordinate problem. Fig. 1.2 depicts the situation for the collinear A + BC $\rightarrow$ AB + C reaction. If one were treating only an inelastic scattering process (i.e. vibrational excitation),

$$A + BC(n) \rightarrow A + BC(n'), \tag{2.28}$$

then the standard Jacobi coordinates (r_a, R_a) are the natural choice, and the coupled-channel expansion of the wavefunction has the form

$$\psi_{n_1} = \sum_n \phi_n(r_a) f_{n \leftarrow n_1}(R_a), \tag{2.29}$$

where $\{\phi_n\}$ are the (known) vibrational eigenfunctions for diatom BC and n_1 denotes the initial vibrational state. Substitution of this expansion into the Schrödinger equation leads to the standard coupled-channel equations for the unknown translational functions

$$0 = (-\frac{h^2}{2\mu}\frac{d^2}{dR_a^2} - E_n) f_{n \leftarrow n_1}(R_a) + \sum_{n'} V_{n,n'}(R_a) f_{n' \leftarrow n_1}(R_a), \tag{2.30}$$

$$V_{n,n'}(R_a) = \int dr_a \phi_n(r_a)(V - v)\phi_{n'}(r_a). \tag{2.31}$$

$E_n = E - \epsilon_n$ is the translational energy for channel n, where E is the (fixed) total energy and ϵ_n the vibrational energy for state n, V is the total potential energy function, and v the potential for the isolated diatom BC.
The "coordinate problem" referred to above for reactive scattering is that the Jacobi coordinates (r_a, R_a) that are natural for describing the reactants A+BC are not appropriate for describing the products, AB+C. There are several ways to deal with this situation, but most of the recent progress in reactive scattering has been based on the formulation [78] in which the Jacobi coordinates for the various "arrangements" (i.e. A+BC, AB+C, AC+B) are all used simultaneously. For the collinear case of Fig. 1.2, for example, the expansion for the wavefunction in this approach is

$$\Psi_{\gamma_1 n_1} = \sum_n \phi_n^a(r_a) f_{an \leftarrow \gamma_1 n_1}(R_a) + \sum_n \phi_n^c(r_c) f_{cn \leftarrow \gamma_1 n_1}(R_c), \tag{2.32}$$

where $\gamma = a$(A+BC), b(B+AC), or c(C+AB) labels the arrangement of the atoms, and $\{\phi_n^a\}$ and $\{\phi_n^c\}$ are the vibrational eigenstates of diatoms BC and AB, respectively. Note that there are only two independent coordinates (degrees of freedom) in (2.32) for the collinear case shown in Fig. 1.2; i.e., r_a and R_a are functions of r_c and R_c, or vice-versa (specifically, they are linear combinations of each other). The philosophy of this approach is similar to that in quantum chemistry of using multicenter (LCAO = linear combination of atomic orbitals) expansions for molecular orbitals. For a diatomic molecule, for example, the molecular orbital $\chi(r)$ for an electron is expanded in basis functions utilizing the coordinates of the electron with respect to both nuclear centers,

$$\chi(r) = \sum_i a_i \phi_i^a(r_a) + \sum_i b_i \phi_i^b(r_b), \tag{2.33}$$

where r_a are the coordinates of the electron with respect to nucleus a and r_b those with respect to nucleus b. (Note that there are only three independent coordinates in (2.33), i.e., r_a is a function of r_b, or vice-versa, specifically, $r_a = r_b + R_b - R_a$ where R_a and R_b are the coordinates of the nuclei.)
One may also think of this approach to reactive scattering as a generalization of the standard description of electron scattering [79]. Thus in Fig. 1.2, consider the case that atom B = H^+ (a proton), and A and C are electrons, i.e. the collinear version of electron-hydrogen atom scattering. In this case $m_B >> m_A, m_C$ and it is clear that the two translational coordinates coincide with the two interparticle coordinates, i.e. $R_c = r_a$ and $R_a = r_c$ and that the two sets of terms in (2.32) are related to one another simply by exchange of the electrons. (By symmetry, the two sets of terms are the same, with a + or - combination corresponding to the singlet and triplet case, respectively.) Thus even if one did not know that the (spatial) two-electron wavefunction should be symmetric or antisymmetric upon exchange of the two electrons, the fact that the electrons can actually interchange by virtue of the collision (a "chemical reaction") requires that the wavefunction include both sets of terms in (2.32). (The chemical reaction H+IH $\rightarrow$ HI+H is a molecular case very close to the e - H atom limit.) The general chemical reaction is more complicated than the electron scattering case because the finite mass of all atoms makes the relation between the various sets of Jacobi coordinates more complicated than simply exchanging them, but the basic idea is the same.
The expansion of the wavefunction in (2.32) is also essentially the same basic idea as the "resonating group model" (RGM) used in nuclear physics [80]. The different sets of Jacobi coordinates define different "groups" (or groupings) of atoms, and the fact that the wavefunction is a linear combination of these different terms allows for "resonance" (i.e. coupling, interaction) between them if there are non-zero matrix elements of the Hamiltonian ("resonance integrals") connecting them.
(2.32) is thus a natural and efficient way to represent a reactive scattering wavefunction, but it introduces the complexity that the coupling between terms corresponding to different arrangements are nonlocal, exchange type interactions. The coupled-channel equations (2.30) are thus generalized as follows [78]:

$$\begin{aligned} 0 = (-\frac{h^2}{2\mu_a}\frac{d^2}{dR_a^2} - E_n^a) f_{an\leftarrow\gamma_1 n_1}(R_a) + \sum_{n'} V_{an,an'}(R_a) f_{an'\leftarrow\gamma_1 n_1}(R_a) \\ - \sum_{\gamma\neq a}\sum_{n'}\int dR_\gamma V_{an,\gamma n'}(R_a,R_\gamma) f_{\gamma n'\leftarrow\gamma_1 n_1}(R_\gamma) \end{aligned} \tag{2.34}$$

The exchange interaction (the last term in the above equation), which couples states of different arrangements, is analogous to electron exchange interactions in quantum chemistry that arise from matrix elements in which the electron coordinates have been permuted (i.e. exchanged). The coupled integro-differential equations for the translational functions, (2.34), are thus analogous to the Hartree-Fock equations of electronic structure theory, and as such they cannot be solved by finite difference algorithms.
Indeed, it is the presence of the exchange interaction in this formulation of reactive scattering that until recently has stymied this approach. Wolken and Karplus [81] made some early attempts using it, but these were not completely successful. It has ultimately become clear that the most satisfactory way of dealing with exchange is analogous to what quantum chemists do in the Hartree-Fock problem, namely to expand the unknown wavefunctions in a basis set and determine the expansion coefficients via a variational principle.
The variational approach received a major boost also when it was realised [82] that the simplest variational method - the Kohn variational principle, which is essentially the Rayleigh-Ritz variational principle for eigenvalues modified to incorporate scattering boundary conditions - is free of anomalous (i.e., spurious, unphysical) singularities if it is formulated with S-matrix type boundary conditions rather than standing wave boundary conditions as had been typically used previously. It is useful first to state the Kohn variational approach for the general inelastic scattering. Thus the variational expression for the S-matrix is

$$S\left[\Psi_f, \Psi_i\right] = S_{fi}^{(0)} + \frac{i}{\hbar}\left\langle \Psi_f | H - E | \Psi_i \right\rangle , \tag{2.35}$$

where Ψ_f and Ψ_i are variational ("trial") wavefunctions of the form that satisfy the correct boundary conditions [cf. (2.16)]

$$\Psi_l(\xi, r) \sim -\frac{e^{-ik_l r}}{v_l^{\frac{1}{2}}}\phi_l(\xi) + \sum_j \frac{e^{ik_j r}}{v_j^{\frac{1}{2}}}\phi_j(\xi) S_{j,l}^{(0)} , \tag{2.36}$$

for $l = i$ and f. In practice we have taken the trial function to be of the form

$$\Psi_l(\xi, r) = \Phi_l(\xi, r) + \sum_j \Phi_j(\xi, r)^* C_{j,l} + \sum_k \chi_k(\xi, r) C_{k,l} , \tag{2.37}$$

where $\Phi_l(\xi, r)$ is an asymptotically incoming radial wave in channel l,

$$\Phi_l(\xi, r) \sim \frac{e^{-ik_l r}}{v_l^{\frac{1}{2}}}\phi_l(\xi), \tag{2.38}$$

and Φ_l^* is a corresponding outgoing wave. The functions $\{\chi_k\}$ in (2.37) are an L^2 basis that describes the interaction (small r) region of the composite molecular system. The coefficients $\{C_{j,l}\}$ and $\{C_{k,l}\}$ in (2.37) are the variational parameters with respect to which (2.35 for the S-matrix is extremized;

i.e., substituting the functions Ψ_f and Ψ_i of the form of (2.37) into (2.35) gives the S-matrix as a quadratic function of these coefficients, and the variational condition

$$0 = \frac{\partial}{\partial C_\lambda} S(\{C_{j,f}\}, \{C_{l,f}\}, \{C_{j,i}\}, \{C_{l,i}\}), \tag{2.39}$$

for each of the coefficients $C_\lambda = C_{j,f}, C_{l,f}$, etc., leads to linear equations for the coefficients which are solved by matrix inversion. Using these variationally optimum coefficients in the expression for the S-matrix then gives the following variationally optimum result (within the given basis set) for the S-matrix,

$$S_{f,i} = \frac{i}{\hbar}(M_{f,i} - \mathbf{M_f^T M^{-1} M_i}), \tag{2.40}$$

where

$$M_{f,i} = \langle \Phi_f | H - E | \Phi_i \rangle , \tag{2.41}$$

$$\mathbf{M_l} = \left\{ \begin{array}{l} \langle \Phi_j^* | H - E | \Phi_l \rangle \\ \langle \chi_k | H - E | \Phi_l \rangle \end{array} \right\} , \tag{2.42}$$

for $l = i$ and f and

$$\mathbf{M} = \left\{ \begin{array}{l} \langle \Phi_{j'}^* | H - E | \Phi_j \rangle , \langle \Phi_{j'}^* | H - E | \chi_k \rangle \\ \langle \chi_{k'} | H - E | \Phi_j \rangle , \langle \chi_{k'} | H - E | \chi_k \rangle \end{array} \right\} . \tag{2.43}$$

Thus the scattering problem has been cast in the form of a standard quantum mechanical calculation, i.e., computing matrix elements of the Hamiltonian with respect to a set of basic functions and then performing a linear algebra calculation (i.e., the matrix inverse in (2.40)).
The power of this variational result is that it applies as written also for reactive scattering provided one expands the definition of the channel label also to include an arrangement label. Thus for an atom-diatom reaction, A + BC $(v, j, m) \rightarrow$ AB (v', j', m') + C, the initial channel index i denotes the collection $\equiv (a, v, j, m)$, labelling the arrangement a and quantum state (v, j, m) of that arrangement; the final channel label in this case is $f = (c, v', j', m')$. The only modification of the above formulae in (2.35)-(2.43) is in (2.38), noting that the coordinates appropriate for asymptotic channel l may be different for different channels, i.e.,

$$\Phi_l \sim -\frac{e^{-ik_l r_l}}{v_l^{\frac{1}{2}}} \phi_l(\xi_l). \tag{2.44}$$

Miller [74] discusses how this strategy of using different coordinates for different basis functions is the same as that in the LCAO approach for constructing molecular orbitals in electronic structure theory by using atomic orbitals which are expressed in terms of spherical coordinates referenced to (i.e., "centered on") various nuclei.

Many of the recent accurate quantum reactive scattering calculations have utilised the above approach [34, 82, 83, 84, 85, 86]. Methods using hyperspherical coordinates have been the primary alternative [87, 88, 89]. Complete state-to-state differential cross section calculations have been carried out for the $H+H_2$ reaction, its isotopic variants [84, 86] and also for the $F+H_2 \to HF + H$ reaction [87]. Calculations for many other reactions have been carried out mostly for $J = 0$ only.
It is also useful to note that methods have been developed which allow one to calculate the cumulative reaction probability (CRP) for a reaction directly, without having to solve for the individual state-to-state S-matrix elements [90, 91, 92, 93, 94]. This subject will be discussed in this volume by a contribution of U. Manthe.

3. General remarks: Quantum scattering, scattering matrix, Møller operators, etc.

The time evolution of any system is determined (in the Schrödinger picture of quantum mechanics) by the Schrödinger equation ($\hbar = 1$) [33]:

$$i\frac{d}{dt}|\psi_t >= H|\psi_t > . \tag{3.1}$$

For conservative systems (which we shall always be considering) the Hamiltonian H is independent of t and the general solution of the Schrödinger equation has the form:

$$|\psi_t >= U(t)|\psi >= e^{-iHt}|\psi > . \tag{3.2}$$

It follows from a basic theorem on linear operators that, since H is selfadjoint, the evolution operator $U(t)$ is unitary (Jordan [95]). The evolution operator maps the state vector for time zero (that is, $|\psi >$) onto the corresponding vector for time t.
The description of quantum scattering closely parallels the classical formalism. In lieu of the classical orbit x(t) satisfying Newton's equation, we now have a state vector $|\psi_t >$ satisfying the time-dependent Schrödinger equation (3.1). $|\psi_t >$ is any vector in the appropriate Hilbert space $\mathcal{H}$.We shall adopt the classical terminology and refer to the solution $U(t)|\psi >$ as an *orbit*, although of course it is no longer an orbit in real space R^3. Every orbit $U(t)|\psi >$ can be uniquely identified by the fixed vector $|\psi >$, which is just the state vector at the instant $t = 0$.
We are considering a single spinless particle in a fixed local potential. Let us suppose that the orbit $U(t)|\psi >$ describes the evolution of some scattering experiment. This means that when followed back to a time well before the collision $U(t)|\psi >$ represents a wave packet that is localized far away from the scattering center and, therefore, behaves like a $free$ wave packet. Now, the motion of a free particle is given by the free evolution operator

$$U^0(t) = e^{-iH^0 t} \tag{3.3}$$

and we therefore expect that as $t \to -\infty$,

$$U(t)|\psi> \to_{t\to-\infty} U^0(t)|\psi_{in}> \tag{3.4}$$

for some vector $|\psi_{in}>$. The limit (3.4) simply means that the difference of the two vectors tends to zero and, hence, that the actual state $U(t)|\psi>$ becomes experimentally indistinguishable from the freely evolving state $U^0(t)|\psi_{in}>$. Similarly, after the collision the particle moves away again and we expect that

$$U(t)|\psi> \to_{t\to+\infty} U^0(t)|\psi_{out}> \tag{3.5}$$

for some $|\psi_{out}>$. These two limits are analogous to the classical limits, and in analogy with the classical terminology we shall call the asymptotic free orbits of (3.4) and (3.5) the in and out asymptotes of the actual orbit $U(t)|\psi>$. It is convenient to label the quantum asymptotes (3.4) and (3.5) by the fixed vectors $|\psi_{in}>$ and $|\psi_{out}>$. We do not expect that every orbit $U(t)|\psi>$ will have asymptotes. We expect rather that there will be certain scattering orbits that do have asymptotes, and that the scattering states together with the bound states will span the space $\mathcal{H}$ of *all* states.
Every vector in $\mathcal{H}$ (labelled $|\psi_{in}>$ or $|\psi_{out}>$) does represent the asymptote of some actual orbit; that is, for every vector $|\psi_{in}>$ in $\mathcal{H}$ there is a solution $U(t)|\psi>$ of the Schrödinger equation that is asymptotic to the free orbit $U^0(t)|\psi_{in}>$ as $t \to -\infty$; and likewise for every $|\psi_{out}>$ as $t \to +\infty$. This result is known as the asymptotic condition. If the potential $V(r)$ falls off fast enough (for $r \to \infty$), then for every $|\psi_{in}>$ in $\mathcal{H}$ there is a $|\psi>$ such that

$$U(t)|\psi> - U^0(t)|\psi_{in}> \to_{t\to-\infty} 0 \tag{3.6}$$

and likewise for every $|\psi_{out}>$ in $\mathcal{H}$ as $t \to +\infty$.
The asymptotic condition guarantees that any $|\psi_{in}>$ in $\mathcal{H}$ is in fact the in asymptote of some actual orbit $U(t)|\psi>$. The actual state $|\psi>$ of the system at $t = 0$ is linearly related to the in asymptote $|\psi_{in}>$; specifically,

$$|\psi> = \lim_{t\to-\infty} U(t)^\dagger U^0(t)|\psi_{in}> \equiv \Omega_+|\psi_{in}> . \tag{3.7}$$

Similarly the actual state $|\psi>$ at $t = 0$ that will evolve into the out asymptote labelled by $|\psi_{out}>$ is

$$|\psi> = \lim_{t\to+\infty} U(t)^\dagger U^0(t)|\psi_{out}> \equiv \Omega_-|\psi_{out}> . \tag{3.8}$$

The two operators $\Omega_\pm$, defined as the limits

$$\Omega_\pm = \lim_{t\to\mp\infty} U(t)^\dagger U^0(t) \tag{3.9}$$

are called the Møller wave operators. They are the limits of a unitary operator and so are isometric. Acting on any vector in $\mathcal{H}$, they give the actual state at

$t = 0$ that would evolve from (or to) the asymptote represented by that vector. It is usual and convenient to introduce the following additional notation:

$$\Omega_+|\phi> \equiv |\phi^+> \qquad [\text{any}|\phi>] \tag{3.10}$$

and

$$\Omega_-|\chi> \equiv |\chi^-> \qquad [\text{any}|\chi>] \tag{3.11}$$

The vector $|\phi^+>$ represents the actual state of the system at $t = 0$, if the in asymptote was $|\psi_{in}> = |\phi>$; the vector $|\chi^->$ represents the actual state at $t = 0$ if the out asymptote were going to be $|\psi_{out}> = |\chi>$.
The various notations can be summarised as follows:

$$\begin{array}{ccccc} \text{in asymptote} & \stackrel{\Omega_+}{\rightarrow} & \left\{ \begin{array}{c}\text{actual state} \\ \text{at } t=0\end{array} \right\} & \stackrel{\Omega_-}{\leftarrow} & \text{out asymptote} \\ |\psi_{in}> & \rightarrow & |\psi> & \leftarrow & |\psi_{out}> \\ |\phi> & \rightarrow & |\phi^+> & & \\ & & |\chi^-> & \leftarrow & |\chi> \end{array} \tag{3.12}$$

Every $|\psi_{in}>$ (or($|\psi_{out}>$) in $\mathcal{H}$ labels the in (or out) asymptote of a unique orbit $U(t)|\psi_{out}>$ and the Møller operators $\Omega_\pm$ map reach $|\psi_{in}>$ (or $|\psi_{out}>$) in $\mathcal{H}$ onto the corresponding scattering state $|\psi>$ in $\mathcal{R}$.
The Scattering Operator: So far we have expressed the actual scattering state at t = 0 in terms of either of its two asymptotes. Our ultimate goal is to express the out asymptote in terms of the in asymptote without reference to the experimentally uninteresting actual orbit. Because Ω_- is isometric, the relation $|\psi> = \Omega_-|\psi_{out}>$ can be inverted. In fact, since $\Omega_-^\dagger \Omega_- = 1$, we simply multiply on the left by $\Omega_-^\dagger$ to give

$$|\psi_{out}> = \Omega_-^\dagger|\psi> = \Omega_-^\dagger \Omega_+|\psi_{in}> . \tag{3.13}$$

If we define the scattering operator as

$$S = \Omega_-^\dagger \Omega_+ \tag{3.14}$$

this equation becomes

$$|\psi_{out}> = S|\psi_{in}> \tag{3.15}$$

which is the desired result.
The scattering operator S gives $|\psi_{out}>$ directly in terms of $|\psi_{in}>$; if a particle enters the collision with in asymptote $|\psi_{in}>$, then it leaves with out asymptote $|\psi_{out}> = S|\psi_{in}>$. Since only the asymptotic free motion is observable in practice, the single operator S contains all information of experimental interest. If we know how to calculate S, then the scattering problem is solved.
In terms of S we can calculate the experimentally relevant scattering probabilities. The particle emerges from the accelerator moving freely along the in asymptote $U^0(t)|\psi_{in}>$ where $|\psi_{in}> = |\phi>$ (for instance) is characteristic of the accelerator. The experimental counter arrangement monitors for some definite out asymptote, given by $|\psi_{out}> = |\chi>$, say. The quantity of interest

is therefore the probability that a particle that entered the collision with in asymptote $|\phi>$ will be observed to emerge with out asymptote $|\chi>$. To evaluate this probability we note that the actual state at $t=0$, which will evolve from the in asymptote $|\phi>$ is $|\phi^+>=\Omega_+|\phi>$, while the actual state at $t=0$, which would evolve into the out asymptote $|\chi>$ is $|\chi^->=\Omega_-|\chi>$. Because the required probability amplitude is just the scalar product of the actual states at any given time ($t=0$, for instance), we find that the probability is:

$$P(\chi \leftarrow \phi) = |<\chi^-|\phi^+>|^2 \tag{3.16}$$

$$= |<\chi\Omega_-^\dagger\Omega_+\phi>|^2 \tag{3.17}$$

$$= |<\chi|S|\phi>|^2 \tag{3.18}$$

The probability amplitude for the process $(\chi \leftarrow \phi)$ is just the S-matrix element $<\chi|S|\phi>$.
In practice even the quantity $P(\chi \leftarrow \phi)$ is not directly observable; this is because one cannot actually produce or identify uniquely defined wave packets $|\phi>$ and $|\chi>$. However the quantity that is experimentally observable, the differential cross-section, can be expressed directly in terms of the matrix elements of S.

4. Coordinate systems: collinear, planar, 3D, reduced degrees of freedom

4.1 Introduction

For the description of the nuclear dynamics all coordinate systems are physically equivalent. The typical picture of the potential in the different coordinate systems can look differently. For a triatomic molecule ABC the positions of the three atoms in the plane are defined by six coordinates: the three internal coordinates ($\mathrm{R}_{\text{A-B}}$, $\mathrm{R}_{\text{A-C}}$ and $\mathrm{R}_{\text{B-C}}$) (Fig. 4.1) and the three Euler angles of a space-fixed coordinate system. The potential energy depends on the internal coordinates: $V=V(\mathrm{R}_{\text{A-B}}, \mathrm{R}_{\text{A-C}}, \mathrm{R}_{\text{B-C}})$. If only the collinear configuration is of interest, the potential depends only on $\mathrm{R}_{\text{A-BC}}$(or $\mathrm{R}_{\text{A-B}}$)

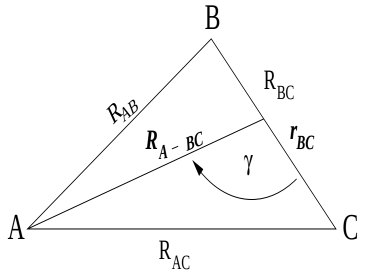

Fig. 4.1. Atomic distances $\mathrm{R}_{\text{A-B}}$, $\mathrm{R}_{\text{A-C}}$, $\mathrm{R}_{\text{B-C}}$ and Jacobi coordinates $R_{\text{A-BC}}$, r_{BC}, γ of the triatomic system ABC. $R_{\text{A-BC}}$ is the distance between the atom A and the center-of-mass of the molecule BC.

and $R_{B\text{-}C}$. A representation of the potential $V(R_{A\text{-}BC}, R_{B\text{-}C})$ is given in Fig. 4.2a.
In reactive scattering in principle one needs coordinates which are convenient in describing reactant and product arrangements simultaneously and which have the correct asymptotic behaviour that leads not to a coupling by the kinetic energy for the separated fragments (e.g. atom and diatom). But, there is not such a unique coordinate system and so one has to make a compromise between practicability, numerical efficiency and physical insight and interpretation of the reaction dynamics.

Which coordinate system for which quantum reactive procedure?
In the review of Manolopolous and Clary [14] the different quantum reactive procedures are classified by the used coordinate systems.

In the next subsection we give a short introduction into the most popular coordinate systems.

4.2 Jacobi coordinates

If one changes the coordinates in case of a collinear configuration in such a form that the kinetic energy operator T becomes "simpler" (i.e. no mixed derivatives), i.e. using Jacobi-coordinates or mass-scaled Jacobi-coordinates (see Fig. 4.1),

$$\begin{aligned} R_{A-BC} &= R_{AB} + [m_C/(m_B+m_C)]R_{BC} \\ r_{BC} &= \sqrt{\frac{m_{BC}}{m}} R_{BC} \qquad (4.1) \\ m &= \frac{m_A(m_B+m_C)}{(m_A+m_B+m_C)} \end{aligned}$$

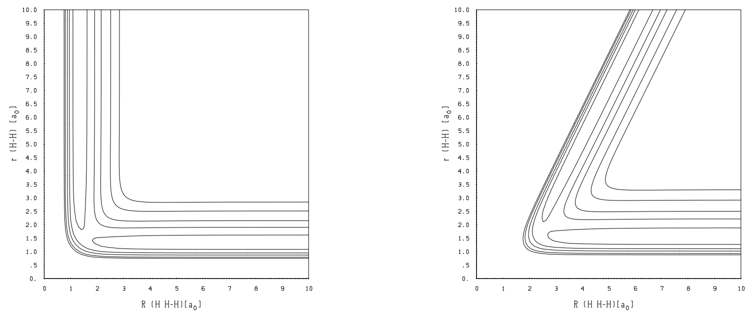

Fig. 4.2. Contour lines (0.35- 3.0 [eV]) for the $H+H_2$ Porter-Karplus potential: (a) internal coordinates (R_{AB}, R_{BC}), (b) mass-weighted Jacobi coordinates (R_{A-BC}, r_{BC})

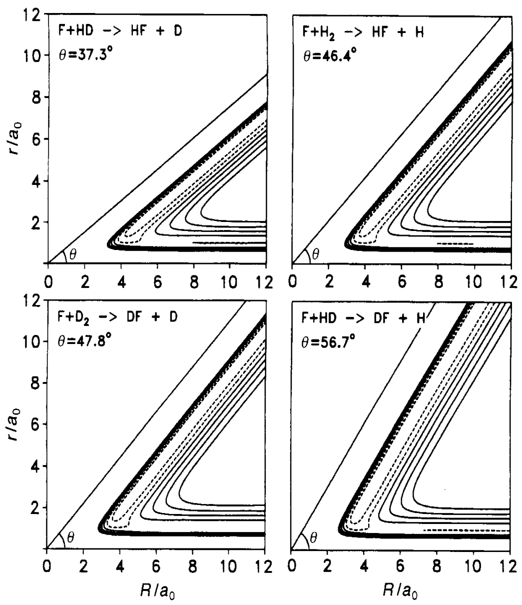

Fig. 4.3. Collinear potential-energy contours and kinematic skewing angles for the four deuterium-substituted isotopomers of the F + H_2 reactions. (Reprinted, by permission, from J. F. Castillo, D. E. Manolopolous, Faraday Discuss. **110** 119, 1998. Copyright 1998 by Royal Society of Chemistry.)

$$m_{BC} \;=\; \frac{m_B m_C}{(m_B + m_C).} \tag{4.2}$$

$$T = -\frac{\hbar^2}{2m}\left(\frac{\partial^2}{\partial R^2_{A-BC}} + \frac{\partial^2}{\partial r^2_{BC}}\right). \tag{4.3}$$

The representation of the potential changes (see Fig. 4.2b) with the skewing angle φ_α depending on the masses of the atoms:

$$\varphi_\alpha = \arctan[m_B(m_A + m_B + m_C)/(m_A m_B)]^{1/2}. \tag{4.4}$$

The skewing angle is for such systems large (maximum 90^o) when $m_B >> m_A, m_C$ and small (minimum 0^o) when $m_B << m_A, m_C$. In case of equal masses (H+H_2) the value for the skewing angle is 60^o. The effect of changing translational energy of the reactants into vibrational energy for the products can be easily explained with the pictures of potential energy surface in skewed coordinates. If the skewing angle becomes very small, calculations can become problematic [100]. In the case of I+HI the skewing angle is 7^o and mass-weighted Jacobi coordinates are not optimal. In such cases hyperspherical coordinates are appropriate [101]. Different representations for the collinear configuration of FHD are given in Fig. 4.3. More detailed information is given in a later section.

4.2.1 Reactant and product coordinates. If one is not fixed on collinear configurations one has three independent sets of Jacobi-coodinates: A + BC (R_α, r_α), AB + C (R_β, r_β) and AC + B (R_γ, r_γ). R_α is the distance of the center of mass of diatom BC and r_α the distance in BC. With $\mathbf{x}_i$ and m_i (i=1,2,3 or A,B,C) the positions and masses of three particles, the centre of mass is

$$\mathbf{X} = \sum_{i=1}^{3} m_i \mathbf{x}_i / M \tag{4.5}$$

and the three types of mass normalised Jacobi coordinates are given as

$$\mathbf{r}_k = (\mathbf{x}_j - \mathbf{x}_i)/d_k \tag{4.6}$$

$$\mathbf{R}_k = d_k[\mathbf{x}_k - \frac{m_i \mathbf{x}_i + m_j \mathbf{x}_j}{m_i + m_j}], \tag{4.7}$$

with the total mass M and the scaling parameters d_k

$$M = \sum_{i=1}^{3} m_i, \quad d_k = \sqrt{(1 - m_k/M) m_k/\mu} \tag{4.8}$$

and the reduced mass

$$\mu = \sqrt{m_1 m_2 m_3 / M}, \tag{4.9}$$

where (i, j, k) is a cyclic permutation of $(1, 2, 3)$.
The relation of all different coordinate configurations (α, β, γ) is given in Fig. 4.4. The transformation between the mass-weighted coordinates [103] in configuration α (reactant coordinate) and configuration β (product coordinate) is given as:

$$\begin{pmatrix} \mathbf{R}_\beta \\ \mathbf{r}_\beta \end{pmatrix} = \begin{pmatrix} -\sqrt{\frac{m_A m_C}{(m_A+m_B)(m_C+m_B)}} & -\sqrt{\frac{m_B(m_A+m_B+m_C)}{(m_A+m_B)(m_C+m_B)}} \\ \sqrt{\frac{m_B(m_A+m_B+m_C)}{(m_A+m_B)(m_C+m_B)}} & -\sqrt{\frac{m_A m_C}{(m_A+m_B)(m_C+m_B)}} \end{pmatrix} \begin{pmatrix} \mathbf{R}_\alpha \\ \mathbf{r}_\alpha \end{pmatrix} \tag{4.10}$$

or

$$\begin{pmatrix} \mathbf{R}_\beta \\ \mathbf{r}_\beta \end{pmatrix} = \begin{pmatrix} \cos\phi_{\alpha\beta} & -\sin\phi_{\alpha\beta} \\ \sin\phi_{\alpha\beta} & \cos\phi_{\alpha\beta} \end{pmatrix} \begin{pmatrix} \mathbf{R}_\alpha \\ \mathbf{r}_\alpha \end{pmatrix}. \tag{4.11}$$

The skewing angle $\phi_{\alpha\beta}$ lies between π and $\pi/2$. More detailed information is given in a later section.

4.3 Hyperspherical coordinates

There are many different ways of defining hyperspherical coordinates, which in the case of a collinear atom-diatom reaction are polar coordinates. The collinear Delves [104] coordinates are defined in terms of the mass-scaled Jacobi vectors of the reactant arrangement a(A + BC) as

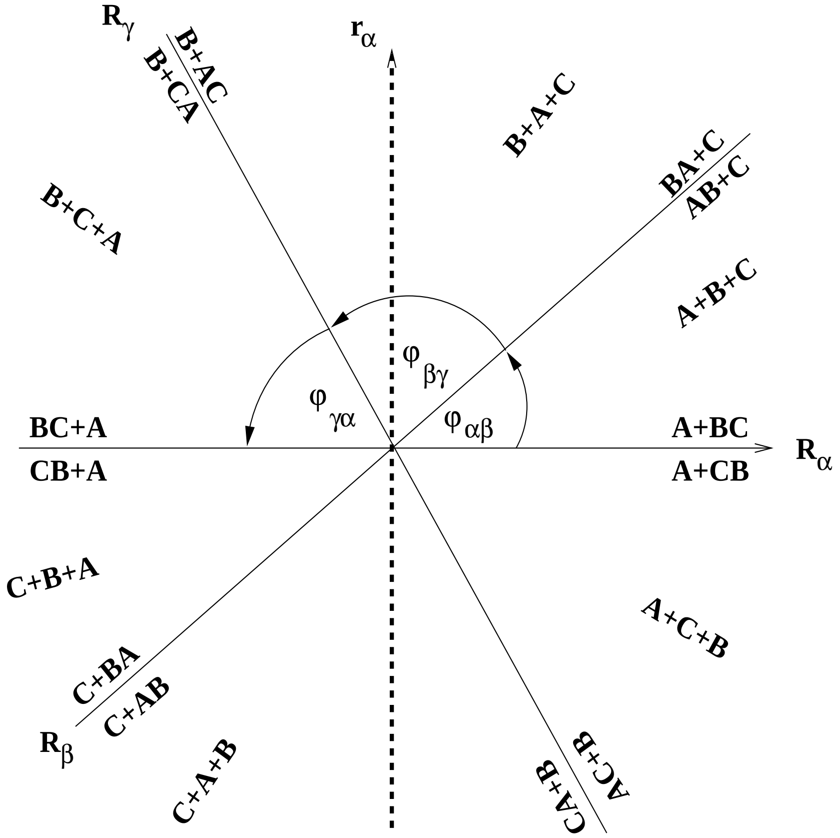

Fig. 4.4. Configuration space of a triatomic system ABC with the arrangements α, β, γ. (Adapted, from Launay, J.M.: *Dynamical Processes in Molecular Physics*, Delgado-Barrio, G. (Ed.) (Institute of Physics Publishing, Bristol and Philadelphia, 1991)

$$\rho = \sqrt{R_a^2 + r_a^2} \tag{4.12}$$

and

$$\theta_a = \tan^{-1}(r_a/R_a) \tag{4.13}$$

where R_a is a mass-scaled distance between A and the centre-of-mass of BC and r_a is a mass-scaled distance between B and C. The hyperradius ρ in (4.12) is universal, in the sense that it can equally well be defined in terms of mass-scaled Jacobi vectors of the product arrangement c(AB+C). However the Delves hyperangle θ_a is a function of the arrangement for which it is defined. In fact the reactant hyperangle θ_a and the product hyperangle θ_c are related by $\theta_a + \theta_c = \theta_{ac}$, where

$$\theta_{ac} = \tan^{-1}(m_B/\mu) \tag{4.14}$$

with

$$\mu = (\frac{m_C m_B m_C}{m_a + m_B + m_C})^{1/2} \tag{4.15}$$

the skewing angle shown in Fig. 1.2c.

To begin with, one invariably solves the Schrödinger equation in hyperspherical coordinates in two distinct steps. The bound θ_a motion is solved first, at the centres of a number of different 'sectors' in the hyperradial coordinate ρ. This gives a set of 'surface' eigenfunctions and eigenvalues within each sector, which are then substituted back into the Schrödinger equation to leave a system of coupled second order linear differential equations in ρ. These 'close-coupled' equations have exactly, the same form as those encountered in inelastic scattering, and so can be solved using well known, and highly efficient, numerical techniques [19].

Unfortunately, however, the surface eigenfunctions and eigenvalues are themselves often quite difficult to obtain. The fundamental reason for this, which should be clear from Fig. 1.2c, is that the reactant and product arrangement channels are confined to smaller and smaller regions of the available hyperangular (θ_a) space as ρ increases. This unavoidable feature of hyperspherical coordinates, which is exacerbated in 3D, makes it difficult to devise numerical methods for solving the surface eigenproblem that work equally well for all required values of ρ. However, some progress has been made in this direction in recent years.

Two final comments on the hyperspherical coordinate approach: (a) the solution of the surface eigenvalue problem is completely independent of the scattering energy E. Once this eigenvalue problem has been solved all that remains is to call a standard close-coupled equation solver at each energy required [19]. Since this is comparatively straightforward, calculations can be performed on a tight energy grid, which greatly facilitates the analysis of narrow scattering resonances due to short-lived meta-stable states [105]. (b) the hyperspherical coordinates may well be the only practical approach to certain physical regimes. In particular heavy-light-heavy reactions, which have a small skewing angle θ_{ac} and collision induced dissociation, which occurs between the two arrangement channel regions in Fig. 1.2c are both much more difficult to study using any other approach.

While the collinear Delves hyperspherical coordinates are essentially unique, several different possibilities arise when one moves to 3D for triatomics. A highly detailed account of these possibilities is given in the introductory section of the work of Pack and Parker [46].

A recent overview of the "hyperspherical view" about dynamics on reactive potential energy surfaces is given by Aquilanti et al [106]. Hyperspherical coordinates in four-atom systems is discussed by Clary and Echave [107] and Kuppermann [108].

For reactive scattering Johnson [?], Pack and Parker [46], Linderberg [35] and Hinze and Wolniewicz [?] have chosen so-called "democratic" hyperspherical coordinates. These coordinates differ from other coordinates (Fock, Launay and LePetit citelaunayr15), that all channels can be treated equally. The coordinates that Kuppermann [123] has chosen, are not so optimal for treating the Pauli-principle for identical nuclei. The hyperspherical coordinates are chosen such that the Euler angles α, β and γ define the orientation of the body-fixed frame, with the z-axis pointing in the direction of the vector product

$$\mathbf{A} = \frac{1}{2}(\mathbf{r} \times \mathbf{R}). \tag{4.16}$$

The remaining internal coordinates ρ, θ and ϕ are given as

$$\rho^2 = |\mathbf{r}| + |\mathbf{R}| \tag{4.17}$$

$$\cos\theta = 4|\mathbf{A}|/\rho^2 \tag{4.18}$$

and

$$\cos\phi_k = 2(\mathbf{r}_k \cdot \mathbf{R}_k)/(\rho^2 \sin\theta), \tag{4.19}$$

where only ϕ depends on k the index of the particular set of Jacobi coordinates. The different sets of Jacobi coordinates are connected via kinematic rotations, i.e. different origins for the angle ϕ. The distance between the particles is obtained as

$$|\mathbf{x}_j - \mathbf{x}_i| = d_k\rho[1 + \sin\theta\sin\phi_k]^{\frac{1}{2}}, \quad d_k = \sqrt{(1 - m_k/M)m_k/\mu} \tag{4.20}$$

$$\mu = m_1 m_2 m_3/M, M = m_1 + m_2 + m_3. \tag{4.21}$$

The volume element in these coordinates is

$$d^6v = \frac{1}{8}\rho^5 d\rho \sin\theta\cos\theta d\theta d\phi d\omega \tag{4.22}$$

with

$$d\omega = d\alpha \sin\beta d\beta d\gamma \tag{4.23}$$

and the range of the coordinates is

$$\begin{aligned} &0 \le \rho \le \infty, 0 \le \theta \le \frac{\pi}{2}, 0 \le \phi \le 4\pi, \\ &0 \le \alpha \le 2\pi, 0 \le \beta \le \pi, 0 \le \gamma \le 2\pi. \end{aligned} \tag{4.24}$$

Pack, Parker and coworkers [46] use a combination of different coordinates for different interaction regions: (a) adiabatically adjusting principal-axis hyperspherical (APH) coordinates for the strong interaction region and Delves hyperspherical coordinates outside the APH-region, where there is strong coupling within each arrangement channel, but negligible coupling between the arrangement channel. Just beyond the Delves region one has the Jacobi

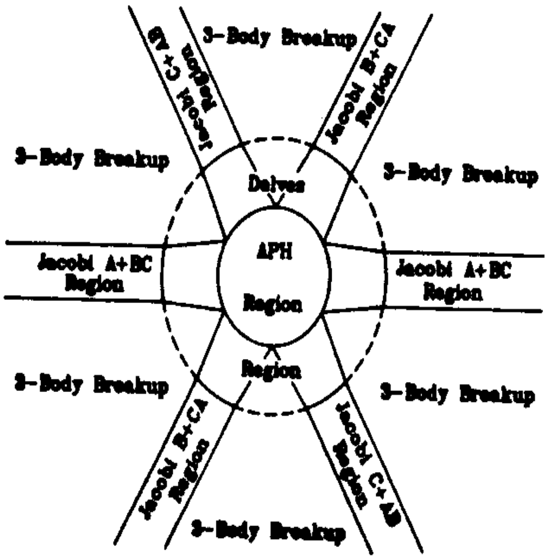

Fig. 4.5. Schematic showing the two hyperspherical regions (APH and Delves) and the Jacobi region. There are six arrangement channels as a result of covering the configuration space twice. (Reprinted, by permission, from Pack, R.T., Parker, G.A.: *J. Chem. Phys.* **87** (1987) 3888. Copyright 1987 by the American Institute of Physics.)

region where the coupling within each arrangement channel varies from moderate to zero.
Definitions by Pack, Parker and coworkers [46]: Six mass scaled Jacobi coordinate components (S_τ,$\widehat{S}_\tau$,s_τ,$\widehat{s}_\tau$) are the space-fixed (SF) Jacobi coordinates, whereas the coordinates (S_τ, s_τ, Θ_τ, α_τ, β_τ, γ_τ) are the body-fixed (BF) Jacobi coordinates. The angles $\widehat{S}_\tau$ and $\widehat{s}_\tau$ are the two sets of polar and azimuthal angles associated with the vectors $\mathbf{S}_\tau$ and $\mathbf{s}_\tau$ respectively, and the angle between these vectors is

$$\Theta_\tau = \cos^{-1}[\frac{\mathbf{S}_\tau \cdot \mathbf{s}_\tau}{\mathbf{S}_\tau \ \mathbf{s}_\tau}]. \tag{4.25}$$

The three Euler angles $(\alpha_\tau, \beta_\tau, \gamma_\tau)$ of the BF system are usually chosen to orient the body-fixed z-axis along $\mathbf{S}_\tau$ or $\mathbf{s}_\tau$ depending on the relative masses of the particles involved. Delves hyperspherical coordinates for arrangement τ are (see Fig. [?]):

$$\rho = (S_\tau^2 + s_\tau^2)^{\frac{1}{2}} \tag{4.26}$$

and

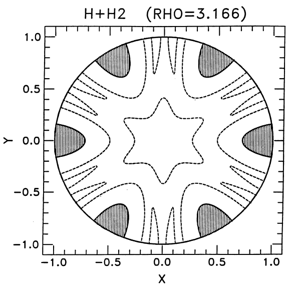

Fig. 4.6. Stereographic projection of a contour plot of the H_3 PES at ρ=3.166 a_0

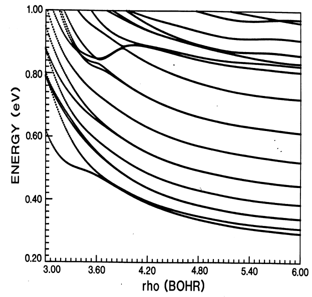

Fig. 4.7. Surface function eigenvalues vs ρ for H_3 for $J = \Lambda = p = 0$ and even j_i. (Reprinted, by permission, from Pack, R.T., Parker, G.A.: *J. Chem. Phys.* **87** (1987) 3888. Copyright 1987 by the American Institute of Physics.)

$$\theta_{D\tau} = \tan^{-1}(\frac{s_\tau}{S_\tau}). \tag{4.27}$$

In addition to ρ and $\theta_{D\tau}$, the four SF or four BF angles of the arrangement complete the Delves coordinate set.
APH coordinates (see Fig. [?]):

$$\rho = (S_\tau^2 + s_\tau^2)^{\frac{1}{2}} \tag{4.28}$$

$$\tan\theta = \frac{[(S_\tau^2 - s_\tau^2)^2 + (2\mathbf{S}_\tau \cdot \mathbf{s}_\tau)^\mathbf{2}]^{\frac{1}{2}}}{\mathbf{2S}_\tau \mathbf{s}_\tau \sin\Theta_\tau} \tag{4.29}$$

$$\sin(2\chi_\tau) = \frac{2\mathbf{S}_\tau \cdot \mathbf{s}_\tau}{[(\mathbf{S}_\tau^\mathbf{2} - \mathbf{s}_\tau^\mathbf{2})^\mathbf{2} + (\mathbf{2S}_\tau \cdot \mathbf{s}_\tau)^\mathbf{2}]^{\frac{1}{2}}} \tag{4.30}$$

$$\cos(2\chi_\tau) = \frac{(S_\tau^2 - s_\tau^2)^2}{[(S_\tau^2 - s_\tau^2)^2 + (2\mathbf{S}_\tau \cdot \mathbf{s}_\tau)^\mathbf{2}]^{\frac{1}{2}}}. \tag{4.31}$$

To complete the APH coordinate specification one chooses the Euler angles $(\alpha_\tau, \beta_\tau, \gamma_\tau)$ to orient the body-fixed z-axis along the smallest principal moment of inertia. These coordinates minimize the Coriolis coupling for reactions that are collinearly dominated. A contour plot for the H_3 potential energy surface and the lowest surface function eigenvalues in hyperspherical

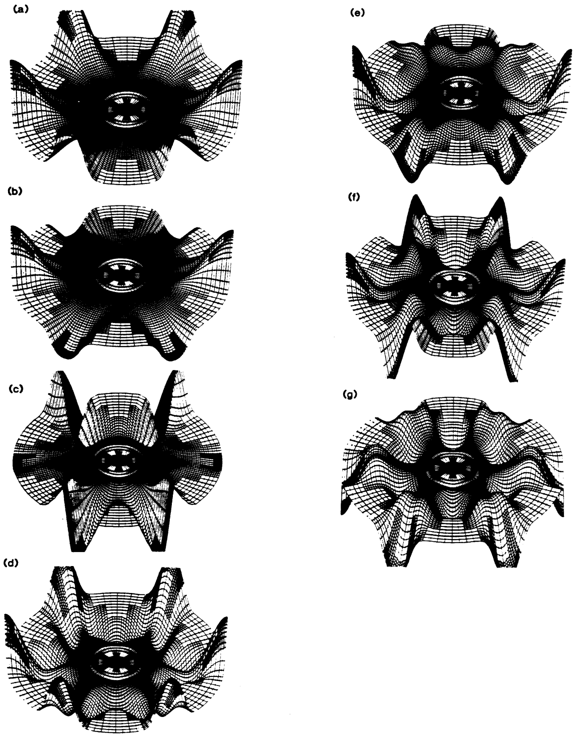

Fig. 4.8. Perspective plots of the first 7 surface eigenfunctions Φ_{t0}^{00} at ρ=3.166 a_0 for H_3. (Reprinted, by permission, from Pack, R.T., Parker, G.A.: *J. Chem. Phys.* **87** (1987) 3888. Copyright 1987 by the American Institute of Physics.)

coordinates are given in Fig. [?] and perspective plots of the first 7 surface eigenfunctions for H_3 are presented in Fig. [?].

4.4 Natural coordinates

In the earliest "exact" 3D quantum reactive scattering calculations for H + H_2 of Kuppermann and Schatz [11, 110, 111], Elkowitz and Wyatt [112] and Walker, Stechel and Light [113] extensions of the 'natural collision coordinates', introduced by Marcus [114], have been used. For the simple case of a collinear atom-diatom reaction the natural collision coordinates swung smoothly from the reactants, A + BC, to the products, AB + C, as shown in Fig. 1.2b. Here s is the 'translational' coordinate, which asymptotically describes a mass-scaled separation between the atom, A or C, and the diatom, BC or AB. It is along this coordinate, from minus infinity to plus infinity, that the reaction actually proceeds. Similarly the 'vibrational' coordinate u asymptotically describes a mass-scaled separation of the two atoms in the diatomic, BC or AB. The vibrational transitions that occur during the course

of the reaction are easily rationalized in terms of coupling between the nuclear motions along a and u, one convenient model of which is based simply on the curvature of the reaction path [115].
This easy physical interpretation of natural collision coordinates, combined with the fact that the translational motion along the reaction path can be solved using essentially standard inelastic scattering techniques [116, 117], led to the success of the early H + p-H_2 $\rightarrow$ o-H_2 + H calculations and appeared to bode wellh for future applications of the approach [118]. Unfortunately, attempts to generalize methods based on these coordinates beyond the simplest 3D reaction soon ran into technical difficulties which seemed impossible to overcome. These difficulties are not immediately apparent in the simple collinear model of Fig. 1.2b, but the following two observations should at least give the general idea:
(a) For an A + BC atom-diatom reaction in 3D, at each value of the conserved total angular momentum quantum number J, the vibrational coordinate u in Fig. 1.2b becomes a 2D (rovibrational) surface in the 3D internal coordinate space which specifies the size and shape of the three-atom triangle. This surface typically has quite complicated metric properties [119], which in turn lead to lengthy algebra in the development of any new numerical approach.
(b) In general a third (B + CA) arrangement must also be considered in 3D, and this makes the idea of a translational 'reaction coordinate' somewhat more difficult to grasp. In practice one can avoid the problem by introducing 'matching surfaces' between the three arrangements, but this is a great deal easier to do for the symmetric H + H_2 reaction than it is for anything else.
Light and coworkers had these tremendous technical difficulties finally been overcome. Webster and Light describe in their papers complete and general 3D atom-diatom reactive scattering methodology [120] and apply it to the calculation of $J = 0$ reaction probabilities for the seven deuterium substituted isotopomers of H + H_2 $\rightarrow$ H_2 + H [121]. Although these calculations were quite successful, the difficulties associated with natural collision coordinates have still tended to direct recent research towards more convenient coordinate schemes.

4.5 Coordinates used in the 'early' H + H_2 calculations

4.5.1 Collinear triatomic reaction coordinates. Now we want to be more specific (the next section is taken as an extraction from Kuppermann [10]). Let r'_α be the BC internuclear distance and R'_α the distance between A and the center of mass G_{BC} of BC. These coordinates (the prime (') stands for: unscaled, non-mass weighted) are convenient for the description of the A + BC reagents. Similarly, let r'_γ be the AB internuclear distance and R'_γ the distance of C to the center of mass G_{AB} of AB, coordinates which are useful for the description of the final state of the products. These two sets of coordinates are depicted in Fig. 4.9a. Equipotential curves for a representative potential energy function (surface) V are depicted in Fig. 4.9b in terms of the α coordinates. This function is obtained by solving the electronic motion problem in three dimensions for all (R'_α, r'_α) collinear ABC configurations. Its central characteristic is that it displays a line of steepest ascents and descents, the minimum energy path depicted by the dashed line in Fig. 4.9b. Along lines orthogonal to that path, the potential function increases in both directions, portraying a behavior similar to that of a diatomic molecule. This is true everywhere along the minimum energy path, including the saddle point, denoted in that Fig. 4.9b by a cross. It is this basic property that suggests methods for solving the dynamic problem. Physically, the reaction consists of (quantum mechanical) motion of the system from the reagent region of the R'_α, r'_α configuration space, denoted by A + BC in Fig. 4.9b, to the product region, denoted by AB + C. The energy of the system is assumed to be significantly below the dissociative plateau region, denoted by A + B + C, so that the region of configuration space sampled by the scattering wave function is limited to the relatively narrow, curved gully, identified by the hatching in Fig. 4.9b, and located between the repulsive walls of the surface corresponding to small values of r'_α and/or r'_γ (for compressed configurations) and large values of these variables (for stretched configurations). The line in Fig. 4.9a that passes through the origin and makes an angle θ' with the R'_α axis is the one for which $r'_\gamma = 0$, i.e., for which A coincides with B. The potential along that line, as well as along the R'_α axis, for which $r'_\alpha = 0$ and C coincides with B, is quite large and can be taken to be infinite for the present purposes. This leads to the nonpenetrability of B by either A or C, and the relative ordering of the three atoms along the fixed straight line to which they are confined is maintained throughout their motion. The angle θ', in the range $\pi/4$ to $\pi/2$, is given by

$$\theta' = \tan^{-1}[1 + m_B/m_C] \tag{4.32}$$

and is introduced for comparison purposes with the dynamically important angle θ to be considered in Fig. 4.10 and (4.40).
If one neglects spin interactions, which are very small compared with the other energies being considered, the nuclear motion Hamiltonian, after removal of the motion of the center of mass of the system, can be written in terms of either α or γ coordinates as

$$\begin{aligned} H = & -\frac{\hbar^2}{2\mu_{A,BC}}\frac{\partial^2}{\partial {R'_\alpha}^2} - \frac{\hbar^2}{2\mu_{BC}}\frac{\partial^2}{\partial {r'_\alpha}^2} + V_\alpha(R'_\alpha, r'_\alpha) \\ = & -\frac{\hbar^2}{2\mu_{C,BA}}\frac{\partial^2}{\partial {R'_\gamma}^2} - \frac{\hbar^2}{2\mu_{BA}}\frac{\partial^2}{\partial {r'_\gamma}^2} + V_\gamma(R'_\gamma, r'_\gamma), \end{aligned} \tag{4.33}$$

where

$$\mu_{A,BC} = \frac{m_A(m_B + m_C)}{m_A + m_B + m_C}, \quad \mu_{BC} = \frac{m_B m_C}{m_B + m_C} \tag{4.34}$$

represent, respectively, the reduced masses of the A + BC and BC systems, similar definitions being valid for $\mu_{C,BA}$ and μ_{BA} with the roles of atoms A and C interchanged. The symbols m$_X$ represent the masses of atoms X (=

A, B, C). The first two terms in each of the two expressions for H given by (4.33) represent, respectively, the kinetic energy of the relative motion of the atom with respect to the center of mass of the diatom, and of the internal diatom vibration.

4.5.2 Scaled coordinates in 2D. A very convenient conceptual and computational simplification can be achieved if we introduce a coordinate scaling that results in the four reduced masses in (4.33) being replaced by a single reduced mass. This can be accomplished by the scaling transformations

$$\begin{aligned} R_\alpha = a_\alpha R'_\alpha \quad r_\alpha = (a_\alpha)^{-1} r'_\alpha \quad a_\alpha = (\mu_{A,BC}/\mu_{BC})^{1/4} \\ R_\gamma = a_\gamma R'_\gamma \quad r_\gamma = (a_\gamma)^{-1} r'_\gamma \quad a_\gamma = (\mu_{C,BA}/\mu_{BA})^{1/4} \end{aligned} \tag{4.35}$$

introduced by Delves [122]. In terms of the scaled coordinates R_α, r_α and R_γ, r_γ, the nuclear motion Hamiltonian becomes

$$\begin{aligned} H = & -\tfrac{\hbar^2}{2\mu}\left(\tfrac{\partial^2}{\partial R_\alpha^2} + \tfrac{\partial^2}{\partial r_\alpha^2}\right) + V_\alpha(R_\alpha, r_\alpha) \\ = & -\tfrac{\hbar^2}{2\mu}\left(\tfrac{\partial^2}{\partial R_\gamma^2} + \tfrac{\partial^2}{\partial r_\gamma^2}\right) + V_\gamma(R_\gamma, r_\gamma). \end{aligned} \tag{4.36}$$

The single reduced mass μ is independent of whether we use α or γ scaled coordinates and is given by the expression

$$\mu = [(m_A m_B m_C)/M]^{1/2}, \quad M = m_A + m_B + m_C, \tag{4.37}$$

where the masses of the three atoms play equivalent roles. Furthermore, the $(R_\alpha, r_\alpha) \rightarrow (r_\gamma, R_\gamma)$ transformation is a 2-MD coordinate-axis rotation in the scaled configuration space:

$$\begin{pmatrix} r_\gamma \\ R_\gamma \end{pmatrix} = \begin{pmatrix} \cos\omega & -\sin\omega \\ \sin\omega & \cos\omega \end{pmatrix} \begin{pmatrix} R_\alpha \\ r_\alpha \end{pmatrix}. \tag{4.38}$$

The clockwise rotation angle ω lies in the $0 - \pi/2$ range and is given by

$$\omega = \tan^{-1}[(m_A m_C)/(m_B M)]^{1/2}. \tag{4.39}$$

In this scaled configuration space the (R_α, r_α) and (r_γ, R_γ) systems of axes are both orthogonal and can be depicted simultaneously, as indicated in Fig. 4.10. Under this rotation, the r_α axis transforms into the R_γ axis, and the R_α into the r_γ. This interchange of the R and r is a peculiarity of the collinear world. The important fact is that, under the $\alpha \rightarrow \gamma$ transformation in the scaled configuration space, the equipotential surface does not change shape; this is not the case for the unscaled (R'_α, r'_α) configuration space.
As a consequence of these properties, the nuclear motion of the ABC triatomic system on a laboratory-fixed straight line is completely isomorphic with that of a single particle of mass μ moving in the 2-MD scaled configuration space and subject to the potential V. In particular, the skew angle θ between the R_α and R_γ axes now has dynamic significance and is given by

$$\theta = \tan^{-1}[(m_B M)/(m_A m_C)]^{1/2}. \tag{4.40}$$

An analogous isomorphism property is valid for general reacting triatomic or even polyatomic systems in the three physical dimensional (3-PD) world. This is a very useful conceptual simplification, since it permits the extension of the ideas developed for single-particle quantum mechanics to multiparticle systems.

4.5.3 3D scaled coordinates. It is convenient to begin by introducing the 3-PD counterpart of the 1-PD scaled coordinates. We label the three atoms $A = A_\alpha$, $B = A_\beta$, and $C = A_\gamma$. Let $\lambda\nu\kappa$ be a cyclic permutation of the indices $\alpha\beta\gamma$. We define the λ coordinates ($\lambda = \alpha, \beta, \gamma$) as $\mathbf{r}'_\lambda$, the internuclear vector from A_ν to A_κ, and $\mathbf{R}'_\lambda$ the position vector of A_λ with respect to the center of mass $G_{A_\nu A_\kappa}$ of the $A_\nu A_\kappa$ diatom. The angle in the 0-π range between these two vectors is labelled γ_λ. These coordinates are displayed in Fig. 4.11. In terms of them, the nuclear motion Hamiltonian H, after removal of the motion of the center of mass of the system, is

$$H = -\frac{\hbar^2}{2\mu_{\lambda,\nu k}}\nabla^2_{\mathbf{R}'_\lambda} - \frac{\hbar^2}{2\mu_{\nu k}}\nabla^2_{\mathbf{r}'_\lambda} + V_\lambda(R'_\lambda, r'_\lambda, \gamma'_\lambda), \tag{4.41}$$

where the reduced masses are analogous to those given by (4.34) and $\nabla^2_{\mathbf{R}'_\lambda}$ and $\nabla^2_{\mathbf{r}'_\lambda}$ are the Laplacian operators with respect to the coordinates $\mathbf{R}'_\lambda$ and $\mathbf{r}'_\lambda$, respectively. The potential energy functions now depends on γ_λ, in addition to R'_λ and r'_λ. We now introduce the scaled position vector coordinates $\mathbf{R}_\lambda$, $\mathbf{r}_\lambda$ as a three dimensional generalization of (4.35):

$$\begin{aligned} \mathbf{R}_\lambda = a_\lambda \mathbf{R}'_\lambda,\ \mathbf{r}_\lambda = (a_\lambda)^{-1}\mathbf{r}'_\lambda, \\ a_\lambda = (\mu_{\lambda,\nu k}/\mu_{\nu k})^{1/4},\ \lambda = \alpha, \beta, \gamma. \end{aligned} \tag{4.42}$$

In terms of these coordinates, (4.41) becomes

$$H = -(\hbar^2/2\mu)(\nabla^2_{\mathbf{R}_\lambda} + \nabla^2_{\mathbf{r}_\lambda}) + V_\lambda(R_\lambda, r_\lambda, \gamma_\lambda). \tag{4.43}$$

The reduced mass μ, which is independent of λ, is the same as that given for the collinear case by (4.34).

The transformation from λ coordinates to ν coordinates is now given by

$$\begin{pmatrix} \mathbf{R}_\nu \\ \mathbf{r}_\nu \end{pmatrix} = \begin{pmatrix} \cos\alpha_{\nu\lambda} & -\sin\alpha_{\nu\lambda} \\ \sin\alpha_{\nu\lambda} & \cos\alpha_{\nu\lambda} \end{pmatrix} \begin{pmatrix} \mathbf{R}_\lambda \\ \mathbf{r}_\lambda \end{pmatrix}, \tag{4.44}$$

where

$$\begin{aligned} \cos\alpha_{\nu\lambda} &= -\{m_\lambda m_\nu/[(m_\lambda + m_k)(m_\nu + m_k)]\}^{1/2} \\ \sin\alpha_{\nu\lambda} &= \{m_k M/[(m_\lambda + m_k)(m_\nu + m_k)]\}^{1/2}. \end{aligned} \tag{4.45}$$

Equations (4.44) and (4.45) represent a rigid rotation in the six-mathematical dimensional (6-MD) configuration space spanned by the Cartesian components of $\mathbf{R}_\lambda$ and $\mathbf{r}_\lambda$. This is not the case for the corresponding transformation of the unscaled coordinates. The Laplacian operators have the property

$$\nabla^2_{\mathbf{R}_\alpha} + \nabla^2_{\mathbf{r}_\alpha} = \nabla^2_{\mathbf{R}_\beta} + \nabla^2_{\mathbf{r}_\beta} = \nabla^2_{\mathbf{R}_\gamma} + \nabla^2_{\mathbf{r}_\gamma} = \nabla^2, \tag{4.46}$$

where ∇^2 is the 6 - MD scaled configuration space Laplacian, which, as for 3-MD, is invariant under rotations. With this notation, (4.43) can be rewritten as

$$H = -(\hbar^2/2\mu)\nabla^2 + V. \tag{4.47}$$

This Hamiltonian describes the motion of a single particle P of mass μ in the 6-MD scaled configuration space subject to the potential V. Therefore, the motion of the three-particle ABC system in 3-PD space is isomorphic to the motion of P in this 6-MD space. This isomorphism permits an extension of the techniques used to treat the quantum mechanics of single particles in 3-PD space to three-particle (or actually, to many-particle) systems.

4.5.4 Potential energy surface mapping in symmetrised hyperspherical coordinates. In order to facilitate an understanding of the nature of the 3-PD reactive scattering problem, it is useful to be able to visualize the spacial characteristics of the potential energy surface $V_\lambda(R_\lambda, r_\lambda, \gamma_\lambda)$. For the collinear case, for which $\gamma_\lambda = \pi$ or 0, these characteristics were displayed in Fig. 4.10, in which contour lines of constant V were depicted in the 2-MD scaled configuration space R_α, r_α. In the present case, the configuration space is six dimensional, but V is a function of three variables only. It would be convenient therefore to display surfaces of constant V in an appropriately chosen 3-MD space in which for every configuration of the three atoms, there would correspond one and one only point Q. Since, for $\gamma_\lambda = \pi$ that space was 2-MD Cartesian, a first attempt would be to consider $R_\lambda, r_\lambda, \gamma_\lambda$ as the cylindrical coordinates of Q, such that for configurations having a constant γ_λ, $V(R_\lambda, r_\lambda, \gamma_\lambda =$ constant) would be represented by contour lines on the $\gamma_\lambda =$ constant half-plane depicted in Fig. 4.12. If that were done, the spherical polar coordinates of the same point Q would be ρ, η_λ and γ_λ, where

$$\rho = (R_\lambda^2 + r_\lambda^2)^{1/2},\ \eta_\lambda = \tan^{-1}(r_\lambda/R_\lambda),\ 0 \le \eta_\lambda \le \pi/2. \tag{4.48}$$

The quantity ρ is invariant with respect to a $\lambda \to \nu$ transformation and is called a hyperradius. These cylindrical and spherical polar coordinates are also displayed in Fig. 4.12. A typical equipotential surface is displayed schematically in Fig. 4.13a, at an energy below the dissociation energy. This mapping suffers from two crucial defects. First, it does not have the basic one-to-one correspondence property between configurations and points Q. Indeed, for collinear configurations in which A_λ coincides with the center of mass of $A_\gamma A_\kappa$, γ_λ is arbitrary. Therefore, all points on the circle C on the $X_\lambda Y_\lambda$ plane, whose radius is the scaled $A_\nu A_\kappa$ distance, are associated with that single configuration. Second, even if the three atoms A_λ, A_ν and A_κ are identical, as for the H_3 system, the equipotentials of V below the dissociation energy would still have the general shape indicated in Fig. 4.13a, with the shape of the $A_\lambda + A_\nu A_\kappa$ region (in which A_λ is not too far from $A_\nu A_\kappa$) distinct from the shape of the $A_\nu + A_\kappa A_\lambda$ region obtained by an interchange of atoms A_λ and A_ν. In other words, the equipotentials of V, in this map, do not have the symmetry we would desire with respect to the interchange of identical atoms.

A way to eliminate the first of these defects is to choose for the spherical polar coordinates the quantities ρ, $\omega_k = 2\eta_k$ and γ_k as indicated in Fig. 4.12 by point P. This "umbrella opening" transformation on $\rho, \eta_\lambda, \gamma_\lambda$ (in which the colatitudinal angle of every point is doubled) collapses the circles C of Fig. 4.12 into a single point located on the negative half of the Z_λ axis (see Fig. 4.13b). It turns out that in this same $\rho, \omega_\lambda, \gamma_\lambda$ system of polar coordinates, the equipotential surfaces are also symmetric with respect to the interchange of identical atoms [123]! Therefore, for the H_3 system, they display the symmetry properties of the C_{3v} -point group. In Fig. 4.13b we have depicted schematically an equipotential surface at an energy below the dissociation energy for a system of three identical atoms. Actually, we should have indicated only the $Y_\lambda \geq 0$ half-space, since γ_λ lies in the range $0 - \pi$. However, we reflected this surface through the $X_\lambda Z_\lambda$ plane to facilitate visualization. As a result, every triatom configuration (except those for which $\gamma_\lambda = 0$ or $\gamma_\lambda = \pi$) is represented in Fig. 4.13b by a pair of points, symmetric with respect to that plane. The hole around the origin is due to the strong repulsion occurring at configurations for which all three atoms are close together.

This mapping of V has an additional property that is of great usefulness. A $\lambda \to \nu$ coordinate transformation in the 3-MD $X_\lambda Y_\lambda Z_\lambda$ internal configuration subspace of Fig. 4.13b is a rigid rotation around the Y_λ axis [123]. This means that this transformation is equivalent to moving the Z_λ axis to the Z_ν position indicated in Fig. 4.13 while otherwise not changing the shape of the equipotentials. This shape invariance with respect to coordinate transformations indicates that this map represents all regions of configuration space in an equivalent way, regardless of the choice of λ. For this reason, we call the coordinates $\rho, \omega_\lambda, \gamma_\lambda$ *symmetrised* hyperspherical coordinates. At large values of R_λ, the rotational motion of $A_\nu A_\kappa$ is indicated by a rotation of the representative point Q around the Z_λ axis, the vibration of $A_\nu A_\kappa$ by an oscillation of Q perpendicular to that axis, and the approach of A_λ to $A_\nu A_\kappa$ by a motion of Q parallel to the same axis. Similar statements are valid for the $A_\nu + A_\kappa A_\lambda$ and $A_\kappa + A_\lambda A_\kappa$ configurations, with the Z_λ axis replaced by Z_ν and Z_κ, respectively. Therefore, a nonreactive collision would correspond to approaching the origin from the large Z_λ direction and then reversing its general direction, whereas a reactive one involves having Q approach the same way but move out along the Z_ν or Z_κ directions while rotating and vibrating around those axes. The dynamical details of these processes depends on the internal topology of these equipotentials, i.e., the nature of the passageways between the different arrangement channel regions of Fig. 4.13b.

5. Quantum reactive scattering in the nineteen seventies: H + H_2. The matching procedures

1975, the first accurate calculations of the differential and integral cross sections of a simple chemical reaction have been published.

5.1 The Quantum Dynamics of Reactive Collinear Triatomic Reactions

Triatomic exchange reactions of the type A + BC → AB + C, with A, B, and C representing atoms confined to move on a laboratory-fixed straight line, constitute the simplest reactive systems that display a basic characteristic of many chemical reactions: the dissolution of a chemical bond and the formation of a new one. The low mathematical dimensionality of the theory permits a presentation unencumbered by the mathematical complexities of molecular rotations, allowing thereby a fairly direct analysis of the effects of translational and vibrational degrees of freedom. We will consider the case of electronically adiabatic exchange reactions; similar considerations can be extended to electronically nonadiabatic ones. The following overview of the matching procedures, performed for the H + H_2 system, is extracted from the work of Kuppermann [10].

5.2 Reactive scattering formalism

The problem being considered is that of obtaining solutions of the nuclear motion Schrödinger equation

$$H\psi = E\psi \tag{5.1}$$

subject to the asymptotic conditions appropriate for reactive scattering. These are, for A + BC collisions,

$$\psi^{\alpha n'_\alpha} \begin{cases} \sim_{R'_\alpha \to \infty} e^{-ik'_{\alpha n'_\alpha} R'_\alpha} \phi_{\alpha n'_\alpha}(r'_\alpha) + \sum_{n_\alpha} f'^{\alpha n'_\alpha}_{\alpha n_\alpha} e^{ik'_{\alpha n_\alpha} R'_\alpha} \phi_{\alpha n_\alpha}(r'_\alpha) \\ \sim_{R'_\gamma \to \infty} \sum_{n_\gamma} f'^{\alpha n'_\alpha}_{\gamma n_\gamma} e^{ik'_{\gamma n_\gamma} R'_\gamma} \phi_{\gamma n_\gamma}(r'_\gamma). \end{cases} \tag{5.2}$$

The $R'_\alpha \to \infty$ behavior is that of a BC molecule (designated α), initially in vibrational eigenstate $\phi_{\alpha n'_\alpha}$ having vibrational quantum number n'_α, and approaching an atom A with relative motion wave number $k'_{\alpha n'_\alpha}$, plus a superposition of waves representing BC molecules receding from A with relative wave numbers $k'_{\alpha n_\alpha}$ and internal quantum states n_α The $R'_\gamma \to \infty$ behavior represents reactive product AB molecules in internal states $\phi_{\gamma n_\gamma}$ receding from atom C with relative wave numbers $k'_{\gamma n_\gamma}$. Conservation of energy requires that

$$\frac{\hbar^2 k'^2_{\alpha n'_\alpha}}{2\mu_{A,BC}} + E_{\alpha n'_\alpha} = \frac{\hbar^2 k'^2_{\alpha n_\alpha}}{2\mu_{A,BC}} + E_{\alpha n_\alpha} = \frac{\hbar^2 k'^2_{\gamma n_\gamma}}{2\mu_{C,BA}} + E_{\gamma n_\gamma} = E, \tag{5.3}$$

where the $E_{\lambda n_\lambda}(\lambda = \alpha, \gamma)$ are the vibrational energies associated with state $\phi_{\lambda n_\lambda}(r'_\lambda)$ and are all referred to a common origin of measurement of energy. It should be noted that although the $E_{\lambda n_\lambda}$ are quantized, the $k'_{\lambda n_\lambda}$ are not, and neither is E. Furthermore, in contrast with bound-state problems, the value of E is assumed known, since we can prepare reagents in known internal states moving with respect to one another with known relative kinetic energy. For values of $E_{\lambda n_\lambda} > E$, (5.3) furnishes $k'^2_{\lambda n_\lambda} < 0$. The corresponding terms in (5.2) are said to be associated with closed channels, and are needed for the mathematical completeness of the expansions on the right-hand side. The values of $k'_{\lambda n_\lambda}$ for such channels are pure positive imaginary, and the corresponding exponentials are real negative, decaying with increasing R'_α or R'_γ. The complex coefficient $f'^{\alpha n'_\alpha}_{\lambda n_\lambda}$ $(\lambda = \alpha, \gamma)$ is called the scattering amplitude from initial state $\alpha n'_\alpha$ to final state λn_λ. If the latter is open, the flux associated with the corresponding term is $v'_{\lambda n_\lambda}|f'^{\alpha n'_\alpha}_{\lambda n_\lambda}|^2$ (where $v'_{\lambda n_\lambda}$ is the relative motion velocity in that channel), whereas the flux associated with the initial collision term is $v'_{\alpha n'_\alpha}$. The collision cross section, for this one-physical-dimensional (1-PD) world (which, however, is a two-mathematical dimensional (2-MD) world), for the $\alpha n'_\alpha \to \lambda n_\lambda$, processes, is dimensionless and is a probability [see (5.27)] given by the ratio of those fluxes:

$$P^{\alpha n'_\alpha}_{\lambda n_\lambda} = (v'_{\lambda n_\lambda}/v'_{\alpha n'_\alpha})|f'^{\alpha n'_\alpha}_{\lambda n_\lambda}|^2. \tag{5.4}$$

A more convenient notation can be introduced by considering that the bound vibrational wave functions $\phi_{\lambda n_\lambda}(r'_\lambda)$ differ significantly from zero only over a relatively small range of r'_λ of atomic dimensions. Furthermore, considering also C + BA collisions, (5.2) can be rewritten as

$$\psi^{\lambda' n'_{\lambda'}} \sim \sum_{\lambda n_\lambda} [\delta^{\lambda' n'_{\lambda'}}_{\lambda n_\lambda} \exp(-ik'_{\lambda n_\lambda} R'_\lambda) + f'^{\lambda' n'_{\lambda'}}_{\lambda n_\lambda} \exp(ik'_{\lambda n_\lambda} R'_\lambda)]\phi_{\lambda n_\lambda}(r'_\lambda). \tag{5.5}$$

In this expression, $\lambda' n'_{\lambda'}$ denotes the initial state of the reagents (which are A + BC for $\lambda' = \alpha$ and C + BA for $\lambda' = \gamma$, where B is always the central atom), the $\sim$ sign indicates that we are considering asymptotically the regions of configuration space in which either $R'_\alpha \to \infty$ with r'_α finite or $R'_\gamma \to \infty$ with r'_γ finite, and $\delta^{\lambda' n'_{\lambda'}}_{\lambda n_\lambda}$ is the Kronecker symbol, which is unity if $\lambda' = \lambda$ and $n'_{\lambda'} = n_\lambda$ and vanishes otherwise. The probability of $\lambda' n'_{\lambda'} \to \lambda n_\lambda$ process (with $\lambda' n'_{\lambda'}$ and λn_λ corresponding to open channels) is then

$$P^{\lambda' n'_{\lambda'}}_{\lambda n_\lambda} = (v'_{\lambda n_\lambda}/v'_{\lambda' n'_{\lambda'}})|f'^{\lambda' n'_{\lambda'}}_{\lambda n_\lambda}|^2. \tag{5.6}$$

5.3 The scattering and reactance matrices and boundary conditions

Before attempting to solve (5.1), subject to the boundary conditions of (5.5), it is convenient to define the scattering matrix $\mathbf{S}$ and the reactance matrix $\mathbf{R}$.

This permits us to decouple the problem of obtaining arbitrary solutions of the Schrödinger equation from the problem of imposing asymptotic conditions appropriate for collision processes on these solutions.
In the λ arrangement channel region of the scaled configuration space $R_\lambda \to \infty$ as r_λ remains finite) we may expand the eigenfunction $\psi^{\lambda' n'_{\lambda'}}$ in the basis set $\phi_{\lambda n_\lambda}(r_\lambda)$, which is forced to be complete and discrete by setting the diatomic potential $v_\lambda(r_\lambda) = V(R_\lambda \to \infty, r_\lambda)$ in that channel equal to zero at and beyond a value $r_{\lambda_{max}}$ of r_λ, a region that the scattering wave function, at the energies considered, does not sample. We write

$$\psi^{\lambda' n'_{\lambda'}} \sim \sum_{\lambda n_\lambda} g_{\lambda n_\lambda}^{\lambda' n'_{\lambda'}}(R_\lambda)\phi_{\lambda n_\lambda}(r_\lambda), \tag{5.7}$$

where

$$-\frac{\hbar^2}{2\mu}\frac{d^2\phi_{\lambda n_\lambda}}{dr_\lambda^2} + v_\lambda(r_\lambda)\phi_{\lambda n_\lambda} = E_{\lambda n_\lambda}\phi_{\lambda n_\lambda} \tag{5.8}$$

and

$$\phi_{\lambda n_\lambda}(0) = \phi_{\lambda n_\lambda}(r_{\lambda_{max}}) = 0. \tag{5.9}$$

Replacement of (5.7) into (5.1) with H given by (4.36), multiplication of both sides by $\phi^*_{\bar\lambda \bar n_\lambda}(r_{\bar\lambda})$ integration over $r_{\bar\lambda}$ and, in the end, replacement of $\bar\lambda$ by λ leads to the set of asymptotic uncoupled differential equations

$$-\frac{\hbar^2}{2\mu}\frac{d^2 g_{\lambda n_\lambda}^{\lambda' n'_{\lambda'}}}{dR_\lambda^2} \sim (E - E_{\lambda n_\lambda}) g_{\lambda n_\lambda}^{\lambda' n'_{\lambda'}}, \tag{5.10}$$

whose solutions can be written as

$$g_{\lambda n_\lambda}^{\lambda' n'_{\lambda'}} \sim_{R_\lambda \to \infty} v_{\lambda n_\lambda}^{-1/2}[\mathcal{I}_\lambda(R_\lambda) A_{\lambda n_\lambda}^{\lambda' n'_{\lambda'}} - \mathcal{O}_{\lambda n_\lambda}(R_\lambda) B_{\lambda n_\lambda}^{\lambda' n'_{\lambda'}}], \tag{5.11}$$

where the $A_{\lambda n_\lambda}^{\lambda' n'_{\lambda'}}$ and $B_{\lambda n_\lambda}^{\lambda' n'_{\lambda'}}$ coefficients are integration constants, $v_{\lambda n_\lambda}$ is the channel velocity $\hbar |k_{\lambda n_\lambda}|/\mu$, $k_{\lambda n_\lambda}$ is the channel wave number given by

$$k_{\lambda n_\lambda} = \hbar^{-1}[2\mu(E - E_{\lambda n_\lambda})]^{1/2} \tag{5.12}$$

and $\mathcal{I}_{\lambda n_\lambda}$ and $\mathcal{O}_{\lambda n_\lambda}$ are the incoming and outgoing waves given by

$$\mathcal{I}_{\lambda n_\lambda}(R_\lambda) = \begin{cases} e^{-ik_{\lambda n_\lambda} R_\lambda} & \text{for open channels} \\ e^{|k_{\lambda n_\lambda}| R_\lambda} & \text{for closed channels} \end{cases} \tag{5.13}$$

$$\mathcal{O}_{\lambda n_\lambda}(R_\lambda) = \begin{cases} e^{ik_{\lambda n_\lambda} R_\lambda} & \text{for open channels} \\ e^{-|k_{\lambda n_\lambda}| R_\lambda} & \text{for closed channels.} \end{cases} \tag{5.14}$$

The superscripts $\lambda' n'_{\lambda'}$ are allowed to scan the same range of values as the subscripts λn_λ. (5.11) can be put in the matrix form

$$\mathbf{g} \sim \mathbf{v}^{-1/2}[\mathcal{I}\mathbf{A} - \mathcal{O}\mathbf{B}], \tag{5.15}$$

where $\mathbf{g}$, $\mathbf{A}$, and $\mathbf{B}$ are the matrices whose λn_λ row and $\lambda' n'_{\lambda'}$ column elements are given, respectively, by $g_{\lambda n_\lambda}^{\lambda' n'_{\lambda'}}$, $A_{\lambda n_\lambda}^{\lambda' n'_{\lambda'}}$, and $B_{\lambda n_\lambda}^{\lambda' n'_{\lambda'}}$ and $\mathbf{v}, \mathcal{I}$ and $\mathcal{O}$ are diagonal matrices whose diagonal elements are $v_{\lambda n_\lambda}, \mathcal{I}_{\lambda n_\lambda}, \mathcal{O}_{\lambda n_\lambda}$, respectively. We now define the scattering matrix $\mathbf{S}$ by the relation

$$\mathbf{B} = \mathbf{S}\mathbf{A}. \tag{5.16}$$

In other words, $\mathbf{S}$ is the matrix that upon left multiplying the matrix $\mathbf{A}$ of incoming wave coefficients, generates the matrix $\mathbf{B}$ of outgoing wave coefficients. This means that if we know what the state and flux of the reagents coming into a collision is, the scattering matrix permits us to obtain the states and fluxes of the outgoing products. This matrix has a set of properties that stems directly from the mathematical structure of the Schrödinger equation. We state here the more important ones. The important review article by Lane and Thomas [124] presents the proofs for the three-dimensional case.

(1) $\mathbf{S}$ is unique, i.e., is independent of the choice of $\mathbf{A}$. In other words, if we arbitrarily pick two coefficient matrices $\mathbf{A_1}$ and $\mathbf{A_2}$ that are non-singular, the Schrödinger equation forces the corresponding $\mathbf{B_1}$ and $\mathbf{B_2}$ to satisfy the relation $\mathbf{B_1 A_1^{-1}} = \mathbf{B_2 A_2^{-2}}$. $\mathbf{S}$ does, however, depend on the total energy E of the system.

(2) $\mathbf{S}$ is symmetric. This basic property leads to the quantum mechanical principle of microscopic reversibility or detailed balancing.

(3) The open part $\mathbf{S}^\circ$ of $\mathbf{S}$, formed from its open channel rows and columns, is unitary. This results in conservation of particle flux.

(5.15) can also be put in the equivalent form

$$\mathbf{g} \sim \mathbf{v}^{-1/2}[\mathcal{S}\mathbf{C} + \mathcal{C}\mathbf{D}], \tag{5.17}$$

where $\mathbf{g}$ and $\mathbf{v}$ have been previously defined, $\mathbf{C}$ and $\mathbf{D}$ are new integration constant matrices, and $\mathcal{S}$ and $\mathcal{C}$ are diagonal sine and cosine stationary wave matrices whose diagonal elements are given by

$$\mathcal{S}_{\lambda n_\lambda}(R_\lambda) = \begin{cases} \sin(k_{\lambda n_\lambda} R_\lambda) & \text{for open channels} \\ e^{|k_{\lambda n_\lambda}| R_\lambda} & \text{for closed channels} \end{cases} \tag{5.18}$$

$$\mathcal{C}_{\lambda n_\lambda}(R_\lambda) = \begin{cases} \cos(k_{\lambda n_\lambda} R_\lambda) & \text{for open channels} \\ e^{-|k_{\lambda n_\lambda}| R_\lambda} & \text{for closed channels.} \end{cases} \tag{5.19}$$

The reactance matrix $\mathbf{R}$ (sometimes called the $\mathbf{K}$ matrix) is defined by the relation

$$\mathbf{D} = \mathbf{R}\mathbf{C}. \tag{5.20}$$

It can be shown to have the following properties [124]:

(1) $\mathbf{R}$ is unique;

(2) $\mathbf{R}$ is real;

(3) the open part $\mathbf{R}^\circ$ of $\mathbf{R}$ is symmetric.

From (5.15) - (5.20), the following relation between $\mathbf{R}^\circ$ and $\mathbf{S}^\circ$ can easily be obtained:

$$\mathbf{S}^\circ = (\mathbf{I} + i\mathbf{R}^\circ)(\mathbf{I} - i\mathbf{R}^\circ)^{-1}. \tag{5.21}$$

Here $\mathbf{I}$ stands for the identity matrix spanned by the open row and column indices λn_λ and $\lambda' n'_{\lambda'}$.
The sine and cosine standing waves associated with $\mathbf{R}$ do not carry flux. However, this matrix has the advantage of being real, and calculable using real quantities only. From it, the complex $\mathbf{S}^\circ$ matrix can be obtained using (5.21), which is equivalent to

$$\mathbf{S}^\circ = \mathrm{Re}\mathbf{S}^\circ + i\mathrm{Im}\mathbf{S}^\circ,$$
$$\mathrm{Re}\mathbf{S}^\circ = (\mathbf{I} - \mathbf{R}^{\circ^2})(\mathbf{I} + \mathbf{R}^{\circ^2})^{-1}, \quad \mathrm{Im}\mathbf{S}^\circ = 2\mathbf{R}^\circ(\mathbf{I} + \mathbf{R}^{\circ^2})^{-1}. \tag{5.22}$$

It can also easily be shown that the scaled configuration-space scattering amplitude $f_{\lambda n_\lambda}^{\lambda' n'_{\lambda'}}$ [defined by the unprimed version of (5.5)] is related to $\mathbf{S}^\circ$ by

$$f_{\lambda n_\lambda}^{\lambda' n'_{\lambda'}} = (v_{\lambda' n'_{\lambda'}}/v_{\lambda n_\lambda})^{1/2}\mathbf{S}^{\circ\,\lambda' n'_{\lambda'}}_{\lambda n_\lambda}, \tag{5.23}$$

where the $v_{\lambda n_\lambda}$ are the scaled channel velocities defined after (5.11). It is also true that the probabilities $P_{\lambda n_\lambda}^{\lambda' n'_{\lambda'}}$ can also be expressed in terms of scaled channel quantities by an expression analogous to (5.6):

$$P_{\lambda n_\lambda}^{\lambda' n'_{\lambda'}} = (v_{\lambda n_\lambda}/v_\lambda)|f_{\lambda n_\lambda}^{\lambda' n'_{\lambda'}}|^2. \tag{5.24}$$

As a result of the last two equations we have, finally:

$$P_{\lambda n_\lambda}^{\lambda' n'_{\lambda'}} = |S^{\circ\,\lambda' n'_{\lambda'}}_{\lambda n_\lambda}|^2. \tag{5.25}$$

Thus, once the open part of the scattering matrix is known, so are all the reaction probabilities at the same total energy. From the symmetry of $\mathbf{S}$ we have

$$P_{\lambda' n'_{\lambda'}}^{\lambda n_\lambda} = P_{\lambda n_\lambda}^{\lambda' n'_{\lambda'}}, \tag{5.26}$$

which is the principle of microscopic reversibility for this collinear system, and from the unitarity of $\mathbf{S}^\circ$ we have

$$\sum_{\lambda n_\lambda} P_{\lambda n_\lambda}^{\lambda' n'_{\lambda'}} = 1, \tag{5.27}$$

where the sum is extended over the open channnels. (5.27) constitutes the property of flux conservation, and justifies the use of the term probability for the quantities $P_{\lambda n_\lambda}^{\lambda' n'_{\lambda'}}$.

5.4 Computational methodology in collinear systems

From the considerations of the previous section, we conclude that to determine the transition probabilities $P_{\lambda n_\lambda}^{\lambda' n'_{\lambda'}}$, which include the reactive $(\lambda \neq \lambda')$

as well as the nonreactive ($\lambda = \lambda'$) ones, it suffices to obtain the reactance matrix **R**. This in term can be determined by calculating a sufficiently large number of linearly independent solutions of the Schrödinger equation, and putting the associated **g** matrix in the form of (5.17). From this, the square coefficient matrices **C** and **D** can be obtained, and **R** calculated from (5.20) as long as care has been taken to as certain that **C** is nonsingular.

Over the years, different approaches have been used to obtain such linearly independent solutions of the Schrödinger equation and many references are given in [10]. As an illustration, only one of these methods, i.e. of Kuppermann [139, 140] will be presented. In this method, the scaled configuration space is divided into three regions (denoted by I, II, and III in Fig. 5.1) and called, respectively, the reagent, the strong interaction, and the product regions. In each of these regions different coordinates and different basis sets for expanding the wave function are used. The value of R_α for points P_1 and P_2 is sufficiently large for $V_\alpha(R_\alpha, r_\alpha)$ along the line P_1P_2 to have assumed the asymptotic behavior $v_\alpha(r_\alpha)$. Similarly, $V_\gamma(R_\gamma, r_\gamma)$ along P_6P_7 equals $v_\gamma(r_\gamma)$. The point P_0 is located sufficiently inside the dissociated plateau region for the wave function to vanish along the line $P_1P_0P_7$. Similarly, P_2 is chosen so as to have a sufficiently low value of r_α and P_6 of r_γ for the wave function along the line $P_2P_4P_6$ to vanish. To integrate the Schrödinger equation, Cartesian coordinates (R_α, r_α) and (R_γ, r_γ) are used in regions I and III, respectively, and in region II circular polar coordinates (ρ, ψ) with origin P_0 are used (see Fig. 5.1). The nuclear motion Hamiltonian in terms of (R_α, r_α) and (R_γ, r_γ) is given by (4.36), whereas in the (ρ, ψ) coordinates it is

$$H = -\frac{\hbar^2}{2\mu}[\frac{1}{\rho^{1/2}}\frac{\partial^2}{\partial\rho^2}\rho^{1/2} + \frac{1}{\rho^2}\frac{\partial^2}{\partial\phi^2}] + V(\rho, \phi) - \frac{\hbar^2}{8\mu\rho^2} \ . \tag{5.28}$$

We now subdivide region I into n_{I}, subregions separated by lines of constant R_α at $R_\alpha = R_\alpha^\circ, R_\alpha^1 ..., R_\alpha^{nI}$ where $R_\alpha^0 = R_{\alpha 1}$ and $R_\alpha^{nI} = R_{\alpha_0}$ are, respectively, the R_α coordinate of points P_1, and P_0 of Fig. 4. The range of the ith subregion is $R_\alpha^{i-1} < R_\alpha < R_\alpha^i$. For expanding the wave function in that subregion we choose as basis functions the eigenfunctions $\phi_{\alpha n_\alpha}(r_{\alpha_i}; R_\alpha^{io})$ of the reference potential $V_{ref}^{\alpha_1}(r_\alpha; R_\alpha^{io}) = V(R_\alpha^{io}, r_\alpha)$ where R_α^{io} is a value of R_α belonging to the ith subregion, such as its midpoint. These basis functions satisfy the equations

$$[-\frac{\hbar^2}{2\mu}\frac{d^2}{dR_\alpha^2} + V_{ref}^\alpha(r_\alpha; R_\alpha^{io})]\phi_{\alpha n_\alpha}(r_\alpha; R_\alpha^{io}) = E_{\alpha n_\alpha}(R_\alpha^{io})\phi_{\alpha n_\alpha}$$

$$\phi_{\alpha n_\alpha}(r_{\alpha 1}; R_\alpha^{io}) = \phi_{\alpha n_\alpha}(r_{\alpha 2}; R_\alpha^{io}) = 0, \tag{5.29}$$

where $r_{\alpha 1}$ and $r_{\alpha 2}$ are the r_α coordinates of points P_1 and P_2, respectively. The $E_{\alpha n_\alpha}(R_\alpha^{io})$ are the energy levels of the local transverse vibration at $R_\alpha = R_\alpha^{io}$ and the local basis set $\phi_{\alpha n_\alpha}(r_\alpha; R_\alpha^{io})$ furnishes a better representation of the scattering wave functions than do the diatom eigenfunctions $\phi_{\alpha n_\alpha}(r_\alpha; R_\alpha \to \infty)$. We now expand those wave functions according to

$$\psi^{\lambda' n'_{\lambda'}} = \sum_{n_\alpha} g_{\alpha n_\alpha}^{\lambda' n'_{\lambda'}}(R_\alpha; R_\alpha^{io}) \phi_{\alpha n_\alpha}(r_\alpha; R_\alpha^{io}). \tag{5.30}$$

Substituting this expression into (5.1) with H given by the first part of (4.36), multiplying both sides by $\phi^*_{\alpha \bar{n}_\alpha}(r_\alpha; R_\alpha^{io})$ and integrating over r_α from an $r_{\alpha 2}$ to $r_{\alpha 1}$ leads to the following set of coupled equations, written in matrix form:

$$-\frac{\hbar^2}{2\mu}\frac{d^2\mathbf{g}^{\mathrm{I}}}{d\mathbf{R}_\alpha^2} + \mathbf{V}^{\mathrm{I}}(R_\alpha; R_\alpha^{io})\mathbf{g}^{\mathrm{I}} = \mathbf{E}^{\mathrm{I}}(R_\alpha^{io})\mathbf{g}^{\mathrm{I}}. \tag{5.31}$$

All matrices appearing in this equation are square, with dimensions equal to the number of terms N used in expansion (39). Although in principle this expansion should be infinite, it is truncated at a finite N, which is greater than the number of open channels at the energy being considered [i.e., expansion (39) includes closed channels], and convergence with respect to increasing N is determined numerically. The elements of $\mathbf{g}^{\mathrm{I}}$ are the $g_{\alpha n_\alpha}^{\lambda' n'_{\lambda'}}$, with n_α and $n'_{\lambda'}$, the row and column indices, respectively. $\mathbf{E}^{\mathrm{I}}$ is the diagonal matrix whose diagonal elements are $E - E_{\alpha n_\alpha}(R_\alpha^{io})$. Finally, $\mathbf{V}^{\mathrm{I}}$ is the interaction potential matrix whose n_α, n'_α, element is given by

$$V_{n_\alpha}^{\mathrm{I} n'_\alpha}(R_\alpha; R_\alpha^{io}) = \langle \phi_{\alpha n_\alpha}(r_\alpha; R_\alpha^{io}) | V_\alpha(R_\alpha, r_\alpha) - V_\alpha(R_\alpha^{io}, r_\alpha) | \phi_{\alpha n'_\alpha}(r_\alpha; R_\alpha^{io}) \rangle. \tag{5.32}$$

The Schrödinger equation is integrated in region **I** for N independent solutions by choosing $\mathbf{g}^{\mathrm{I}}(R_{\alpha 1}; R_\alpha^{io}) = d\mathbf{g}_0^{\mathrm{I}}$ and $d\mathbf{g}^{\mathrm{I}}(R_{\alpha 1}; R_\alpha^{io})/dR_\alpha = \mathbf{g}_0^{\mathrm{I}}$ arbitrarily, but not simultaneously zero. One such choice is to make the first equal to the identity matrix and the second equal to the null matrix. This corresponds to a choice of initial conditions at the starting value $R_{\alpha 1}$ of R_α, One then integrates the coupled equations (40) through subregion I, changes to the basis set for subregion 2 at the boundary between these subregions, and continues in this manner until one reaches the end of region I. The change in vibrational basis sets at the boundary between subregions i and $i+1$ is accomplished by imposing the condition that the wave function $\psi^{\lambda' n'_{\lambda'}}$ and its derivative with respect to R_α be continuous at that boundary. This results in the relations

$$\mathbf{g}^{\mathrm{I}}(R_\alpha^i; R_\alpha^{i+1,o}) = \mathbf{S}_i^{\mathrm{I}}\mathbf{g}^{\mathrm{I}}(R_\alpha^i, R_\alpha^{io}), \quad \frac{d\mathbf{g}^{\mathrm{I}}(R_\alpha^i; R_\alpha^{i+1,o})}{dR_\alpha} = \mathbf{S}_i^{\mathrm{I}}\frac{\mathbf{g}^{\mathrm{I}}(R_\alpha^i; R_\alpha^{io})}{dR_\alpha} \tag{5.33}$$

where $\mathbf{S}_i^{\mathrm{I}}$ is the overlap matrix between the basis functions for subregions i and $i+1$, its n_α, n'_α element being given by

$$S_{i n_\alpha}^{\mathrm{I} n'_\alpha} = \langle \phi_{\alpha n_\alpha}(r_\alpha; R_\alpha^{i+1,o}) | \phi_{\alpha n'_\alpha}(r_\alpha; R_\alpha^{io}) \rangle. \tag{5.34}$$

If the expansion (5.30) were complete $\mathbf{S}_i^{\mathrm{I}}$ would be orthogonal. For the truncated expansions required by practical considerations, it still must be nearly orthogonal in order for the scattering matrix that results at the end to satisfy flux conservation with acceptable accuracy.

Proceeding to region II, it is also subdivided into subregions by lines of constant ϕ at $\phi = \phi^0, \phi^1, ..., \phi^{n\mathrm{II}}$ where $\phi^0 = 0$ and $\phi^{n\mathrm{II}} = \phi_{max}$ are, respectively, the ϕ coordinate of points P_3 and P_5. In analogy with region I, the range of the ith subregion is $\phi^{i-1} < \phi < \phi^i$. We note that cuts of the potential energy function $V(\rho, \phi)$ along lines of constant ϕ, when plotted as a function of ρ, have the shape of diatomic molecule potential energy functions. This is a crucial property, which not only serves as a fundamental basis for reactive scattering calculations, but has also been historically used by Eyring [143] as a basic justification for transition state theory. We make use of this characteristic behavior by choosing as basis functions for the ith subregion the eigenfunctions $\psi_{\mathrm{II}}(\rho; \phi^{io})$ of the reference potential $V^{\mathrm{II}}_{ref}(\rho; \phi^{io}) = V(\rho, \phi^{io})$ where ϕ^{io} is a value of ϕ in that subregion. These functions are defined by the eigenvalue equation

$$[-\frac{\hbar^2}{2\mu}\frac{d^2}{d\rho^2} + V^{\mathrm{II}}_{ref}(\rho; \phi^{io})]\phi_{\mathrm{II}n}(\rho; \phi^{io}_\lambda) = E_{\mathrm{II}n}(\phi^{io})\phi_{\mathrm{II}n} \tag{5.35}$$

and the boundary conditions

$$\phi_{\mathrm{II}n}(\rho^i_{max}; \phi^{io}) = \phi_{\mathrm{II}n}(\rho = 0; \phi^{io}) = 0, \tag{5.36}$$

where ρ^i_{max} is the value of ρ for the intersection point between the $\phi = \phi^{io}$ line and the line $\mathrm{P}_3\mathrm{P}_4\mathrm{P}_5$. As in region I, ϕ_{II_n} and E_{II} are local transverse vibrational eigenfunctions and eigenvalues that lead to a much more rapidly converging expansion of the scattering wave function in subregion IIi than would the eigenfunctions of the isolated diatom reagent or product. We now expand that wave function according to

$$\psi^{\lambda' n'_{\lambda'}} = \rho^{-1/2} \sum_n g^{\lambda' n'_{\lambda'}}_{\mathrm{II}n}(\phi; \phi^{io})\phi_{\mathrm{II}n}(\rho; \phi^{io}). \tag{5.37}$$

Substituting this expression into (5.1) with H given by (5.28) and proceeding analogously to region I, we obtain the following matrix differential equation:

$$-\frac{\hbar^2}{2\mu}\frac{d^2\mathbf{g}^{\mathrm{II}}}{d\phi^2} + \rho^2(\phi^{io})\mathbf{V}^{\mathrm{II}}(\phi; \phi^{io})\mathbf{g}^{\mathrm{II}} = \rho^2\mathbf{E}^{\mathrm{II}}(\phi^{io})\mathbf{g}^{\mathrm{II}}. \tag{5.38}$$

All the matrixes in this expression are N x N square matrices, with the same dimensions as those in (5.31). The elements of $\mathbf{g}^{\mathrm{II}}$ are the $\mathbf{g}^{\lambda' n'_{\lambda'}}_{\mathrm{II}n}$ with n and $n'\lambda'$, the row and column indices, respectively; $\rho^2, \mathbf{V}^{\mathrm{II}}$ and $\mathbf{E}^{\mathrm{II}}$ are defined by

$$\begin{aligned} \rho^{2n'}_n(\phi^{io}) &= \langle\phi_{\mathrm{II}n}(\rho; \phi^{io})|\rho^2|\phi_{\mathrm{II}n'}(\rho; \phi^{io})\rangle \\ V^{\mathrm{II}n'}_n(\phi; \phi^{io}) &= \langle\phi_{\mathrm{II}n}(\rho; \phi^{io})|V(\rho, \phi) - V(\rho, \phi^{io}) - \frac{\hbar^2}{8\mu\rho^2}|\phi_{\mathrm{II}n'}(\rho; \phi^{io})\rangle \\ E^{\mathrm{II}n'}_n(\phi^{io}) &= \delta^{n'}_n[E - E_{\mathrm{II}n}(\phi^{io})] \end{aligned} \tag{5.39}$$

The condition that at the boundary between regions I and II, and $\psi^{\lambda' n'_{\lambda'}}$ its derivative with respect to R_α, are continuous, leads to the following relations between the initial values of g^{II} or its ϕ derivative and the final values of g^{I} or its R_α derivative:

$$\mathbf{g}^{\mathrm{II}}(\phi = 0; \phi^{1o}) = \rho^{1/2}\mathbf{g}^{\mathrm{I}}(R_{\alpha 0}; R_\alpha^{n}\mathrm{I}^{o}) \tag{5.40}$$

$$\mathbf{dg}^{\mathrm{II}}(\phi = 0; \phi^{io})/d\phi = -\rho^{3/2}[d\mathbf{g}^{\mathrm{I}}(R_{\alpha 0}; R_\alpha^{n}\mathrm{I}^{o})/dR_\alpha], \tag{5.41}$$

where

$$\rho_n^{bn'} = (\phi_{\mathrm{II}n}(\rho; \phi^{io})|\rho^b|\phi_{\mathrm{II}n'}(r_{\alpha 1} - \rho; R_\alpha^{n}\mathrm{I}^{o})),\ b = \frac{1}{2}, \frac{3}{2}. \tag{5.42}$$

The change in vibrational basis set at the boundary between subregions IIi and IIi + 1 is accomplished by equations analogous to (42) and (43). Using them and (5.40) we can integrate (5.38) from the beginning through the end of region II.

For region III we use equations analogous to (5.29) - (5.34) with I and α replaced by III and γ respectively, and other obvious notational changes. At the boundary between regions II and III, equations analogous to (5.40) are applicable, with a plus rather than a minus sign in the right-hand side of the second of these equations to indicate that both ϕ and R_γ increase in the direction of integration.

With the help of this procedure, we can integrate the Schrödinger equation from the beginning of region I to the end of region III. The numerical method used for integrating the coupled second-order differential equations (5.31), (5.38), and the region III equivalent of (5.31), is arbitrary. It should, however, be an efficient method, because otherwise the computation time may be excessive, since it grows with the cube of the number N of coupled equations. Three such methods commonly used are those of Gordon [144], Magnus [24], and Light and Walker [142].

A numerical complication that should be mentioned is that due to the necessary inclusion of closed channels in the expansion of $\psi^{\lambda' n'_{\lambda'}}$ the columns of the $\mathbf{g}$ matrices tend to become linearly dependent, as the integration proceeds, thereby destroying the needed linear independence of the $\psi^{\lambda' n'_{\lambda'}}$ This can be avoided by reorthogonalization procedures, one of which involves right multiplying $\mathbf{g}$ and $\mathbf{g'}$ by $\mathbf{g^{-1}}$, which means continuing the integration with $\mathbf{g}_{new} = \mathbf{I}$ and $\mathbf{g}'_{new} = \mathbf{g}^{\mathrm{I}}\mathbf{g}^{-1}$. This corresponds to obtaining n solutions with the modified initial conditions $\mathbf{g}^{\mathrm{I}}_{0new} = \mathbf{g}^{\mathrm{I}}_0\mathbf{g}^{-1}$ and $\mathbf{g}^{\mathrm{I}'}_{0new} = \mathbf{g}^{\mathrm{I}'}_0\mathbf{g}^{-1}$ Each time a reorthogonalization procedure is performed anywhere in regions I, II, or III, the initial conditions of region I must be modified accordingly. The efficient integration method recently developed by Light and Walker (1976) has elegantly bypassed this complication.

Let us label by $\mathbf{g}_f^{\mathrm{III}}$ the final $\mathbf{g}^{\mathrm{III}}$ matrix at the end of region III and by $\mathbf{g}_0^{\mathrm{I}}$ the corresponding (modified) initial $\mathbf{g}^{\mathrm{I}}$ matrix at the beginning of region I, and let us use an equivalent notation for the derivatives with respect to R_γ

and R_α, respectively. Similarly, let us perform integrations of the Schrödinger equation starting at the beginning of region III (i.e., line P_6P_7 of Fig. 5.1) and terminating at the end of region I (line P_1P_2). Let $\mathbf{g}_o^{\mathbf{III}}$ and $\mathbf{g}_f^{\mathbf{I}}$ be the corresponding initial and final matrices, with a similar notation for their derivatives. With the help of these several matrices we can determine the $\mathbf{R}$ matrix as follows.

We define the global $\mathbf{g}$ and $\mathbf{g}'$ matrices by

$$\mathbf{g} = \begin{pmatrix} \mathbf{g}_0^{\mathbf{I}} & \mathbf{g}_f^{\mathbf{I}} \\ \mathbf{g}_f^{\mathbf{III}} & \mathbf{g}_0^{\mathbf{III}} \end{pmatrix}, \qquad \mathbf{g}' = \begin{pmatrix} \mathbf{g}_0^{\mathbf{I}'} & \mathbf{g}_f^{\mathbf{I}'} \\ \mathbf{g}_f^{\mathbf{III}'} & \mathbf{g}_0^{\mathbf{III}'} \end{pmatrix}. \tag{5.43}$$

Since along lines P_2P_1 and P_6P_7, the potential function V has assumed its asymptotic behavior $v_\alpha(r_\alpha)$ and $v_\gamma(r_\gamma)$, respectively, $\mathbf{g}$ must have assumed the form given by (5.17):

$$\mathbf{g} = \mathbf{v}^{-1/2}[\mathcal{S}\mathbf{C} + \mathcal{C}\mathbf{D}]. \tag{5.44}$$

Similarly, its derivative must be given by

$$\mathbf{g}' = \mathbf{v}^{-1/2}[\mathcal{S}'\mathbf{C} + \mathcal{C}'\mathbf{D}], \tag{5.45}$$

where $\mathcal{S}'$ and $\mathcal{C}'$ are the diagonal matrices whose diagonal elements are the derivatives with respect to R_λ of (5.18) and (5.19), evaluated, as are $\mathcal{S}$ and $\mathcal{C}$, at $R_\alpha = R_{\alpha_1}$ and $R_\gamma = R_{\gamma_7}$.

In (5.44) and (5.45), all matrices except $\mathbf{C}$ and $\mathbf{D}$ are now known. From these equations we can therefore obtain these unknowns and from them $\mathbf{R}$ by using (5.20). From the open part $\mathbf{R}^\circ$ of $\mathbf{R}$ we obtain $\mathbf{S}^\circ$ from either (5.21) or (5.22), and finally the transition probabilities $P_{\lambda n_\lambda}^{\lambda' n'_{\lambda'}}$ by using (5.25). In this manner, once V is given, these probabilities can be calculated.

5.5 Electronically nonadiabatic exchange reactions

When a chemical reaction occurs that involves a change in the electronic state of the triatomic system, the theoretical formulation of the exchange reaction given by (5.2) and (5.5) must be extended. In one form of the general theory, we consider a family of electronically diabatic potential energy surfaces as well as a family of coupling potential energy surfaces. If the lowest two of these surfaces interact and the others are at energies that are high compared to the collision energy being considered, we may use the two-state approximation, in which (5.1), in scaled coordinates, is replaced by the system of equations

$$\begin{aligned}
(-\frac{\hbar^2}{2\mu}(\frac{\partial^2}{\partial R_\alpha^2} + \frac{\partial^2}{\partial r_\alpha^2}) + V_1(R_\alpha, r_\alpha) - E)\psi_1(R_\alpha, r_\alpha)] &= -V_{12}(R_\alpha, r_\alpha)\psi_2(R_\alpha, r_\alpha) \\
(-\frac{\hbar^2}{2\mu}(\frac{\partial^2}{\partial R_\alpha^2} + \frac{\partial^2}{\partial r_\alpha^2}) + V_2(R_\alpha, r_\alpha) - E)\psi_2(R_\alpha, r_\alpha) &= \\
-V_{21}(R_\alpha, r_\alpha)\psi_1(R_\alpha, r_\alpha)&
\end{aligned} \tag{5.46}$$

where V_1 and V_2 are the two electronically diabatic surfaces being considered and V_{12} us the coupling potential energy surface.

$$\psi^{i\lambda' n'_{\lambda'}} \sim \sum_{\lambda n_\lambda} [e^{(-ik_{i\lambda n_\lambda} R_\lambda} \delta^{\lambda' n'_{\lambda'}}_{\lambda n_\lambda} + e^{ik_{i\lambda n_\lambda} R_\lambda} f^{\lambda' n'_{\lambda'}}_{\lambda n_\lambda}] \phi_{i\lambda n_\lambda}(r_\lambda), \quad i = 1,2$$

$$\psi^{j\lambda' n'_{\lambda'}} \sim \sum_{\lambda n_\lambda} f^{\lambda' n'_{\lambda'}}_{\lambda n_\lambda} e^{ik_{j\lambda n_\lambda} R_\lambda} \phi_{j\lambda n_\lambda}(R_\lambda), j \neq i, \quad j = 1,2 \tag{5.47}$$

5.6 The Quantum Dynamics of Three-Dimensional Reactive Triatomic Systems

In this section we generalize the description of the electronically adiabatic reactive scattering of collinear triatomic systems to three physical dimensions (3-PD). The corresponding formalisms are analogous. The restrictions on the total energy will be the same as those for the 1-PD systems. One difference is that the partial first derivatives with respect to the two scalar distances are replaced by the gradients with respect to the corresponding position vectors, and appropriate spherical scattered waves replace the corresponding collinear plane waves. An additional difference is that for A + BC reagents, two reactive product arrangement channels (AB + C and AC + B) are allowed, rather than only one. This results in an interesting "bifurcation" problem, not encountered in the collinear case. The scattering and reactance matrices are introduced analogously to the 1-PD case, after an appropriate partial wave expansion.

5.7 Reactive-scattering formalism

We start out by choosing a system of coordinates that spans the 6-MD configuration space in which the motion of the triatomic system, after removal of the motion of the center of mass, takes place. Let $Oxyz$ be a system of coordinates whose origin 0 is the center of mass of the system and whose axes are parallel to a system of laboratory-fixed axes. We will call $Oxyz$ the laboratory-fixed system. The spherical polar coordinates of the scaled $\mathbf{R}_\lambda$ in this system are $R_\lambda, \theta_\lambda, \phi_\lambda$. Let us also define a body-fixed coordinate system $OX_\lambda Y_\lambda Z_\lambda$ (not to be confused with the axes of Figs. 4.12 and 5.2 obtained by rotating the $Oxyz$ axis by the Euler angles $\phi_\lambda, \theta_\lambda, 0$. The resulting OZ_λ axis points along the $\mathbf{R}_\lambda, \mathbf{r}_\lambda$ in the space-fixed system are $\mathbf{r}^{sf}_\lambda = (r_\lambda, \theta_{r\lambda}, \phi_{r\lambda})$ and in body-fixed system are $r^{\mathrm{bf}}_\lambda(r_\lambda, \gamma_\lambda, \psi_\lambda)$ where γ_λ is, as before, the angle between $\mathbf{R}_\lambda$ and $\mathbf{r}_\lambda$ and ψ_λ is a tumbling angle around the $(\mathbf{R}_\lambda, Oz)$ plane. In this presentation we chose body-fixed coordinates because they lead to simpler final expressions for the cross sections and to a simpler solution to the bifurcation problem. However, space-fixed coordinates can also be used (Pack [145]). In terms of these body-fixed coordinates, we wish to find the solutions of the Schrödinger equation:

$$H\psi^{\lambda' n'_{\lambda'}} = E\psi^{\lambda' n'_{\lambda'}}, \tag{5.48}$$

which satisfy the asymptotic condition for large $R_\lambda(\lambda = \alpha, \beta, \gamma)$

$$\psi^{\lambda' n'_{\lambda'}} \sim \exp(ik_{\lambda' c'_{\lambda'} j'_{\lambda'}} R_{\lambda'_z}) \Phi_{\lambda' n'_{\lambda'}}(\mathbf{r}^{sf}_{\lambda'}) +$$
$$\sum_{\lambda n_\lambda} f^{\lambda' n'_{\lambda'}}_{\lambda n_\lambda}(\theta_\lambda, \phi_\lambda)(R_\lambda)^{-1} \exp(ik_{\lambda c_\lambda j_\lambda} R_\lambda) \phi_{\lambda n_\lambda}(\mathbf{r}^{\mathrm{bf}}_\lambda). \tag{5.49}$$

In these expressions λ and λ' designate the final and initial arrangement channels, respectively, and n_λ is the set of quantum numbers $c_\lambda, j_\lambda, m_{j_\lambda}$ of the $A_\nu A_k$ isolated diatom where c_λ, is the vibrational quantum number, j_λ its rotational angular momentum quantum number, and m_{j_λ} the quantum number associated with the projection of the diatom's rotational angular momentum along the direction of the final relative wave-number vector $\mathbf{k}_{\lambda c_\lambda j_\lambda}$ (i.e., the helicity polarization quantum number) which, as $R_\lambda \sim \infty$, lies in the $\theta_\lambda, \phi_\lambda$ direction. Similarly, $n'_{\lambda'}$ represents the corresponding quantum numbers $c'_{\lambda'} j'_{\lambda'} m'_{j'\lambda'}$ of the initial diatomic reagent $A_{\nu'} A_{k'}$ where the axis of quantization for, $m'_{j'_{\lambda'}}$ is the direction of the initial relative wave-number vector $\mathbf{k}_{\lambda' c'_{\lambda'} j'_{\lambda'}}$, that has been chosen to lie along the laboratory-fixed Oz axis. $R_{\lambda'_z}$ is the component of $\mathbf{R}_{\lambda'}$ along that axis. As $R_{\lambda'} \sim \infty$ $\mathbf{R}_{\lambda'}$ lies in the $-\mathbf{k}_{\lambda' c'_{\lambda'} j'_{\lambda'}}$ direction, i.e., in the negative Oz direction. In other words, in the helicity representation, the axis of quantization for the reagent and product diatoms are, respectively, the initial and final relative wave-number vectors. This particular choice of representation greatly simplifies the expression for the scattering amplitude given by (5.68).

The $\phi_{\lambda n_\lambda}(\mathbf{r}^{\mathrm{bf}}_\lambda)$ and $\phi_{\lambda' n'_{\lambda'}}(\mathbf{r}^{sf}_{\lambda'})$ in (5.49) represent the diatomic product and reagent rovibrational eigenfunctions, respectively, in scaled coordinates, and in the helicity representation; $(R_\lambda)^{-1} exp(ik_{\lambda c_\lambda j_\lambda})$ represents a spherical radial scattered wave and $exp(ik_{\lambda' c'_{\lambda'} j'_{\lambda'}} R_{\lambda'_{z'}})$ is a plane wave representing the initial relative motion of the atom A_λ with respect to the diatomic molecule $A_{\nu'} A_{k'}$ in scaled coordinates; and finally $f^{\lambda' n'_{\lambda'}}_{\lambda n_\lambda}(\theta_\lambda, \phi_\lambda)$ is the scaled coordinate scattering amplitude from initial state $\lambda' n'_{\lambda'}$ of the reagent to final state λn_λ of the product, for initial and final relative atom-diatom wave-number vectors $\mathbf{k}_{\lambda' c'_{\lambda'} j'_{\lambda'}}$ and $\mathbf{k}_{\lambda c_\lambda j_\lambda}$ respectively, $\theta_\lambda \phi_\lambda$ being the polar angles of the latter with respect to the former in the $Oxyz$ system whose Oz axis lies along $\mathbf{k}_{\lambda' c'_{\lambda'} j'_{\lambda'}}$. The magnitudes of these wave numbers satisfy the energy conservation relation

$$(\hbar^2 k^2_{\lambda' c'_{\lambda'} j'_{\lambda'}}/2\mu) + E_{\lambda' c'_{\lambda'} j'_{\lambda'}} =$$
$$(\hbar^2 k^2_{\lambda c_\lambda j_\lambda}/2\mu) + E_{\lambda c_\lambda j_\lambda} = E,\ \lambda = \alpha, \beta, \gamma, \tag{5.50}$$

where $E_{\lambda' c'_{\lambda'} j'_{\lambda'}}$ and $E_{\lambda c_\lambda j_\lambda}$ are, respectively, the rovibrational energy of the initial and final diatoms and E is the total energy of the system. The unscaled coordinate scattering amplitude $f'^{\lambda' n'_{\lambda'}}_{\lambda n_\lambda}(\theta_\lambda, \phi_\lambda)$ is related to the scaled one by:

$$f'^{\lambda' n'_{\lambda'}}_{\lambda n_\lambda}(\theta_\lambda, \phi_\lambda) = (a_\lambda)^{-1}(a_\lambda/a_{\lambda'})^{1/2} f^{\lambda' n'_{\lambda'}}_{\lambda n_\lambda}(\theta_\lambda, \phi_\lambda), \tag{5.51}$$

where the a_λ terms have been defined in (4.42), and the differential cross section for the $\lambda' n'_{\lambda'} \to \lambda n_\lambda$ process can be obtained from $f'^{\lambda' n'_{\lambda'}}_{\lambda n_\lambda}$ by the expression

$$\sigma^{\lambda' n'_{\lambda'}}_{\lambda n_\lambda}(\theta_\lambda, \phi_\lambda) = (v'_{\lambda n_\lambda}/v'_{\lambda' n'_{\lambda'}})|f'^{\lambda' n'_{\lambda'}}_{\lambda n_\lambda}(\theta_\lambda, \phi_\lambda)|^2, \tag{5.52}$$

where $v'_{\lambda n_\lambda}$ and $v'_{\lambda' n'_{\lambda'}}$ are the final and initial unscaled coordinate velocities, respectively.
The sum in the right-hand side of (5.49) includes the closed-channel terms, for which $E_{\lambda c_\lambda j_\lambda} > E$, for the reasons given following (5.3).
In the present formulation the A_α, A_β, and A_γ, atoms have been considered distinguishable. When they are not, the scattering wave function must be made to satisfy the Pauli principle. This can be achieved a posteriori, after solving the Schrödinger equation and ignoring this principle.

5.8 Scattering and reactance matrices and boundary conditions

As in the collinear case, it is convenient to introduce scattering and reactance matrices in order to separate the problem of finding solutions of the Schrödinger equation (5.48), satisfying arbitrary asymptotic conditions, from the problem of finding the scattering amplitudes of (5.49). We start by defining the functions $\phi^{JM_J}_{\lambda b_\lambda}(\hat{\mathbf{R}}_\lambda, \mathbf{r}^{\mathbf{bf}}_\lambda)$ where $\hat{\mathbf{R}}_\lambda$ is the unit vector in the $\mathbf{R}_\lambda$ direction, defined by the laboratory-fixed polar angles $\theta_\lambda, \phi_\lambda$. This function of the five scalar variables $\theta_\lambda, \phi_\lambda, \gamma_\lambda, \psi_\lambda$ is defined as a simultaneous eigenfunction of the following five operators:
(1) the square of the triatomic system total angular momentum J^2_{op};
(2) the Oz laboratory-fixed component of that angular momentum $J_{z_{op}}$;
(3) the energy of the isolated A_ν A_k diatom $h_{\lambda_{op}}$;
(4) the square of the rotational angular momentum of that isolated diatom $j^2_{\lambda_{op}}$ and
(5) the component of that angular momentum along the body-fixed OZ_λ (i.e., $\mathbf{R}_\lambda$) axis $j_{z_{\lambda_{op}}}$
The quantum numbers associated with that set of operators are $J, M_J, c_\lambda, j_\lambda$ and Ω_λ respectively, and b_λ designates the $c_\lambda, j_\lambda, \Omega_\lambda$ subset. The quantum number Ω_λ associated with the tumbling motion of the triatom around R_λ and described by the tumbling angle ψ_λ will play a special role in the computational methodology described in one of the next sections.
The functions $\phi^{JM_J}_{\lambda b_\lambda}(\hat{\mathbf{R}}_\lambda, \mathbf{r}^{\mathrm{bf}}_\lambda)$ are called surface functions. They form a complete discrete orthonormal set that spans the 5-MD $\theta_\lambda, \phi_\lambda, r_\lambda \gamma_\lambda, \psi_\lambda$ subspace of the 6-MD configuration space. They are given by (Schatz and Kuppermann [11]):

$$\phi^{JM_J}_{\lambda b_\lambda}(\hat{\mathbf{R}}_\lambda, \mathbf{r}^{\mathbf{bf}}_\lambda) = [(2J+1)/4\pi]^{1/2} D^J_{M_j \Omega_\lambda}(\phi_\lambda \theta_\lambda) \Phi_{\lambda c_\lambda j_\lambda \Omega_\lambda}(\mathbf{r}^{\mathbf{bf}}_\lambda), \tag{5.53}$$

where $D^J_{M_j\Omega_\lambda}$ is a Wigner rotation function and $\Phi_{\lambda c_\lambda j_\lambda \Omega_\lambda}(\mathbf{r}^{\mathrm{bf}}_\lambda)$ is a simultaneous eigenfunction of the $h_{\lambda_{op}}$ (Hamiltonian), $j^2_{\lambda_{op}}$ and $j_{z_{\lambda_{op}}}$ operators of the isolated $A_\nu A_k$ diatom in the scaled coordinates $OX_\lambda Y_\lambda Z_\lambda$ body-fixed system of axis. If the electronic state of that molecule is a $\mathbf{S}igma$ state, the $\Phi_{\lambda c_\lambda j_\lambda \Omega_\lambda}$ are given by

$$\Phi_{\lambda c_\lambda j_\lambda \Omega_\lambda}(\mathbf{r}^{\mathbf{bf}}_\lambda) = (r)^{-1}\phi_{\lambda c_\lambda j_\lambda \Omega_\lambda}(r_\lambda) Y_{j_\lambda \Omega_\lambda}(\gamma_\lambda, \psi_\lambda), \tag{5.54}$$

where $Y_{j_\lambda \Omega_\lambda}$ is a spherical harmonic and $\phi_{\lambda c_\lambda j_\lambda \Omega_\lambda}$ satisfies the radial Schrödinger equation

$$[-\frac{\hbar^2}{2\mu}\frac{d^2}{dr^2_\lambda} + v_\lambda(r_\lambda) + \frac{j_\lambda(j_\lambda+1)\hbar^2}{2\mu r^2_\lambda}]\phi_{\lambda c_\lambda j_\lambda}(r_\lambda) = E_{\lambda c_\lambda j_\lambda}\phi_{\lambda c_\lambda j_\lambda}(r_\lambda), \tag{5.55}$$

where $v_\lambda(r_\lambda)$ is the interatomic potential of the isolated $A_\nu A_\kappa$ diatomic molecule.
Let $\psi^{JM_J\lambda' b'_{\lambda'}}$ be a simultaneous eigenfunction of H, J^2_{op} and $J_{z_{op}}$ We can expand it asymptotically for large R_λ in terms of the surface functions according to:

$$\psi^{JM_J\lambda' b'_\lambda} \sim \sum_{\lambda b_\lambda}(R)^{-1}(g^{JM_J})^{\lambda' b'_{\lambda'}}_{\lambda b_\lambda}(R)\phi^{JM_J}_{\lambda b_\lambda}(\hat{\mathbf{R}}_\lambda, \mathbf{r}^{\mathbf{bf}}_\lambda), \tag{5.56}$$

where the radial functions g behave asymptotically as

$$\begin{aligned}(g^{JM_J})^{\lambda' b'_{\lambda'}}_{\lambda b_\lambda}(R_\lambda)R'_\alpha \overset{\sim}{\to} \infty v^{-1/2}_{\lambda c_\lambda j_\lambda}[&\mathcal{I}^J_{\lambda c_\lambda j_\lambda J}(R_\lambda)(A^{JM_J})^{\lambda' b'_{\lambda'}}_{\lambda b_\lambda} \\ &-\mathcal{O}^J_{\lambda c_\lambda j_\lambda J}(R_\lambda)B^{JM_J})^{\lambda' b'_{\lambda'}}_{\lambda b_\lambda}].\end{aligned} \tag{5.57}$$

This expression is the 3-PD counterpart of (5.11) where the symbols have similar meanings. As before, A and B are integration constants, v is the (real) velocity, k is the channel wave number given by an expression analogous to (5.12), and $\mathcal{I}$ and $\mathcal{O}$ are the incoming and outgoing waves given by

$$\mathcal{I}^J_{\lambda c_\lambda j_\lambda J}(R_\lambda) = \begin{cases} e^{-i[k_{\lambda c_\lambda j_\lambda}R_\lambda - \frac{1}{2}(J+j_\lambda)\pi]} \text{ for open channels} \\ e^{-|k_{\lambda c_\lambda j_\lambda}|R_\lambda} \text{ for closed channels}\end{cases} \tag{5.58}$$

$$\mathcal{O}^J_{\lambda c_\lambda j_\lambda J}(R_\lambda) = \begin{cases} e^{i[k_{\lambda c_\lambda j_\lambda}R_\lambda - \frac{1}{2}(J+j_\lambda)\pi]} \text{ for open channels} \\ e^{|k_{\lambda c_\lambda j_\lambda}|R_\lambda} \text{ for closed channels}\end{cases}. \tag{5.59}$$

The phase $\frac{1}{2}(J+j_\lambda)\pi$ in these expressions is introduced for convenience in simplifying subsequent expressions. We can rewrite (5.57) in matrix form as

$$\mathbf{g}^{JM_J} \sim \mathbf{v}^{-1/2}[\mathcal{I}^J\mathbf{A}^{JM_J} - \mathcal{O}^J\mathbf{B}^{JM_J}], \tag{5.60}$$

which is the 3-PD analog of (5.15), the corresponding matrices being defined similarly, with the rows and columns scanned by the quantum numbers λb_λ

and $\lambda' b'_{\lambda'}$ respectively. We now define an intermediate scattering matrix $\bar{\mathbf{S}}^J$ by

$$\mathbf{B}^{JM_J} = \bar{\mathbf{S}}^J \mathbf{A}^{JM_J} \tag{5.61}$$

and the body-fixed helicity scattering matrix $\bar{S}^J$ by

$$(\mathbf{S^J})_{\lambda c_\lambda j_\lambda m_{j_\lambda}}^{\lambda' c'_{\lambda'} j'_{\lambda'} m'_{j_{\lambda'}}} = (\bar{\mathbf{S}}^{\mathbf{J}})_{\lambda c_\lambda j_\lambda, \Omega_{j_\lambda} = m_{j_\lambda}}^{\lambda' c'_{\lambda'} j'_{\lambda'}, \Omega'_{j_{\lambda'}} = -m'_{j'_{\lambda'}}} . \tag{5.62}$$

The negative sign in the column label of this expression is introduced because as $R_{\lambda'} \sim \infty, \mathbf{R}_{\lambda'}$ and $\mathbf{k}_{\lambda' c'_{\lambda'} j'_{\lambda'}}$ become antiparallel. Again, as in the collinear case, the scattering matrix relates the coefficients of the outgoing waves to those of the incoming ones. It has a set of properties analogous to those of the collinear case. They are [124]:
(1) $\mathbf{S}^J$ is unique, i.e., is independent of $\mathbf{A^{JM_J}}$ and of M_J but depends on E and J.
(2) The open part $\mathbf{S}_o^J$ of $\mathbf{S}^J$ is symmetric. This property leads to the principle of microscopic reversibility.
(3) $\mathbf{S}_o^J$ is unitary.
This results in the conservation of particle flux. (5.60) can also be written as

$$\mathbf{g}^{JM_J} \sim \mathbf{v}^{-1/2}[\mathbf{S}^J \mathbf{C}^{JM_J} + \mathbf{C}^J \mathbf{D}^{JM_J}], \tag{5.63}$$

where $\mathbf{g}^{JM_J}$ and v are the same, $\mathbf{C}^{JM_J}$ and $\mathbf{D}^{JM_J}$ are new integration constant matrices and $\mathbf{S}^J$ and $\mathbf{C}^J$ are diagonal sine and cosine stationary wave matrices whose diagonal elements are given by

$$\mathcal{S}^J_{\lambda b_\lambda}(R_\lambda) = \begin{cases} \sin[k_{\lambda c_\lambda j_\lambda} R_\lambda - \frac{1}{2}(J + j_\lambda)\pi] & \text{for open channels} \\ e^{|k_{\lambda c_\lambda j_\lambda} R_\lambda|} & \text{for closed channels} \end{cases} \tag{5.64}$$

$$\mathcal{C}^J_{\lambda b_\lambda}(R_\lambda) = \begin{cases} \cos[k_{\lambda c_\lambda j_\lambda} R_\lambda - \frac{1}{2}(J + j_\lambda)\pi] & \text{for open channels} \\ e^{-|k_{\lambda c_\lambda j_\lambda} R_\lambda|} & \text{for closed channels} \end{cases} . \tag{5.65}$$

The reactance matrices are defined, by analogy to the scattering matrices, by

$$\mathbf{D}^{JM_J} = \mathbf{R}^J \mathbf{C}^{JM_J}, \quad (\mathbf{R}^J)_{\lambda c_\lambda j_\lambda m_{j_\lambda}}^{\lambda' c'_{\lambda'} j'_{\lambda'} m'_{j_{\lambda'}}} = (\bar{\mathbf{R}}^J)_{\lambda c_\lambda j_\lambda, \Omega_{j_\lambda} = m_{j_\lambda}}^{\lambda' c'_{\lambda'} j'_{\lambda'}, \Omega'_{j_{\lambda'}} = -m'_{j'_{\lambda'}}} . \tag{5.66}$$

The body-fixed helicity reactance matrix $\mathbf{R}^J$ has the following very important properties, analogous to those for the collinear case:
(1) $\mathbf{R}^J$ is unique;
(2) $\mathbf{R}^J$ is real; and
(3) the open part $\mathbf{R}_o^J$ of $\mathbf{R}^J$ is symmetric. The following relation, analogous to (5.21), is valid:

$$\mathbf{S}^J_\circ = (\mathbf{I} + i\mathbf{R}^J_\circ)(\mathbf{I} - i\mathbf{R}^J_\circ)^{-1}. \tag{5.67}$$

In addition, expressions analogous to (5.22) are valid.

5.9 Distinguishable atom scattering amplitudes and cross sections

From (5.49) and (5.56) - (5.62) we can derive the following expression fo r the scaled coordinate distinguishable-atom scattering amplitude for the $\lambda' n'_{\lambda'} \to \lambda n_\lambda$ transition in the body-fixed helicity representation [11]:

$$f^{\lambda' n'_{\lambda'}}_{\lambda n_\lambda}(\theta_\lambda, \phi_\lambda) = (\frac{v_{\lambda' c'_{\lambda'} j'_{\lambda'}}}{v_{\lambda, c_\lambda j_\lambda}})^{1/2} \frac{\exp(i m_{j_\lambda} \phi_\lambda)}{2k_{\lambda' c'_{\lambda'} j'_{\lambda'}}} i^{j'_{\lambda'} - j_\lambda + 1} \sum_{J=0}^{\infty} (2J+1) d^J_{m'_{j'_{\lambda'}} m_{j_\lambda}}(\theta_\lambda)(\mathbf{T}^J_0)^{\lambda' n'_{\lambda'}}_{\lambda n_\lambda} \quad (5.68)$$

where the transition matrix $\mathbf{T}^J_o$ is defined by

$$\mathbf{T}^J_\circ = \mathbf{I} - \mathbf{S}^J_\circ. \quad (5.69)$$

This expression is reminiscent of that for the scattering of a single particle by a central fi eld. Its simplicity results from the choice of the body-fixed helicity representation. The corresponding unscaled coordinate scattering amplitudes f' can be obtained from (5.68) and (5.51).
From (5.68), (5.51), and (5.52) we can derive the following expression for the $\lambda' n'_{\lambda'} \to \lambda n_\lambda$ distinguishable-atom differential cross section [11]:

$$\sigma^{\lambda' n'_{\lambda'}}_{\lambda n_\lambda}(\theta_\lambda) = (4k'^2_{\lambda' c'_{\lambda'} j'_{\lambda'}})^{-1} | \sum_{J=0}^{\infty} (2J+1) d^J_{m'_{j'_{\lambda'}} m_{j_\lambda}}(\theta_\lambda)(\mathbf{T}^J_0)^{\lambda' n'_{\lambda'}}_{\lambda n_\lambda} |^2, \quad (5.70)$$

where k' denotes the initial wave number in unscaled coordinates. Several consequences result from this expression. One of them deals with the nature of the dependence of σ on θ_λ We note that the functions $d^J_{m'_{j'_{\lambda'}} m_{j_\lambda}}$ are real and that the associated Legendre functions are particular cases of these d functions, with either m_{j_λ} or $m'_{j'_{\lambda'}}$ equal to zero [146]. The d^J terms display an oscillatory dependence on θ_λ the higher the value of J, the faster is the rate of oscillation. Nevertheless, for direct reactions, such as the distinguishable atom $H + H_2$ exchange reaction, the variation of σ with θ_λ is monotonic. The reason is that the phases and amplitudes of the $\mathbf{T}^J_o$ matrix elements bear a relationship to each other that leads, for such reactions, to the disappearance of the oscillations in σ. As a result, if differential cross sections devoid of spurious oscillations are to be obtained from ab initio quantum mechanical scattering calculations, a sufficiently accurate scattering matrix must be obtained from such calculations [111]. More specifically, not only must we accurately calculate the absolute values of its elements, but the corresponding phases must be determined accurately as well.
We also notice that although the scattering amplitudes depend on θ, the differential cross sections do not. The reason is that the initial probability density is cylindrically symmetric al around the quantization axis, and therefore so must the final one be, in the absence of extern al fields. In addition, since $d^J_{m'm}(0) = \delta_{m'm}$ and $d^J_{m'm}(\pi) = (-1)^{J+m}\delta_{m'-m}$ we conclude from (5.70) that for $m'_{j'_{\lambda'}} \neq m_{j_\lambda}, \sigma^{\lambda' n'_{\lambda'}}_{\lambda n_\lambda}(\pi)$ vanishes, and from $m'_{j'_{\lambda'}} \neq -m_{j_\lambda}, \sigma^{\lambda' n'_{\lambda'}}_{\lambda n_\lambda}(\pi)$

vanishes. These rigorous selection rules for forward and backward scattering are related to the conservation of J_z [111].
The integral cross section $Q_{\lambda n_\lambda}^{\lambda' n'_{\lambda'}}$, defined as the integral of the differential cross section over all scattering directions, can be obtained from (5.70) as

$$Q_{\lambda n_\lambda}^{\lambda' n'_{\lambda'}} = \frac{\pi}{k'^2_{\lambda' c'_{\lambda'} j'_{\lambda'}}} \sum_{J=0}^{\infty} (2J+1) |(\mathbf{T_0^J})_{\lambda n_\lambda}^{\lambda' n'_{\lambda'}}|^2. \tag{5.71}$$

In contrast to the differential cross section, we do not need accurate phases of the transitio n matrix to obtain accurate integral cross sections. Therefore, the latter cross sections are easier to calculate than the former.
The unitarity of $\mathbf{S}_o^J$ permits us to define the $\lambda' n'_{\lambda'} \to \lambda n_\lambda$ J partial wave reaction probability as

$$P_{\lambda n_\lambda}^{J^{\lambda' n'_{\lambda'}}} = |(\mathbf{S_0^J})_{\lambda n_\lambda}^{\lambda' n'_{\lambda'}}|^2 \tag{5.72}$$

in terms of which the $\lambda' n'_{\lambda'} \to \lambda n_\lambda$ integral cross section for transitions other than the elastic one (i.e., for $\lambda' n'_{\lambda'} \neq \lambda n_\lambda$) can be written as

$$Q_{\lambda n_\lambda}^{\lambda' n'_{\lambda'}} = \frac{\pi}{k'^2_{\lambda' c'_{\lambda'} j'_{\lambda'}}} \sum_{J=0} (2J+1) P_{\lambda n_\lambda}^{J^{\lambda' n'_{\lambda'}}}, \quad \lambda n_\lambda \neq \lambda' n'_{\lambda'}. \tag{5.73}$$

Both $\sigma_{\lambda n_\lambda}^{\lambda' n'_{\lambda'}}$ and $Q_{\lambda n_\lambda}^{\lambda' n'_{\lambda'}}$ may be averaged over the initial $m'_{j'_{\lambda'}}$ and summed over the final m_{j_λ} to give the degeneracy-averaged quantities $\sigma_{\lambda c_\lambda j_\lambda}^{\lambda' c'_{\lambda'} j'_{\lambda'}}$ and $Q_{\lambda c_\lambda j_\lambda}^{\lambda' c'_{\lambda'} j'_{\lambda'}}$ respectively. The latter can be written, for inelastic or reactive transitions, as

$$Q_{\lambda c_\lambda j_\lambda}^{\lambda' c'_{\lambda'} j'_{\lambda'}} = \frac{\pi}{k'^2_{\lambda' c'_{\lambda'} j'_{\lambda'}}} \sum_{J=0}^{\infty} (2J+1) P_{\lambda c_\lambda j_\lambda}^{J^{\lambda' c'_{\lambda'} j'_{\lambda'}}}, \quad \lambda c_\lambda j_\lambda \neq \lambda' c'_{\lambda'} j'_{\lambda'}, \tag{5.74}$$

where $P_{\lambda c_\lambda j_\lambda}^{J^{\lambda' c'_{\lambda'} j'_{\lambda'}}}$ is the opacity function defined as

$$P_{\lambda c_\lambda j_\lambda}^{J^{\lambda' c'_{\lambda'} j'_{\lambda'}}} = (2j'_{\lambda'} + 1)^{-1} \sum_{m_{j_\lambda} m'_{j'_{\lambda'}}} P_{\lambda n_\lambda}^{J^{\lambda' n'_{\lambda'}}}. \tag{5.75}$$

Although the last two expressions were obtained from the body-fixed helicity representation, the same degeneracy-averaged $Q_{\lambda c_\lambda j_\lambda}^{\lambda' c'_{\lambda'} j'_{\lambda'}}$ an partial wave opacity function $P_{\lambda c_\lambda j_\lambda}^{J^{\lambda' n'_{\lambda'} j'_{\lambda'}}}$ would have been obtained if we had started from other representations.
From the properties of the open part of the scattering matrix we can derive related properties
of the cross section, reaction probabilities, and opacity functions. From its unitarity we obt ain:
(1) Conservation of flux for body-fixed helicity transition probabilities,

$$\sum_{\lambda n_\lambda} P^{J^{\lambda' n'_{\lambda'}}}_{\lambda n_\lambda} = 1 \tag{5.76}$$

(2) Conservation of opacity,

$$\sum_{\lambda c_\lambda j_\lambda} P^{J^{\lambda' c'_{\lambda'} j'_{\lambda'}}}_{\lambda c_\lambda j_\lambda} = 1 \tag{5.77}$$

From the symmetry of $\mathbf{S}^J_o$ we obtain:
(3) Microscopic reversibility for body-fixed helicity transition probabilities,

$$P^{J^{\lambda' n'_{\lambda'}}}_{\lambda n_\lambda} = P^{J^{\lambda n_\lambda}}_{\lambda' n'_{\lambda'}} \tag{5.78}$$

(4) Microscopic reversibility for opacity functions,

$$(2j'_{\lambda'} + 1) P^{J^{\lambda' c'_{\lambda'} j'_{\lambda'}}}_{\lambda c_\lambda j_\lambda} = (2j_\lambda + 1) P^{J^{\lambda c_\lambda j_\lambda}}_{\lambda' c'_{\lambda'} j'_{\lambda'}} \tag{5.79}$$

(5) Microscopic reversibility for body-fixed integral helicity cross sections,

$$k'^2_{\lambda' c'_{\lambda'} j'_{\lambda'}} Q^{\lambda' n'_{\lambda'}}_{\lambda n_\lambda} = k'^2_{\lambda c_\lambda j_\lambda} Q^{\lambda n_\lambda}_{\lambda' n'_{\lambda'}} \tag{5.80}$$

(6) Microscopic reversibility for degeneracy-averaged integral cross sections,

$$(2j'_{\lambda'} + 1) k'^2_{\lambda' c'_{\lambda'} j'_{\lambda'}} Q^{\lambda' c'_{\lambda'} j'_{\lambda'}}_{\lambda c_\lambda j_\lambda} = (2j_\lambda + 1) k'^2_{\lambda c_\lambda j_\lambda} Q^{\lambda c_\lambda j_\lambda}_{\lambda' c'_{\lambda'} j'_{\lambda'}} \tag{5.81}$$

(7) Microscopic reversibility for body-fixed helicity differential cross sections,

$$k'^2_{\lambda' c'_{\lambda'} j'_{\lambda'}} \sigma^{\lambda' n'_{\lambda'}}_{\lambda n_\lambda}(\theta_\lambda) = k'^2_{\lambda c_\lambda j_\lambda} \sigma^{\lambda n_\lambda}_{\lambda' n'_{\lambda'}}(\theta_{\lambda'} = \theta_\lambda). \tag{5.82}$$

(5.76) - (5.82) relate properties of forward ($\lambda' \to \lambda$) and backward ($\lambda \to \lambda'$) processes occurring at the same total energy E, and care must be taken not to apply them, by mistake, to such collisions occurring at equal translational energies.

5.10 Cross sections for systems containing identical atoms

If the three atoms of the triatomic system being considered are not all distinguishable, we must include the effects of the Pauli principle on the reactive scattering problem. The interaction energies between the nuclear spin and the orbital motions are in general several orders of magnitude smaller than the Born-Oppenheimer interaction potential in the regions of configuration space of interest to the scattering process. We will therefore neglect those spin-orbit interactions in the present considerations. Under these conditions, the Pauli principle may be introduced by the techniques of post-antisymmetrization (for identical fermions) or post-symmetrization (for identical bosons). For example, for the H_3 system, there are only two independent sets of distinguishable scattering amplitudes: reactive (or exchange) f'^R and nonreactive (or direct), ${f'}^N$. The appropriately antisymmetrized scattering wave functions can be obtained by taking linear combinations of those of the distinguishable atom (Kuppermann et al., 1976), and, as a result, the correct antisymmetrized differential cross sections can be expressed in terms of t he ${f'}^R$ and ${f'}^N$ [11] as:

(1) para $\rightarrow$ para(j', j even)

$$\sigma_{pn}^{pn'} = \frac{v'_{cj}}{v'_{c'j'}} |{f'_n}^{Nn'} - {f'_n}^{Rn'}|^2 \tag{5.83}$$

(2) para $\rightarrow$ ortho (j' even j odd)

$$\sigma_{on}^{pn'} = 3\frac{v'_{cj}}{v'_{c'j'}} |{f'_n}^{Rn'}|^2 \tag{5.84}$$

(3) ortho $\rightarrow$ para (j' odd, j even)

$$\sigma_{pn}^{on'} = \frac{v'_{cj}}{v'_{c'j'}} |{f'_n}^{Rn'}|^2 \tag{5.85}$$

(4) ortho $\rightarrow$ ortho (j', j odd)

$$\sigma_{on}^{on'} = \frac{v'_{cj}}{v'_{c'j'}} (|{f'_n}^{Nn'} + {f'_n}^{Rn'}|^2 + 2|{f'_n}^{Rn'}|^2). \tag{5.86}$$

In these expressions, the indices λ and λ' were omitted, due to the identicity of the three atoms. As before, the v' quantities are the channel velocities and n stands for the set of diatom quantum numbers c, j, m in the body-fixed helicity representation. Although the calculations that furnish the ${f'}^R$ and ${f'}^N$ are for distinguishable atoms, for which the Pauli principle is ignored, (5.83) - (5.86) furnish the correct cross sections, which can be comp ared with experimental results. It should be noticed that in (5.83) and (5.86), to which both ${f'}^N$ and ${f'}^R$ contribute, interference effects between these two scattering amplitudes are present due to the ${f'}^N \pm {f'}^R$ terms.

5.11 Computational methodology

So far we have indicated how once the scattering matrix of a reactive system is known, the scattering amplitudes and cross sections can be obtained. In this section we outline how that matrix can be calculated once the system's electronically adiabatic potential energy function $V_\lambda(R_\lambda, r_\lambda, \gamma_\lambda)$ is known.
As in the collinear case, several approaches are possible. However, only three coupled-channel methods have been used so far in crosssection calculations for 3-PD systems. One of them, developed by Elkowitz and Wyatt [147, 148], uses natural collision coordinates (NCC) and local hindered asymmetric-top-vibrator basis sets, as reviewed recently by Wyatt [42]. Another, developed by Kuppermann and Schatz [110], uses asymptotic free rotor and local vibrator

basis sets, and different coordinates in different regions of configuration space, similar to those described in earlier sections. The advantage of Elkowitz and Wyatt's approach is that their basis functions furnish an efficient representation of the local motion and contain very useful interpretive information in the form of asymmetric top-rotational energy correlation diagrams. However, the NCC are more cumbersome to use in the representation of the potential energy function and in the calculation of the matrix elements that appear in the coupled-channel equations. The third method was developed by Walker et al. [52, 149] and has elements in common with both the Elkowitz and Wyatt and the Kuppermann and Schatz approaches. Here we review Schatz and Kuppermann [11]. We first define the complete discrete orthonormal body-fixed basis set:

$$\mathcal{Y}^{JM_J}_{j_\lambda \Omega_\lambda}(\theta_\lambda, \phi_\lambda, \gamma_\lambda, \psi_\lambda) = \left(\frac{2J+1}{4\pi}\right)^{1/2} D^J_{M_J \Omega_\lambda}(\phi_\lambda, \theta_\lambda, 0) Y_{j_\lambda \Omega_\lambda}(\gamma_\lambda, \psi_\lambda). \tag{5.87}$$

These are simultaneous eigenfunctions of the operators $J^2_{op}, J_{z_{op}}$ and $j^2_{\lambda_{op}}$ defined at the beginning of an earlier section. They span the 4-MD subspace degned by the angular coordinates $\theta_\lambda, \phi_\lambda, \gamma_\lambda, \psi_\lambda$. We now expand, in this basis set, the wave functions $\psi^{JM_J}_\lambda$ which are simultaneous eigenfunctions of H, J^2_{op} and $J_{z_{op}}$ expressed in λ arrangement channel coordinates $\mathbf{R}_\lambda, \mathbf{r}^{\mathrm{bf}}_\lambda$:

$$\psi^{JM_J}_\lambda(\mathbf{R}_\lambda, \mathbf{r}^{\mathrm{bf}}_\lambda) = \sum_{\Omega_\lambda=-J}^{J} \sum_{j_\Omega=|\Omega_\lambda|}^{\infty} (R_\lambda r_\lambda)^{-1} F^J_{\lambda j_\lambda \Omega_\lambda}(R_\lambda, r_\lambda) \mathcal{Y}^{JM_J}_{j_\lambda \Omega_\lambda}(\theta_\lambda, \phi_\lambda, \gamma_\lambda, \psi_\lambda). \tag{5.88}$$

Replacement of this expansion in the Schrödinger equation furnishes the following set of coupled-channel partial differential equations for the functions $F^J_{\lambda j_\lambda, \Omega_\lambda}$

$$t^{J\lambda j_\lambda}_{\Omega_\lambda, \Omega_{\lambda-1}} F^J_{\lambda j_\lambda, \Omega_{\lambda-1}} + t^{J\lambda j_\lambda}_{\Omega_\lambda, \Omega_\lambda} F^J_{\lambda j_\lambda, \Omega_\lambda} + t^{J\lambda j_\lambda}_{\Omega_\lambda, \Omega_{\lambda+1}} F^J_{\lambda j_\lambda, \Omega_{\lambda+1}} + \sum_{j'\lambda} V^{\lambda \Omega_\lambda}_{j_\lambda j'_\lambda} F^J_{\lambda j_\lambda, \Omega_\lambda} = E F^J_{\lambda j_\lambda, \Omega_\lambda}, \tag{5.89}$$

where the kinetic energy operators t are given by

$$t^{J\lambda j_\lambda}_{\Omega_\lambda, \Omega_\lambda}(R_\lambda, r_\lambda) = -\frac{\hbar^2}{2\mu}\left(\frac{\partial^2}{\partial R^2_\lambda} + \frac{\partial^2}{\partial r^2_\lambda}\right) + \frac{j_\lambda(j_\lambda+1)\hbar^2}{2\mu r^2_\lambda} + \frac{\hbar^2}{2\mu R^2_\lambda}[J(J+1) - 2\Omega^2_\lambda + j_\lambda(j_\lambda+1)] t^{J\lambda j_\lambda}_{\Omega_\lambda, \Omega_{\lambda \pm 1}}(R_\lambda) = -\frac{\hbar^2}{2\mu R^2_\lambda} \xi_\pm(J, \Omega_\lambda) \xi_\pm(j_\lambda, \Omega_\lambda)$$

$$\xi_\pm(j, m) = [j(j+1) - m(m \pm 1)^{1/2}], \ |m| \le j \tag{5.90}$$

and the potential energy function matrix element $V^{\lambda \Omega_\lambda}_{j_\lambda j'_\lambda}$ is

$$V^{\lambda \Omega_\lambda}_{j_\lambda j'_\lambda}(R_\lambda, r_\lambda) = (j_\lambda \Omega_\lambda | V_\lambda(R_\lambda, r_\lambda, \gamma_\lambda) | j'_\lambda \Omega_\lambda). \tag{5.91}$$

In (5.89), $t^{J\lambda j_\lambda}_{\Omega_\lambda,\Omega_{\lambda\pm 1}}$ terms are centrifugal coupling terms that are independent of V and couple $F^J_{\lambda j_\lambda,\Omega_\lambda}$ with $F^J_{\lambda j_\lambda,\Omega_{\lambda\pm 1}}$ They depend only on R_λ and the quantum numbers $J, j_\lambda, \Omega_\lambda$. For reactive systems, the range of total angular momentum quantum numbers J that contribute appreciably to the reactive cross sections is usually much smaller than that which contributes to non-reactive inelastic cross sections, and in many instances these $t^{J\lambda j_\lambda}_{\Omega_\lambda,\Omega_{\lambda\pm 1}}(R_\lambda)$ terms can be neglected. In this case (5.89) becomes diagonal in Ω_λ i.e. the $F^J_{\lambda j_\lambda,\Omega_\lambda}$ for different tumbling angular momenta in arrangement channel λ are decoupled, since the $V^{\lambda\Omega_\lambda}_{j_\lambda j'_\lambda}$ do not couple such functions. This leads to the tumbling decoupling approximation.
(5.89) contains the same two distances R_λ, r_λ as did the Schrödinger equation for collinear triatomic systems. The main difference is that instead of a single equation, we now have, for each J, a system of coupled equations scanned by the rotational quantum numbers j_λ and Ω_λ. The potential energy function couples different j_λ (because of its dependence on γ_λ whereas the angular-momentum tumbling centrifugal terms couple different Ω_λ. In addition, instead of only two arrangement channels (reagents and reactive products), we now have three such channels (one reagent and two product arrangements). The method of solution of these coupled-channel equations is described most easily by considering the internal configuration space $R_\lambda, r_\lambda, \gamma_\lambda$ in the symmetrized hyperspherical coordinate mapping of an earlier section, whose coordinate axes are $X_\lambda Y_\lambda Z_\lambda$ (not to be confused with the axis of Fig. 5.2. In Fig. 5.3, we indicate an outline of a equipotential on the $X_\lambda Z_\lambda$ plane (which coincides with the $X_\nu Z_\nu$ and $X_k Z_k$ planes), and the intersection with that plane of three halfplanes, labeled $\pi_{\lambda\nu}, \pi_{\nu k}$, and $\pi_{k\lambda}$ whose common edge is the Y_λ, axis (which coincides with the Y_ν, and Y_k axes), perpendicular to the plane of the figure. These half-planes divide the internal configuration space into three arrangement-channel subspaces, λ, ν and k. When augmented by the $\theta_\lambda, \phi_\lambda, \psi_\lambda$ space they define three subspaces of the total configuration space. The method of solution consists of integrating the coupled (5.89) over the range of R_λ, r_λ which, together with γ_λ, spans the λ arrangement-channel subspace. This integration is performed by dividing the R_λ, r_λ subspace into regions, as was done in the collinear case, and using appropriate variables and basis sets in each region (Schatz and Kuppermann [11]). We thereby get, in each region, a set of coupled ordinary differential equations that can be integrated numerically by the use of an appropriate efficient algorithm, such as that of Gordon [144] or Light and Walker [142]. This procedure generates a set of linearly independent wave functions $\psi^{JM_J}_{\lambda b_\lambda}(\mathbf{R}_\lambda, \mathbf{r^{bf}}_\lambda)$ that span the λ arrangement-channel subspace, but do not cover the entire configuration space. We similarly generate wave functions $\psi^{JM_J}_{\nu b_\nu}(\mathbf{R}_\nu, \mathbf{r}^{\mathrm{bf}}_\nu)$ and $\psi^{JM_J}_{k b_k}(\mathbf{R}_k, \mathbf{r}^{\mathrm{bf}}_k)$ that span the ν and k arrangement-channel Subspaces. These λ, ν and k solutions overlap on the $\pi_{\lambda\nu}, \pi_{\nu k}$ and $\pi_{k\lambda}$ half-planes, but have in general different values on those surfaces. In order to generate solutions

of the Schrödinger equation for a given J and M_J, which are everywhere continuous and smooth, we take linear combinations of the $\psi^{JM_J}_{\lambda b_\lambda}(R_\lambda, r^{\mathrm{bf}}_\lambda)$ in the λ arrangement-channel subspace, of the $\psi^{JM_J}_{\nu b_\nu}(R_\nu, r^{\mathrm{bf}}_\nu)$ in the ν subspace and of the $\psi^{JM_J}_{k b_k}(R_k, r^{\mathrm{bf}}_k)$ in the k subspace and impose on these three different sets of linear combinations the conditions that they be continuous on the $\pi_{\lambda\nu}, \pi_{\nu k}$ and $\pi_{k\lambda}$ half-planes and that their derivatives normal to these half-planes also be continuous. In this manner, we generate solutions of the Schrödinger equation at a given energy E that are also eigenfunctions of J^2_{op} and $J_{z_{op}}$ corresponding to the quantum numbers J and M_J, respectively, and that are everywhere smoothly continuous. An examination of the asymptotic behavior of these solutions, as described in the section (scattering and reactance matrices), furnishes the desired reactance and scattering matrices. From these, the scattering amplitudes and cross sections are obtained.

5.12 Results for $H + H_2$

In the 1970ies the only system for which accurate 3-PD quantum mechanical reactive scattering cross-section calculations had been performed was the $H + H_2$ system. Such calculations had been done independently by three groups, using three different methods: (a) by Kuppermann and Schatz (KS) [150, 111] using the methodology described in the last sections, (b) by Elkowitz and Wyatt (EW) [147, 148] using a natural collision coordinate method and rotationally adiabatic basis functions. Both groups used the Porter-Karplus H_3 surface (Porter and Karplus [151]). KS expanded it in Legendre polynomials of y, using enough terms for convergence of the results to be achieved. Elkowitz and Wyatt cast the surface in a mathematical form, in terms of natural collision coordinates, convenient for the calculations. As a result, the two surfaces as actually used are not quite the same, differing nonnegligibly from one another in the saddle-point region. KS used sufficient vibrational basis functions in the calculation to achieve convergence of the results to within about 5 %. This required between four and six vibrational basis functions. The third group, Walker et al. [149], reported results on the Porter-Karplus and the SLTH (Truhlar and Horowitz [152]) potential energy surfaces. Further information on these "historical" implementations are given by Wyatt in [4]. References to new calculations on improved surfaces will be presented in later chapters.

A.1 List of abbreviations

BCRLM - bending corrected linear model
BF - body-fixed
BO - Born-Oppenheimer
CG - Clebsch-Gordan

CRP - cumulative reaction probability
DCS - differential cross section
DIM - diatomics-in-molecules
GP - geometric phase
LAB - laboratory
NGP - non geometric phase
PD - physical dimension
PDE - partial differential equation
PES - potential energy surface
QM - quantum mechanical
RIOSA - reactive infinite order sudden approximation
SE - Schrödinger equation
SF - space-fixed
TDSE - time-dependent Schrödinger equation
TISE - time-independent Schrödinger equation

A.2 Credits

The following work from the literature was in some parts extracted and built into this review:

(a) "Manolopoulos, D.E. and Clary, D.C.: *Ann. Rep. C Roy. Soc. of Chem.* **80** (1989) 95" contributed to chapter 1.1, 5.3, 5.4 and 13.
(b) "Mrugala, F.: *Int. Rev. Phys. Chem.* **12** (1993) 1" contributed to chapter 1.2.
(c) "Miller, W.H. in: *Frontiers in Chemical Dynamics*, Yurtsever, E. (Ed.), NATO ASI Series C470 (Kluwer, Dordrecht, 1995)" contributed to chapter 2.1, 2.2 and 2.3.
(d) "Kuppermann, A. in: *Theoretical Chemistry and Perspectives*, 6A, D. Henderson (Ed.) (Academic, NY, 1981)" contributed to chapters 4.5 and 5.

References

1. Baer, M. (Ed.) in: *Theory of Chemical Reaction Dynamics*, Vols. I-IV, CRC Press, Boca Raton, FL, 1985.
2. Clary, D.C. (Ed.) in: *The Theory of Chemical Dynamics* (Reidel,Dordrecht, 1986).
3. Miller, W.H. (Ed.) in : *Dynamics of Molecular Collisions*, Parts A and B (Vols. 1 and 2 of Modern theoretical Chemistry) (Plenum, NY, 1976).
4. Bernstein, R.B. (Ed.) in: *Atom-Molecule Collision Theory: a Guide for the Experimentalist* (Plenum, NY, 1979).
5. Bowman, J.M. (Ed.) in: *Advances in Molecular Vibrations and Collision Dynamics*, Vol. 2 (JAI Press, Greenwich, CT, 1994).

6. Zhang, J.Z.H. and Wyatt, R.E. (Eds.) in: *Dynamics of molecules and chemical reactions* (Dekker, 1996).
7. Tsipis, C.A., Popov, V.S., Herschbach, D.R., Avery, J.S. (Eds.) in: *New methods in quantum theory*, NATO ASI Series 3/8 (Kluwer, Dordrecht, 1997).
8. Cerjan, C. (Ed.) in: *Numerical Grid Methods and their Application to Schrödinger's Equation*, NATO ASI Series C 412 (Kluwer, Dordrecht, 1993).
9. Lagana, A. (Ed.) in: *Supercomputer algorithms for reactivity, dynamics and kinetics of small molecules* (Kluwer, Dordrecht, 1989).
10. Kuppermann, A. in: *Theoretical Chemistry and Perspectives*, **6A**, Henderson, D. (Ed.) (Academic, NY 1981) p. 79.
11. Schatz, G.C., Kuppermann, A.: *J. Chem. Phys.* **65** (1976) 4642.
12. Kouri, D.J., Hoffman, D.K. in: *Multiparticle quantum scattering with applications to nuclear, atomic and molecular physics*, Truhlar, D.G., Simon B. (Eds.) (Springer, NY, 1997).
13. Miller, W.H. in: *Frontiers in Chemical Dynamics*, ed. Yurtsever, E., NATO ASI Series C470 (Kluwer, Dordrecht, 1995)
14. Manolopoulos, D.E. and Clary, D.C., *Ann. Rep. C Roy. Soc. of Chem.* **80** (1989) 95.
15. Mrugala, F.: *Int. Rev. Phys. Chem.* **12** (1993) 1.
16. Launay, J.M. in: *Dynamical Processes in Molecular Physics*, ed. G. Delgado-Barrio (Institute of Physics Publishing Bristol and Philadelphia, 1991) p. 97.
17. Jaquet, R., Kumpf, A., Heinen, M.: *J. Chem. Soc., Farad. Trans.* **93** (1997) 1027.
18. Levine, R.D., Bernstein, R.B. in: *Molecular Reaction Dynamics* (Oxford, 1974).
19. Secrest, D. in [4].
20. Truhlar, D.G., Muckerman in [4].
21. Micha, D.: *Adv. Chem. Phys.* **30** (1975) 7.
22. Kouri, D.J., Baer, M.: in [2] p. 359.
23. Marcus, R. A.: 1966: *J. Chem. Phys.* **45** (1966) 4493, 4500.
24. Light, J.C. in: *Methods in Computational Physics*, Vol. 10, B. Alder, B., Fernbach, S., Rotenberg, M. (Eds.) (Academic,NY, 1971) p. 111.
25. Smith, F.T.: *Phys. Rev.* **118** (1960) 349.
26. Smith, F.T.: *Phys. Rev.* **120** (1960) 1058; **179** (1969) 111.
27. Johnson, B.R.: *J. Comput. Phys.* **13** (19730 445; *J. Chem. Phys.* **67** (1978) 4086; **69** (1978) 4678; **73** (1980) 5051.
28. Walker, R.B., Light, J.C.: *Ann. Rev. Phys. Chem.* **31** (1980) 401.
29. Baer, M.: *Adv. Chem. Phys.* **49** (1982) 191; *Phys. Rev.* **178** (1989) 99.
30. Basilevsky, M. V., Ryaboy, V. M., 1982, in: *Adv. Quant.Chem.* edited by P. 0. Löwdin (NY: Academic), Vol. 15, p. 1.
31. Zhang, J.Z.H., Miller, W.H. : *Chem. Phys. Lett.* **140** (1987) 329.
32. Zhang, J.Z.H., Miller, W.H. : *J. Chem. Phys.* **91** (1989) 1528; 1990, Ibid., 92, 1811.
33. Taylor, J.R. in: Scattering Theory (Wiley, NY, 1972).
34. Manolopoulos, D.E., Wyatt, R.E.: *Chem. Phys. Lett.* **152** (1988) 23 ; 159, (1989) 123; *J. Chem. Phys.* **91** (1989) 6096; **93** (1990) 403.
35. Linderberg, J., Padkjaer, S.B., Öhrn, Y.,, Vessal, B. : *J. Chem. Phys.* **90** (1989) 6254.
36. Schwenke, D.W., Haug, K., Zhao, M., Truhlar, D. G., Sun, Y., Kouri, D.J. : *J. Phys. Chem.* **92** (1988) 3202.
37. Zhang, J.Z.H., Kouri, D.J., Haug, K., Schwenke, D. W., Shima, Y., Truhlar, D. G. : *J. Chem. Phys.* **88** (1988) 2492.
38. Schwenke, D. W., Mladenovic, M., Zhao, M., Truhlar, D.G., Sun, Y., Kouri, D.J. in: [9] p. 131.

39. Sun, Y., Kouri, D.J., Truhlar, D. G., Schwenke, D. W. : *Phys. Rev. A.* **41** (1990) 4837.
40. Sun, Y., Kouri, D.J., Truhlar, D.G.: *Nucl. Phys. A* **508** (1990) 410.
41. Lester, W. A. JR. in: Methods in Computational Physics, 10, edited by B. Adler, S. Fernbach and M. Rotenberg (NY: Academic, 1971); 1976, Dynamics of Molecular Collisions, Part, A, edited by Miller, W.H. (NY: Plenum), p. 1.
42. Wyatt, R.E. in: [4] p.477.
43. Schatz, G.C. in: [2] p. 1.
44. Schatz, G.C.: *Chem. Phys. Lett.* **150** (1988) 92.
45. Schatz, G.C.: *J. Chem. Phys.* **90** (1989) 3582.
46. Pack, R.T., Parker G.A.: *J. Chem. Phys.* **87** (1987) 3888.
47. Pack, R.T., Parker, G.A.: *J. Chem. Phys.* **90** (1989) 3511.
48. Parker, G.A., Pack, R.T., Archer, B. J., Walker, R.B. : *Chem. Phys. Lett.* **137** (1987) 564.
49. Bacic, Z., Kress, J. D., Parker, G.A., Pack, R.T.: *J. Chem. Phys.* **92** (1990) 2344.
50. Darakjian, Z., Hayes, E.F., Parker, G.A., Butcher, E.A., Kress, J.D. : *J. Chem. Phys.* **95** (1991) 2516.
51. Elkowitz, A.B., Wyatt, R.E.: *J. Chem. Phys.* **63** (1975) 702.
52. Walker, R.B., Light, J.C., Altenberger-Sizek, A. : *J. Chem. Phys.* **64** (1976) 1166.
53. Light, J.C., Walker, R.B. : *J. Chem. Phys.* **63** (1976) 1598; Ibid., **65** (1976) 4272.
54. Kuppermann, A., Kaye, J.A., Dwyer, J.P. : *Chem. Phys. Lett.* **74** (1980) 257.
55. Kuppermann, A., Hipes, P.G. : *J. Chem. Phys.* **84** (1986) 5962.
56. Cuccaro, S.A., Hipes, P.G., Kuppermann, A. : *Chem. Phys. Lett.* **154** (1989) 155.
57. Hauke, G., Manz, J., Römelt, J. : *J. Chem. Phys.* **73** (1980) 5040.
58. Römelt, J.: *Chem. Phys. Lett.* **74** (1980) 263; Ibid., **87** 259.
59. Diestler, D.J. : *J. Chem. Phys.* **54** (1971) 4547.
60. Stechel, E.B., Schmalz, T.G., Light, J.C.: *J. Chem. Phys.* **70** (1979) 5640.
61. Top, Z.H., Shapiro, M. : *J. Chem. Phys.* **77** (1983) 5009.
62. Schwenke, D.W., Truhlar, D.G., Kouri, D.J.: *J. Chem. Phys.* **86** (1987) 2772.
63. Y. T. Lee, et al.: *J. Chem. Phys.* **53** (1970) 2123 ; **53** (1970) 3755 ; **55** (1971) 5762; **56** (1972) 1511; **56** (1972) 5801; **59** (1973) 601.
64. Bernstein, R.B., *Adv. Chem. Phys.* **10** (1966) 75.
65. Ford, K.W. and Wheeler, J.A.: *Ann. Phys.* **7** (1959) 259, 287.
66. Berry, M.V., Mount, K.E.: *Rept. Prog. Phys.* **35** (1972) 315.
67. (a) Child M.S. in : *Semiclassical Mechanics with Molecular Applications* (Oxford U. P., 1991). (b) Miller, W.H.: *Science* **233** (1986) 171.
68. (a) Robinson, P.A., Holbrook, R.A. in: *Unimolecular Reactions* (Wiley, NY, 1972). (b) Forst, W. in: *Theory of Unimolecular Reactions* (Academic, NY, 1973). (c) Gilbert, R.G., Smith, S.C. in: *Theory of Unimolecular and Recombination Reactions* (Blackwell, Oxford, 1990).
69. Troe, J.: *J. Chem. Phys.* **97** (1992) 288 and references therein.
70. (a) Lester, W.A. in: [3], p. 1. (b) Light, J.C. in: [4] p. 239. (c) Secrest, D. in: [4] p. 265, 377.
71. (a) Porter, R.N., Raff, L.M. in: [3] p. 1. (b) Hase, W.H. in: [3] p. 121. (c) Pattengill, M.D. in: [4] p. 359. (d) Raff, L.M., Thompson, D.L. in: [1] Vol. III, p. 2.
72. (a) Micha, D.A. in: [3] p. 81. (b) Shin, H.K. in: [3] p. 131. (c) Wyatt, R.E. in: [4] p. 477. (d) Jellinek, J., Kouri, D.J. in: [1] Vol. II, p. 1.
73. Miller, W.H.: *Adv. Chem. Phys.* **25** (1974) 69; **30** (1975) 77.
74. Miller, W.H.: *Ann. Rev. Phys. Chem.* **41** (1990) 245.

75. Lester, W.A. in: [3] p. 1.
76. Light, J.C. in: [4] p. 239.
77. Secrest, D. in: [4] p. 265, 377.
78. Miller, W.H.: *J. Chem. Phys.* **50** (1969) 407.
79. Burke Taylor 1966
80. Tang Mehre Thompson 1978
81. Wolken, G., Karplus, M.: *J. Chem. Phys.* **60** (1974) 351.
82. Miller, W.H., B.M.D.D. Jansen op de Haar: *J. Chem. Phys.* **86** (1987) 6213.
83. Zhang, J.Z.H., S.I. Chu, Miller, W.H.: *J. Chem. Phys.* **88** (1988) 6233.
84. Zhang, J.Z.H., Miller, W.H.: *J. Chem. Phys.* **91** (1989) 1528.
85. (a) Truhlar, D.G., Kouri, D.J. et al.: *J. Chem. Phys.* **91** (1989) 1643. (b) Truhlar, D.G., Kouri, D.J. et al.: *J. Phys. Chem.* **92** (1988) 3202.
86. Mielke, S.L., Truhlar, D.G., D. W. Schwenke: *J. Phys. Chem.* **98** (1994) 1053.
87. Launay, J.M., Le Dournef, M.: *Chem. Phys. Lett.* **169** (1990) 473.
88. Pack, R.T., Butcher, E.A., BParker, G.A.: *J. Chem. Phys.* **99** (1993) 9310.
89. Kuppermann, A. in: [5], earlier references therein.
90. Miller, W.H., *Accts. Chem. Res.* **26** (1993) 174.
91. (a) Miller, W.H., Schwartz, S.D., Tromp, J.W.: *J. Chem. Phys.* **79** (1983) 4889. (b) T. Seideman and Miller, W.H.: *J. Chem. Phys.* **96** (1992) 4412; **97** (1992) 2499.
92. Manthe, U. and Miller, W.H.: *J. Chem. Phys.* **99** (1993) 3411.
93. Thirumalai, D., Garrett, B.C., Berne, B.J.: *J. Chem. Phys.* **83** (1985) 2972.
94. Mandelshtam, V.A., Taylor, H.S.: *J. Chem. Phys.* **99** (1993) 222.
95. Jordan, T.F. in: *Linear Operators for Quantum Mechanics* (Wiley, NY, 1969)
96. Extensive references and many recent papers describing computational methods for the TDSE can be found in Time-Dependent Quantum Molecular Dynamics, eds. J. Broeckhove and L. Lathouwers, NATO ASI Series B: Physics Vol. 299 (Plenum, NY, 1992) and in the thematic volume of Computer Physics Communications, Ed. K. Kulander, Vol. 63 (North-Holland, Amsterdam, 1991).
97. Newton, R.G. in: Scattering Theory of Waves and Particles (Springer, NY, 1982).
98. Powell, J.L., Crasemann, B., in: Quantum Mechanics (Addison-Wesley, Reading, MA, 1961) pp. 96-98.
99. Secrest, D. in: [4], chap. 8.
100. Miller, W.H.: *Annu. Rev. Phys. Com.* **41** (1990) 245.
101. Schatz, G.C.: *J. Chem. Phys.* **90** (1988) 1237, 4847.
102. Castillo, J.F., Manolopolous, D.E.: Faraday Discuss. **110** (1998) 119.
103. Baer, M., ed. in: Theory of Chemical Reaction Dynamics, Vol 1, CRC Press, Boca Raton, Fl, 1985 .
104. Delves, L.M.: Nucl. Phys., 1959, 9, 391; 1960, 20, 275.
105. Kuppermann, A. in: 'Potential Energy Surfaces and Dynamics Calculations', ed. Truhlar, D.G., Plenum Press, NY, 1981, p. 375.
106. Aquilanti in: [5].
107. Clary in: [5].
108. Kuppermann in [6].
109. Pack, R.T., Parker, G.A.: *J. Chem. Phys.* **87** (1987) 3888.
110. Kuppermann, A., Schatz. G.C.: *J. Chem. Phys.* **62** (1975) 2502.
111. Schatz, G.C., Kuppermann, A. (1976). *J. Chem. Phys.* **65** 4668.
112. (a) A. B. Elkowitz and Wyatt, R.E.: *J. Chem. Phys.* **62** (1975) 2504; **62** (1975) 3683; (b) S. A. Harms and Wyatt, R.E.: *J. Chem. Phys.* **62** (1975) 3162; **62** (1975) 3173.
113. Walker et al 1978.
114. Marcus, R.A.: *J. Chem. Phys.* **45** (1966) 4493.

115. Child, M.S. in: 'Molecular Collision Theory', Academic Press, London, 1974, chap. 10.
116. Light, J.C., Walker, R.B.: *J. Chem. Phys.* **65** (1976) 472; Stechel, E.B., Walker, R.B., Light, J.C.: *J. Chem. Phys.* **69** (1978) 3518.
117. Light, J.C., Walker, R.B., Stechel, E.B., Schmalz, T.G., Comp. Phys. Comm, , **17** (1979) 89; Lill, J.V., Schmalz, T.G., Light, J.C.: *J. Chem. Phys.* **78** (1983) 4456.
118. Walker, R.B., Light, J.C.. *Ann. Rev. Phys. Chem.* **31** (1980) 401.
119. Stechel, E.B., Webster, F., Light, J.C.. *J. Chem. Phys.* **88** (1988) 1824.
120. Webster, F., and Light, J.C.: *J. Chem. Phys.* **90** (1989) 265.
121. Webster, F., Light, J.C.: *J. Chem. Phys.* **90** (1989) 300.
122. Delves, L. M. : Nucl. Phys. 9, (1959) 391; Nucl. Phys. 20, (1960) 275.
123. Kuppermann, A. : *Chem. Phys. Lett.* **32** (1975) 374.
124. Lane, A. M., Thomas, R. G. : Rev. Mod. Phys. **30** (1958) 257.
125. Mortensen. E. M., Pitzer, K.S. : J. Chem. Soc., Spec. Publ. 16, (1962) 57-75.
126. Mortensen, E. M. : *J. Chem. Phys.* **48** (1968) 4029.
127. Diestler, D.J., McKoy, V.: *J. Chem. Phys.* **48** (1968) 2951.
128. Truhlar, D.G., Kuppermann, A.: *J. Chem. Phys.* **52** (1970) 3841.
129. Truhlar, D. G., Kuppermann, A. : *J. Chem. Phys.* **56** (1972) 2232.
130. Truhlar, D.G., Kuppermann, A., Adams, J.T. : *J. Chem. Phys.* **59** (1973) 395.
131. McCullough, E. A., Jr., Wyatt, R. E.: *J. Chem. Phys.* **51** (1969) 1253.
132. McCullough, E. A., Jr., Wyatt, R. E. : *J. Chem. Phys.* **54** (1971) 3578, 3592.
133. Sams, W. M., Kouri, D.J. : *J. Chem. Phys.* **51** (1969) 4809, 4815.
134. Adams, J.T., Smith, R.L., Hayes, E. F.: *J. Chem. Phys.* **61** (1974) 2193.
135. Mortensen. E.M., Gucwa, L.D.: *J. Chem. Phys.* **51** (1969) 5695.
136. Askar, A., Cakmak, A.S., Rabitz, H.A. : *Chem. Phys.* **33** (1978) 267.
137. Rankin, C. C., Light, J.C.: *J. Chem. Phys.* **51** (1969) 1701.
138. Miller, G., Light, J.C.: *J. Chem. Phys.* **54** (1971) 1635, 1643.
139. Kuppermann, A. (1970) in: "Proceedings of the Conference on Potential Energy Surfaces in Chemistry" (Lester, W.A., ed.), pp. 121-124. University of California, Santa Cruz.
140. Kuppermann, A. (1972). Proc. Int. Com. Phys. Electron. At. Collisions, 7th, 1971. pp. 3-5.
141. Johnson, B.R.: *Chem. Phys. Lett.* **13** (1972) 172.
142. Light, J.C., Walker, R. B.: *J. Chem. Phys.* **65** (1976) 4272.
143. Eyring, H. : *J. Chem. Phys.* **3** (1935) 107.
144. Gordon, R.G. : *J. Chem. Phys.* **51** (1969) 14.
145. Pack, R,T. : *J. Chem. Phys.* **60** (1974) 633.
146. Davydov, A.S. in: *Quantum Mechanics* chap. VI (Addison Wesley, Reading, MA, 1965).
147. Elkowitz, A.B., Wyatt, R. E. (1975). *J. Chem. Phys.* **62** 2504.
148. Elkowitz, A.B., Wyatt, R. E. (I 975). *J. Chem. Phys.* **63** 702.
149. Walker, R. B., Stechel, E. B. and Light, J.C. (1978). *J. Chem. Phys.* **69** 2922.
150. Schatz, G.C. and Kuppermann, A.: *Phys. Rev. Lett.* **35** (1975) 1266
151. R. N. Porter and M. Karplus: *J. Chem. Phys.* **40** (1964) 1105
152. Truhlar, D. G. and Horowitz, C. G. (1978). *J. Chem. Phys.* **68** 2466.

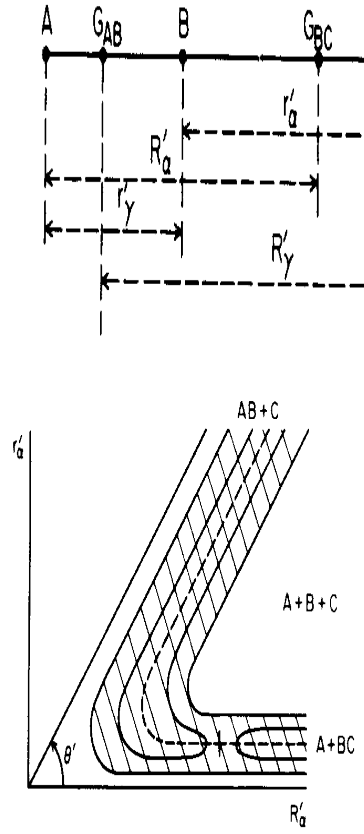

Fig. 4.9. (a) Coordinates for collinear triatomic systems, (b) Potential energy surface V for a collinear triatomic system ABC in the distance coordinates of (a). The solid curves are lines of constant V. The dashed line is the minimum energy path. The angle θ' is given by (4.32) (Reprinted, by permission, from Kuppermann, A. in: *Theoretical Chemistry and Perspectives*, **6A**, Henderson, D. (Ed.) (Academic, NY 1981). Copyright 1981 by Academic Press, Inc.)

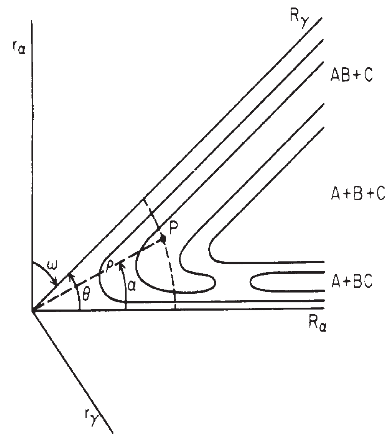

Fig. 4.10. Potential energy surface for a collinear triatomic system ABC in the scaled coordinates (R_α, r_α) and (R_γ, r_γ) of (4.35). The circular polar coordinates (ρ, α) are considered in the next section. The angles ω and θ are given by (4.39) and (4.40). respectively. Both sets of axes (R_α, r_α) and (R_γ, r_γ) are in the same plane. (Reprinted, by permission, from Kuppermann, A. in: *Theoretical Chemistry and Perspectives*, **6A**, Henderson, D. (Ed.) (Academic, NY 1981), Copyright 1981 by Academic Press, Inc.)

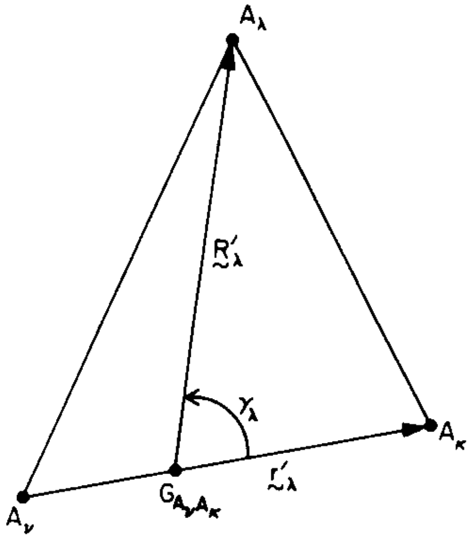

Fig. 4.11. Relative position vectors for triatomic system in three physical dimension (3-PD). (Reprinted, by permission, from Kuppermann, A. in: *Theoretical Chemistry and Perspectives*, **6A**, Henderson, D. (Ed.) (Academic, NY 1981), Copyright 1981 by Academic Press, Inc.)

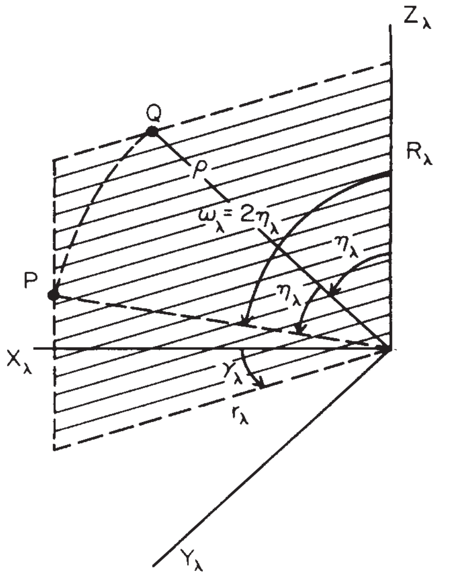

Fig. 4.12. Cylindrical and spherical polar coordinates for mapping potential energy function for noncollinear triatomic system. (Reprinted, by permission, from Kuppermann, A. in: *Theoretical Chemistry and Perspectives*, **6A**, Henderson, D. (Ed.) (Academic, NY 1981), Copyright 1981 by Academic Press, Inc.)

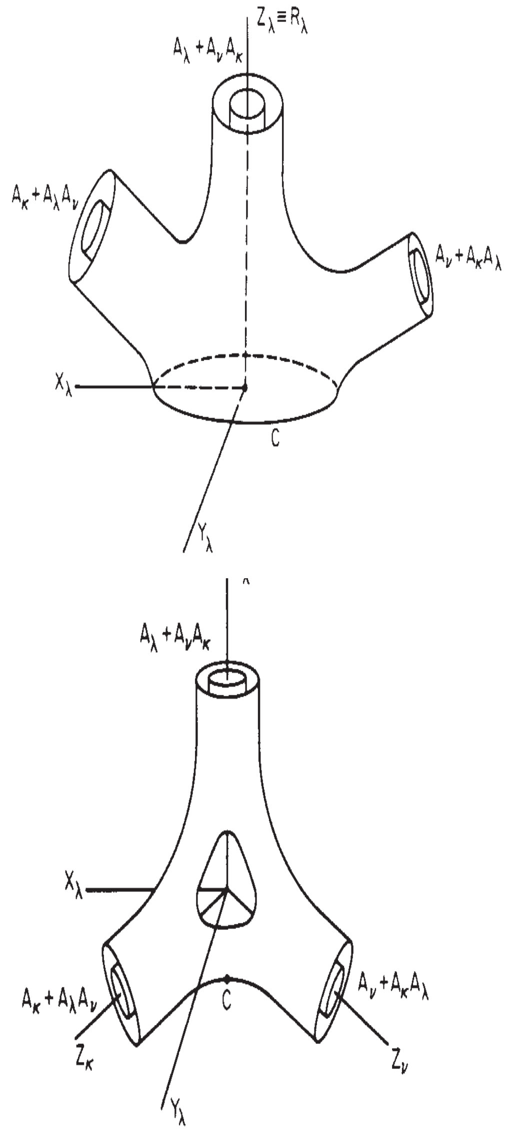

Fig. 4.13. Equipotential surface for noncollinear $A_\lambda A_\nu A_\kappa$ triatomic system in spherical polar coordinates. a) $\rho = (R_\lambda^2 + r_\lambda^2)^{1/2}, \eta_\lambda = \tan^{-1}(r_\lambda/R_\lambda)$ and γ_λ, b) $\rho = (R_\lambda^2 + r_\lambda^2)^{1/2}, \omega_\lambda = 2\tan^{-1}(r_\lambda/R_\lambda)$ andγ_λ. (Reprinted, by permission, from Kuppermann, A. in: *Theoretical Chemistry and Perspectives*, **6A**, Henderson, D. (Ed.) (Academic, NY 1981), Copyright 1981 by Academic Press, Inc.)

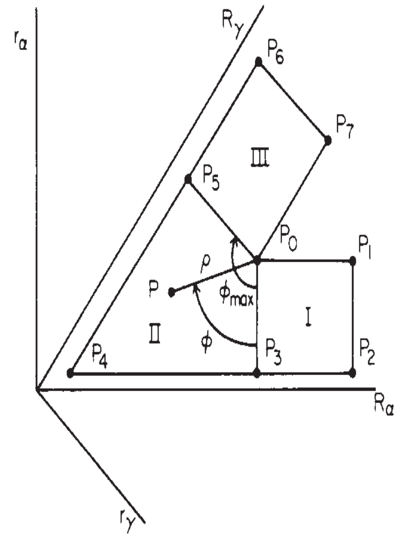

Fig. 5.1. Coordinates and regions of scaled configuration space for integrating the Schrödinger equation for collinear triatomic reactions. (Reprinted, by permission, from Kuppermann, A. in: *Theoretical Chemistry and Perspectives*, **6A**, Henderson, D. (Ed.) (Academic, NY 1981). Copyright 1981 by Academic Press, Inc.)

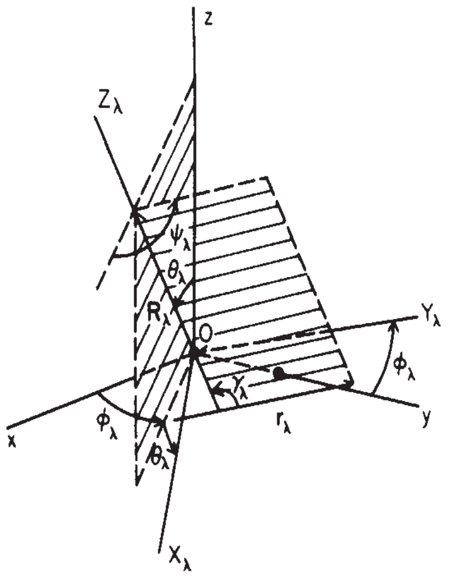

Fig. 5.2. Body-fixed and space-fixed coordinates for triatomic system in three physical dimensions. (Reprinted, by permission, from Kuppermann, A. in: *Theoretical Chemistry and Perspectives*, **6A**, Henderson, D. (Ed.) (Academic, NY 1981). Copyright 1981 by Academic Press, Inc.)

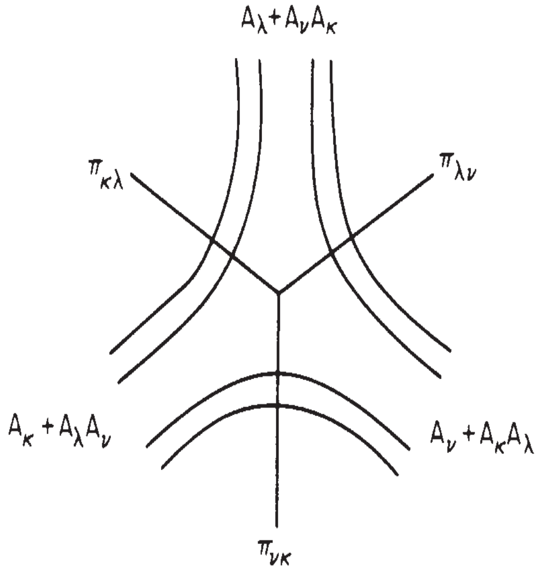

Fig. 5.3. Intersection of matching half-phanes $\pi_{\lambda\nu}, \pi_{\nu k}, \pi_{k\lambda}$ with the $X_\lambda Z_\lambda$ plane of Fig. 4.13b. Curves are intersections of an equipotential surface with that same coordinate plane. (Reprinted, by permission, from Kuppermann, A. in: *Theoretical Chemistry and Perspectives*, **6A**, Henderson, D. (Ed.) (Academic, NY 1981), Copyright 1981 by Academic Press, Inc.)